POLITECNICO DI TORINO

Dipartimento di Ingegneria Strutturale, Edile e Geotecnica

Master of Science in Civil Engineering

Master's Degree Thesis

Comparative study of geometrical properties and preliminary design proposal for concrete arch bridges

Supervisor:

Prof. Giuseppe Carlo Marano

Co-supervisor:

Prof. Leonardo Todisco

Prof. Hugo Corres Peiretti

Dott. Raffaele Cucuzza

Candidates:

Luciano Molner

Giulia Tibaldo

March, 2021

ACKNOWLEDGMENTS

We are very grateful to Politecnico di Torino, which supports its students in undertaking experiences like the one we lived in Spain. In particular, we would like to thank our supervisor Professor Giuseppe Carlo Marano for giving us the opportunity to go to Madrid, for guiding us during the development and writing of this work and for the help in concluding in the best way possible this academic path. We would like to thank also our Italian co-supervisor Raffaele Cucuzza for being like an "older brother" giving us advices and help during this work.

Secondly, we would like to thank the Universidad Politécnica de Madrid (Escuela de Caminos, Canales y Puertos) for welcoming us so warmly despite these hard times due to the Covid19 pandemic, giving us the opportunity to work and to develop a very interesting topic for our master thesis. Thanks to the advices and help of very expert Professors and Engineers Leonardo Todisco and Hugo Corres Peiretti, we had the opportunity to immerse ourselves in the world of reinforced concrete arch bridges, a world that was unknown to us, but which, thanks to this experience, we were able to know and appreciate making this experience unforgettable.

We would like to express our gratitude to our respective families which supported us during this long way. In particular to our parents, who gave us the possibility to go to Madrid, supporting us in all the ways possible; opportunity that would be impossible without their help and love. And, to our brothers and sister, who supported and stand us during these five years of university.

Last but not least, to all our friends, which went through this long journey with us being a kind of "second family", for the help and support they gave us constantly.

Giulia Tibaldo

Luciano Molner

ABSTRACT

The present research is based on the construction of a comprehensive and descriptive database of 58 concrete arch bridges (38 roadways and 20 railways) built in Spain during the last century. The collected information includes geometrical and mechanical data that are used to find out the main relations among different dimensions and parameters of the structures, further assembled to derive specific trends. These information have been combined with data collected by other relevant authors involved in the same issue as Salonga, Gauvreau and Manterola. In this way, a wider dataset has been obtained for bridges with similar features, allowing to have more reliable results. In particular, 112 arch bridges covering a span range from 12 to 384 meters have been employed to investigate relations of a variety of parameters. These are both geometrical, such as flatness, arch and girder dimensions, system bending stiffness, slenderness, effective slab thickness, and mechanical, as dimensionless axial force. Moreover, these empirical relations have been studied and applied to the Tiemblo bridge situated in Avila, Spain, designed by Fhecor, in 1999, whose technical drawings were kindly given by the Designer and the co-supervisor of this work. In this way, a finite element model of the bridge was built to carry more detailed analysis on this type of structures, with the aim to understand the influence of each engineering choices adopted during conceptual design process.

Based on the data collected in the database presented in this work, the authors have proposed a sound procedure for the preliminary design of roadway arch bridges with fixed supports and variable cross-section. Then, a comparison between the results obtained from this procedure and the real data collected into the dataset has been performed, specifically, in terms of dimensionless axial force ν.

The aim of this work is to find a methodology which, although its simplicity, represents a conservative procedure for the preliminary design of arch bridges. The authors are aware that the methodology does not include a complete analysis of the bridges, but the procedure proposed may represent a first approach to the design of such bridges.

SUMMARY

LIST OF FIGURES

LIST OF TABLES

1 INTRODUCTON

In this first chapter of the thesis, it will be given a general overview about the organization of the work. The contributions of each of the two authors given to the development of the present work is reported, the main objectives of the thesis and its structure.

1.1 General overview

Finding an easy and quick methodology for performing a preliminary design of a bridge in the early stages of a project is a typical job of an engineer. Bridge designers are often inspired by existing structures to carry a first structural and geometrical definition of a new bridge, trying to minimize costs and time.

The authors are aware that the methodology proposed and developed in the present work does not include a complete analysis of the bridges, but the procedure proposed may represent a first approach to the design of such bridges.

Due to the large amount of work and data treated to develop in the most comprehensive way as possible the topic proposed, the thesis has been conducted in group. Here below the contributions that each of the two authors made for the development of the present thesis has been reported:

- **Molner Luciano**. He developed in **Chapter 6** a deeper analysis on the real case of Tiemblo bridge through a FE model built with SAP2000, to study and better understand the main structural behavior in terms of resisting response of arch bridges. To validate the model, a comparison between hand-made calculation of the reactions, with the values from the analysis of the model has been done. Then, to find out if the common preliminary design rules suggested by Menn for arch bridges provide close results with those obtained by a FE model, the Tiemblo bridge has been taken as reference, exploiting their limits of applicability. Then, the student proposed the study of the arch shape geometry starting always from the real case of Tiemblo bridge to check if its pressure line was located as close as possible to the one due to dead load to achieve the best structural response from the arch. In **Chapter 7**, instead, he studied the structural response under vertical loads and imposed deformations of the Tiemblo bridge to understand the importance of the degree of constraint of such arch by making comparisons with a two-way hinged arch. In particular it has been analyzed: the influence of the rigidity relation between arch and deck, the embedding of spandrel columns in arch and deck, the Freyssinet connections and the construction processes used for such bridges.

- **Tibaldo Giulia**. She developed the preliminary design process stages and the steps performed to reach that goal. Starting, in **Chapter 4**, with the assembly of the database, which stand at the foundation of this work, ensuring the characterization of the state of art of the concrete deck arch bridges and identifying and describing the most relevant geometrical trends among the set of structures taken into consideration. The database assembled for this work was based on the description of each structure from both the qualitative and quantitative points of view. The collected information concerned the geometry of the bridge in its entirety, as well as each of its single component: deck, arch, and columns. Then the student run in **Chapter 5** an analysis on selected empirical trends among the system parameters, which has been used for the preliminary assessment of a certain pre-design concept as a guide for the designers. In **Chapter 9** a comparison between results obtained with the procedure described in chapter 7 and the value calculated according to the data collected in the dataset has been performed.

Despite remarking each author contribution to the work development, the **Chapter 8**, regarding the proposed sound procedure for the preliminary design of roadway arch bridges with fixed supports and variable cross-section, the core of the thesis, has been elaborated by both the students together.

1.2 Main objectives

The main goal of the present work is to develop a preliminary design process based on a comprehensive collection of existing structures which can be very useful from the designer perspective. This efficient process is based on the fulfillment of a given set of requirements, such as some empirical trends of completed bridges that satisfy similar conditions and for that reason can be used as a starting point. The collected bridges are concrete deck arches in Spain, widely used in modern and ancient engineering permitting to transfer loads from the superstructure to the foundations with low structural weight; moreover, if properly shaped, they become an optimal solution to cross large spans and transfer high loads. A deeper analysis has been also conducted on the real case of Tiemblo bridge, to study and better understand the main structural behavior in terms of resisting response of arch bridges and to validate some of the empirical formulas and considerations proposed by Menn and Manterola. These information have been used by the authors to study fundamental parameters that define the structural behavior of such bridges.

1.3 Thesis structure

The thesis is composed by nine chapters, without considering the acknowledgements, the abstract and the introduction. In Chapter 2 the state of art of arches, has been introduced. Historical and descriptive aspects about arch bridges are presented. The idea was to start with a short history of arch bridges, then proceeding with a general analysis to finish with a deeper description of the deck arch bridges, the ones treated in this study case.

In Chapter 3 of the thesis the main theories and conceptual design concepts based on the arch bridges illustrated by Menn, Leonhardt, and Manterola used to develop the present work have been presented. The entire analysis has been carried out for deck arch bridges, when the deck is located above the arch and it is supported by columns rising from the arch.

Afterwards, in Chapter 4, the realization of the database has been explained, inspired by the research on concrete arch bridges performed by Salonga and Gauvreau in 2014. The dataset presented is constituted by geometrical and mechanical information of 58 Spanish concrete arch bridges, of which 38 roadways and 20 railways to investigate the correlation between parameters with the goal of defining a reliable source for carrying a preliminary sizing of such bridges, topic that will be developed in the following chapters of this work.

Linked to this topic is the Chapter 5, where some empirical trends has been identified and from which it can be deduced that optimization is a key issue for a good design, searching optimal solutions in terms of material consuming, shape section and also from the architectural point of view (Salonga & Gauvreau, 2014).

In Chapter 6 has been performed the analysis of the structural system where, in order to study and better understand the main structural behavior in terms of resisting response of arch bridges, the Tiemblo bridge situated in Avila, Spain, designed by Fhecor in 1999 has been selected.

Another analysis about Tiemblo bridge has been conducted in the Chapter 7 regarding the engineering choices of its design. In particular, the influence of the rigidity's relation between arch and deck, the embedding of spandrel columns in arch and deck, the Freyssinet connections and the construction processes used for such bridges.

Then, in Chapter 8, some simple methods to perform a preliminary design of roadway arch bridges with fixed supports and variable cross-section has been presented, this includes an analysis under permanent and live loads, where no horizontal loads will be considered. The procedure chosen to be followed is based on the observation of the trends deduced from the empirical parameters plots and discussed in Chapter 5.

The Chapter 9 of the present work presents a comparison between the real values collected and the preliminary design results of the geometrical parameters discussed in Chapter 8.

Finally, in Chapter 10, conclusions about the work are performed and the future works to be done are suggested.

2 STATE OF ART

In this chapter historical and descriptive aspects about arch bridges are presented. The idea is to start with a short history of arch bridges, then proceeding with a general analysis to finish with a deeper description of the deck arch bridges, the ones treated in this study case.

2.1 History of arch bridges

Arch structures have been used in construction field, since long time ago, for their structural capability and aesthetical purposes. Even before the beginning of recorded history, humans had a need to cross fast-moving streams and other natural obstacles. Humans soon discovered that a vine attached to a treetop enabled them to swing across a wide river, discover which led to the construction of primitive suspension bridges with cables of vines or bamboo strips twisted into ropes.

The arch came much later as applied to bridge building with the Sumerians around 4000 B.C., when they discovered the advantages of the arch shape and its construction (Fox, 2000).

The general consensus among architectural archaeologists is that in Europe the Etruscans were the first to use the genuine arch bridge in Italy in around 800 B.C. By real arch bridge is meant a structure in which the stone segments are arranged in a radial way, as opposed to false arches composed of cantilevered brick or stone.

Neither the Egyptians nor the Greeks used so much the arch in their construction, although there is evidence to show that they were aware of its existence. It is with the Romans that the arch bridge became the almost universal method of bridge construction right down to the 18th century. If we date civilization from the Mesopotamian cultures that arose in the region between the Tigris and Euphrates rivers, we see that arch bridge-building was a relatively late development, only becoming widespread in Roman times as from about 700 B.C. (Martínez, 2005).

By the time of the Romans, most bridges were constructed as stone arches, also known as masonry or Voussoir arches (Fox, 2000). Empirical rules for dimensioning the shape of the arch and the wedge-shaped stones were developed. The Romans were magnificent builders and many of their masonry bridges are still standing, since stone can support very large compressive forces and it is resistant to corrosive elements (Fox, 2000). Moreover, the arch is stable as long as the thrust line is contained within the cross-sectional area. Today, arch bridges are generally constructed of concrete or structural steel. The 19^{th} century was the century of iron/steel bridges, suspension bridges, trusses, large cantilever bridges, viaducts, but toward its end, also concrete arch bridges began to be constructed, the ones that will be treated and analyzed more deeply in the present work.

2.2 First concrete arches

From John Smeaton's Eddystone Lighthouse of 1759 to the advent of the cement industry at the beginning of the 19^{th} century spanned a period of almost 50 years. Yet it took another 50 years before the appearance of reinforced concrete. During that period is the time of the plain concrete, for the arch bridges only a few works were made out with a compacted plain concrete, some with spans of as much as 36m, in both France and Spain. Just who discovered reinforced concrete and when the discovery was made are matters which, as often occurs in historically research, raise the difficulty of separating the individuals who did something with reinforced concrete and those who actually converted it into a practical building material on a large scale. The first patent taken out was that of Lambot in 1855, he was a gamekeeper who had made a boat out of cement. He was followed by the gardener Monier, who took out successive patents from 1867 onwards and had enough business sense to make commercial use of his invention. In fact, the first reinforced concrete arch to be built, in 1875, was the work of Monier. It was a footbridge in the gardens of the Palace of the Marquis of Tilière de Chazelet (Fig.2.1) (Martínez, 2005).

After the early pioneers came Hennebique who, at the end of the century, making better use of industrial processes and the radically new concept of the franchise, succeeded in extending the use of reinforced concrete around the world. He was given a prize for his efforts at the Paris Exhibition in 1900 and it was Hennebique himself who in 1904 built the Risorgimento Bridge in Rome, with a span of over 100m (Fig.2.2) (Martínez, 2005).

Figure 2.1: Tilière de Chatelet Arch Bridge, France (image taken from Arch evolution and future trends, Martínez)

Figure 2.2: Risorgimento bridge, Italy (image taken from Wikipedia)

In Spain it was Eugenio Ribera who introduced the use of reinforced concrete at the beginning of the 20th century and designed the arches to be used as the official set of reinforced-concrete units for standard road bridges.

In 1899 he began to work as a builder, founding his own company, Hidrocivil and carried out all kinds of works with the new material. In 1901 he built the Golbardo Bridge (Fig.2.3) over the Saja River and later up to about 500 reinforced concrete bridges, built with a rigid frame that was incorporated into the structure. Among the most important are those of Kursaal and María Cristina (Fig.2.4), in San Sebastián, Reina Victoria (Fig.2.5), in Madrid, San Telmo, in Seville, and Valencia de Don Juan, in the province of León. The Amposta suspension bridge (Fig.2.6), over the Ebro, deserves a special mention. All his works were characterized by the search for simplicity and economy. Along this line of simplicity is the Official Collection of arch bridges, which he wrote and with whose models many bridges were built, such as the Barranco Hondo, in the Canary Islands. He also built several aqueducts, starting with Araxes, in Navarra and continuing with La Perera and the large diameter Sosa and Albelda siphons in the Canal de Aragón and

Cataluña. His most spectacular work was the Chorro aqueduct, built between 1904 and 1907 in a gorge a hundred meters high which collapsed in 1904 under construction (Ridruejo, 2018).

Figure 2.3: Golbardo bridge, Spain (image taken from Structurae)

Figure 2.4: Maria Cristina bridge, Spain (image taken from Wikipedia)

Figure 2.5: Reina Victoria bridge, Spain (image taken from Wikipedia)

Figure 2.6: Amposta suspension bridge, Spain (image taken from Wikipedia)

2.3 General analysis of arch bridges

First, an arch is a curved structural element whose transversal section is negligible with respect to its length and generally it rests on piers or columns. The arch constitutes a "compromise" between the horizontal and vertical element, progressively deviating the vertical loads on the piers (or abutments) leading them to the ground. Arches have been created to work in compression, being one of the best construction solutions for covering large spans and bearing structures for absorbing the horizontal thrusts by using cheap foundations. Ideally, it should be subjected only to compressive forces, free of any bending moments and shear forces. In such a case, the arch is extremely efficient because every part of its cross sections is subject to the same stress. To obtain an ideal arch free of bending moments, the arch axis must coincide with the line of thrust caused by all loads acting on it. Nevertheless, in arch bridges, there is no single line of thrust, and sometimes there is more than one arch axis. So, moving loads on the bridge cause changes in the line of thrust (Schanack, 2016).

The biggest problem to build reinforced concrete arches was the difficulty in setting up the scaffolding. With reinforced concrete arches development scaffolding became a key issue, due to the difficulty of assembly and the resulting cost.

The scaffolding for the Salginatobel was designed and constructed by Richard Coray (Fig.2.7). It is a classic ‘curtain’ scaffolding, so called because the uprights are gathered together at foundation points high up on the hillside, thus reducing its height. Not surprisingly, by the mid-20th century reinforced concrete arches had undergone a temporary eclipse, due to the costs involved in their scaffolding construction employed during construction stages and the high material consumptions. To avoid this difficulty, scaffolding to be embedded in the final structure was developed. One of the early structures of this type was that developed in 1898 by the Austrian engineer Josef Melan. He used a steel truss with chords, diagonals and vertical members which was cantilevered out. The bottom chord was a box truss and will acted after as the shuttering itself. The best-known bridge using this system was the Echelsbach Bridge in Austria, constructed in 1929 (Fig.2.8) (Martínez, 2005). However, the procedure never caught on in Europe fully, as the costs of setting up the materials and the truss boxes were more expensive than the bridge itself.

Figure 2.7: Salginatobel scaffolding system, Switzerland (image taken from Arch evolution and future trends, Martínez)

Figure 2.8: Echelsbach Bridge, Austria (image taken from Wikipedia)

Another important issue regarding arch bridges is how to carry loads to the ground, not only the vertical loads but, especially, the thrust of the arch requiring a very competent foundation, in the case of deck arch bridges (Fig.2.9), to support the high vertical and horizontal forces transmitted by the arch. However, most of the through (Fig.2.10) and half-through arches (Fig.2.11) are tied arches, so, the horizontal thrust is tied by the deck and the foundation of the arches only need to support vertical reactions (Schanack, 2016). This is the natural concept of an arch bridge, also known as a true arch. With the coming of concrete, some additional aspects with respect to the masonry arch bridges started to be considered as the deformations due to creep, temperature changes and shrinkage which affect the shape of the arch making joints necessary. The simple concrete conditions, for example, the choice of the arch type, if three-hinged, two-hinged or fixed-end without internal hinges (Leonhardt, 1979), which will be deeply described in the “Analysis of the structural system” chapter.

Arch bridges, as briefly mentioned above, are generally classified into three main types:

a. deck arch bridges, with the crown of the arch located below the deck (Fig.2.9);
b. through arch bridges, where the bridge deck is located at the springing line of the arch (Fig.2.10);
c. half-through arch bridges, where the bridge deck is located at an elevation between a deck arch and a through arch (Fig.2.11).

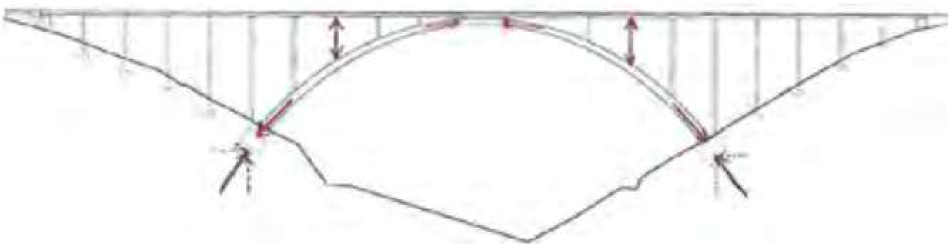

Figure 2.9: Deck arch bridge (image taken from Arch bridges, Schanack and Ramos, 2016)

Figure 2.10: Through arch bridge (image taken from Arch bridges, Schanack and Ramos, 2016)

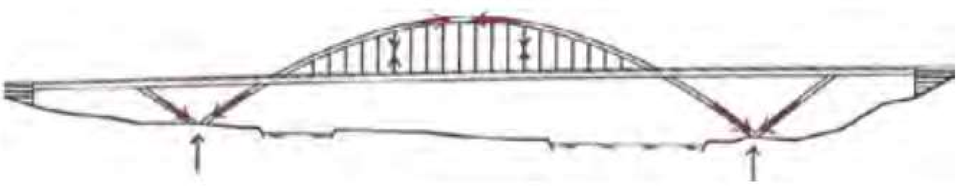

Figure 2.11: Half-through arch bridge (image taken from Arch bridges, Schanack and Ramos, 2016)

Since this study case has been conducted on concrete deck arch bridges, this chapter will only discuss this first typology.

2.4 Investigation of deck arch bridges

As mentioned above, deck arch bridges are structures where the bridge deck, which includes the structure that directly supports the traffic loads, is located above the crown of the arch. The deck arch is also known as a true or perfect arch (Fox, 2000).

To design a deck arch bridge, two requirements must be satisfied:

- enough clearance under the deck to place the arch;
- foundation materials with competent bearing capacity to resist the thrust.

This type of structure can be classified according to different criteria, such as (Schanack, 2016):

a. the arch form;
b. the material used to build the arch;
c. the relation between the arch and the deck;
d. the restraint conditions;
e. the arch cross section.

Regarding the form of the arch, the following types can be identified (Schanack, 2016):

- Rounded or semicircular arch form extensively used by the ancient Romans. There are some examples of arch bridges built by the Romans using the rounded arch in Spain as the Segovia Aqueduct (Fig.2.12) and the Alcántara Bridge (Fig.2.13);

Figure 2.12: Segovia Aqueduct in Segovia, Spain (image taken from Wikipedia)

Figure 2.13: Alcántara Bridge in Alcántara, Spain (image taken from Wikipedia)

- The pointed arch which started to be used in the Middle Ages. A concentrated load on top of the key of this arch type is needed to maintain its structural efficiency. Nowadays, this form is relatively common used in bridges for high-speed railways (HSR) as the Deza bridge in Spain (Fig.2.14);

Figure 2.14: Deza River Railway Viaduct in Galicia, Spain (image taken from Wikipedia)

- Low-rise arch for which a circular arc is used instead of a complete semicircle, frequently used nowadays;
- Parabolic arch, structurally very efficient, given that the parabola is the inverse funicular curve for a uniform load;
- Several circular arcs which is a try to approximate the parabolic arch by chaining circular segments turning into a more easily constructible geometry;

- Polygonal arch which occurs when there are few columns connecting the arch and the deck, the load is not enough uniformly distributed, so a polygonal form is a better approximation of the inverse funicular curve.

Talking about the material used to construct arches, in addition to concrete, which is the most used nowadays and it constitutes one of the cheapest solutions for constructions, there are also (Schanack, 2016):

- Stone arches which was arch bridges built before the 19th century, since the coming of steel and concrete;
- Metal arches which started to be built in the early 19th century. Soon, however, the cast iron was replaced by steel, which became the most used material for arches until the mid-20th century. Today, many arches are still built with steel, but not as many as those made of concrete;
- Concrete-filled steel tubular (CFST) arches, relatively recent type of deck arch.
- High performance concrete (HPC) and Ultra-high-performance concrete (UHPC) arches are suitable solutions nowadays to withstand very high compression forces. Moreover, their use allows smaller cross-section for the arch, so lighter self-weight structures can be realized, easing the erection procedure and lessening the thrust at springing. HPC is commonly used in big deck arch bridges. Many examples can be found in Spain as Los Tilos Bridge in Canary Islands (Fig.2.15), Contreras Reservoir Bridge in Valencia (Fig.2.16), Alcántara Reservoir HSR Bridge (Fig.2.17) and the Almonte River HSR Bridge (Fig.2.18) both in Cáceres.

Figure 2.15: Los Tilos Bridge in Tenerife, Spain (image taken from Wikipedia)

Figure 2.16: Contreras Reservoir Bridge in Valencia, Spain (image taken from Wikipedia)

Figure 2.17: Alcántara Reservoir HSR Bridge in Cáceres, Spain (image taken from Wikipedia)

Figure 2.18: Almonte River HSR Bridge in Cáceres, Spain (image taken from Wikipedia)

For the deck-arch relation, two types of arches can be distinguished (Schanack, 2016):

- Close-spandrel arches, used in ancient stone arch bridges;

- Open-spandrel arches used in modern concrete and steel deck arch. The connection between the deck and the arch is made by means of piers.

The restraint conditions of the arch have been mentioned in the previous paragraph regarding the general analysis of arch bridges and will be deeply described in the "Analysis of the structural system" chapter.

Finally, concerning the arch cross section, a simple distinction between concrete and steel can be done. In concrete arches the cross-section can be mainly solid or n-cell box, instead for steel arches it can be a truss, a solid web girder or a tube filled with concrete (Schanack, 2016).

2.5 Future evolution of concrete arches

In the tender for the Millau viaduct in France, Jean Muller and Alain Spielmann presented a concrete arch solution with a span of 602m. The solution included two variants: one with a concrete deck and the other with a steel deck. The arch (Fig.2.19) had a hexagonal box section with a continuous depth of 8m and variable width from 8m to 18m. The span between piers over the arch was 85m approximately and in the key area, the deck and arch are connected over a 105m stretch. The construction process was like the Guaira bridges. First the arch cantilever starters were built tied to the arch starter pier up to 170m, then a steel truss scaffolding was built with a concreted lower slab and then raised by "lifting" with a weight of 2,300Tm. According to the budgets prepared for this quotation, the solution competed with the multiple spans stay viaduct that was built.

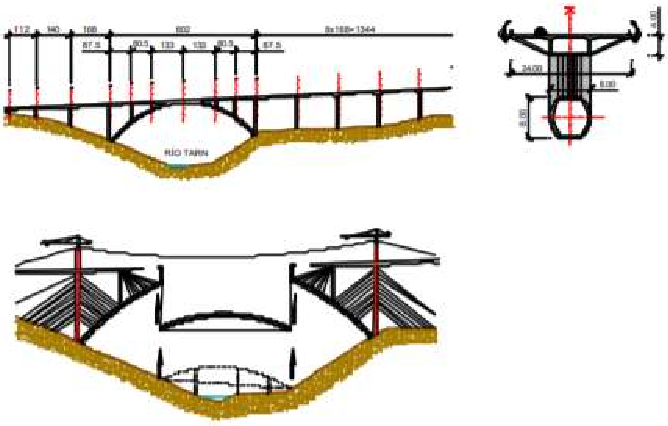

Figure 2.19: Millau arch, dimension, construction, France (image taken from Arch evolution and future trends, Martínez)

3 LITERATURE

In this chapter of the thesis the main theories and conceptual design concepts based on the arch bridges illustrated by Menn, Leonhardt, and Manterola used to develop the present work have been presented (Menn, 1990)(Leonhardt, 1979)(Manterola, 2006).

The entire analysis has been carried out for deck arch bridges, when the deck is located above the arch and it is supported by columns rising from the arch as has been explained in the “State of art” chapter.

3.1 Arch bridges analysis proposed by Menn

3.1.1 Conceptual Design

The cost of falsework and formwork for arch bridges is high with respect to cast-in-place girder bridges. So, arch bridges are economical only in some specific topographical and geotechnical conditions, as for river, canyons, or valleys crossings. The range of reinforced concrete arch spans holds to be more economic goes from 50 up to 200m (Menn, 1990).

As will be explained more in details in the “Empirical (geometrical and material) trends” chapter, the recommended range for the span-to-rise ratio L/f for Menn is between 2 and 10 due to the sensitivity of arches to creep, shrinkage, temperature change, and support displacements which increase with the increasing of L/f. Stresses and deformations due to these actions are smaller when L/f is less than 4. As L/f approaches to 10, it may be necessary to reduce or eliminate redundant moments caused by the restrained deformations, providing hinges at the springing lines and at the crown. If the span-to-rise ratio is greater than 10, excessive deformations are inevitable; on the other hand, if the L/f is smaller than 2, the arch will appear with a strange shape and a substantial increasing of construction cost (Menn, 1990).

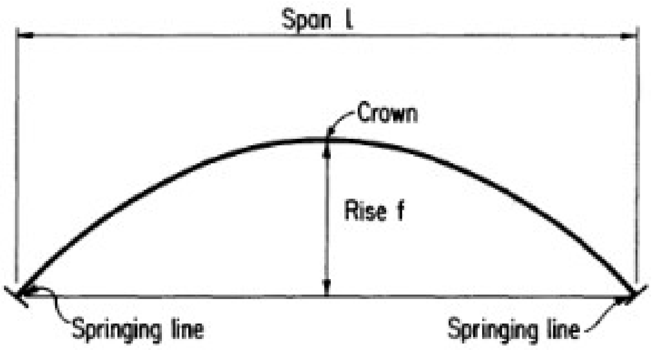

Figure 3.1: Terminology of arch bridges (image taken by C. Menn)

The moments arising in the system can be divided into two components: fixed system moments, produced when the arch vertical deformations are restrained and so equal the continuous beam moments in the girder and flexible system ones which correspond to the arch vertical displacements generally shared by both the arch and the girder. From this initial distinction, two limit cases in terms of bending stiffness can be identified: stiff arches, where the arch alone resists to the entire flexible system moment, and deck-stiffened arches, where the entire flexible system moment is instead resisted by the girder (Menn, 1990).

Moments due to arch displacements can be further subdivided into two components: dead load and live load. To minimize the bending in the arch due to dead load, which displaces the arch away from the pressure line, the axis of the arch should be located along the pressure line (Menn, 1990),.

The stiffness of the arch can be useful both during the construction process and the service life of the bridge carrying the dead load of arch, columns, and girder without counting on the girder stiffness for the global stability. The stability of the entire system is generally guaranteed by the continuity of the girder (Menn, 1990).

3.1.2 Design of the cross-section

Regarding the arch depth, which is chosen early in the design process due to its effect on visual qualities and structural response of a given bridge, Menn does not recommend any specific value. Regarding the cross-section type, instead, Menn says: "*The cross section of the arch is primarily a function of the arch **span length** and the **ratio of arch stiffness to girder stiffness** [..]*" (Menn, 1990), suggesting some threshold values of span length *L*: for *L* smaller than 120m the section can be consider a slab one, which appears slender and elegant but a bit expensive; for *L* up to 150m, twin ribs can be an economical choice, reducing the cost of the top forms; for L greater than 200m, box section can be used, diminishing the weight of the section especially for long-span arches (Menn, 1990).

3.1.3 Prestressing Concept and Tendon Layout

In the arch region, which has to resist to both positive and negative bending moments, the tendon layout is placed at the top and at the bottom of the section. An efficient use of prestressing occurs when the prestressing and the minimum reinforcing steel are sufficient to resist the ultimate bending moments produced by the dead load and the live one at the locations of lowest stress. It is suggested that the entire girder be fully prestressed for dead load. Avoiding permanent cracks is desirable for durability reasons and for the increasing in stiffness which improves the global stability of the system (Menn, 1990).

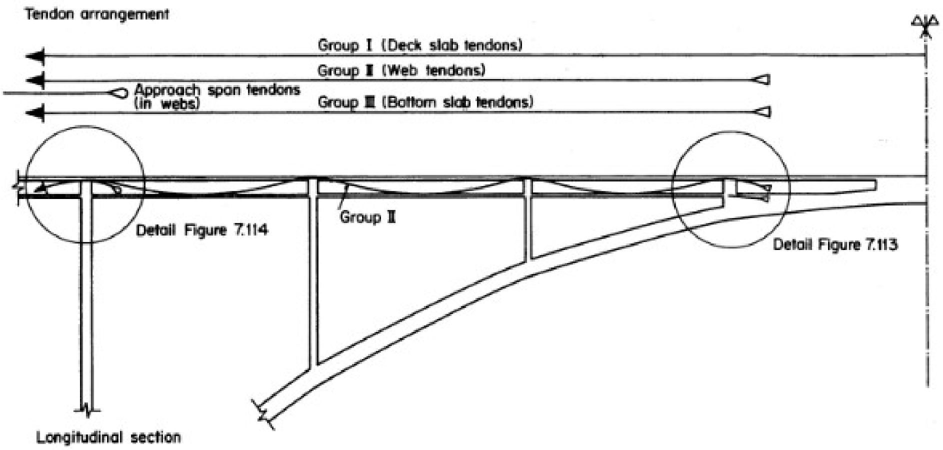

Figure 3.2: Tendon layout for arch bridges

The tendon arrangement shown in Fig.3.2 is recommended by Menn for hollow-box girders. Web tendons, designed to balance the dead load of the girder in the fixed system, are provided over the entire length of the bridge, overlapped at the columns above the arch abutments and are terminated just before the crown. The interior spans above the arch are often progressively shortened towards the crown. By stressing the web tendons at the columns above the arch abutments, the prestressing force decreases towards the crown to match the reduction in span length. Tendons in the top and bottom slabs are provided only in the arch region and they should be placed as close to the webs as possible. The bottom slab tendons terminate just before the crown. Top slab tendons, which are continuous over the crown, can help to balance the eccentrically applied arch force at this location. The overlapping of the tendons is recommended since negative moments in the girder are normally highest at this location (Menn, 1990).

3.1.4 Preliminary Design

According to Menn's preliminary design process, the load configuration should be as in Fig.3.3, where the arch axis is located as close as possible to the pressure line due to dead load, the weight of the girder and columns is applied as concentrated loads at the base of each column, and the slope of the pressure line will be discontinuous at these points.

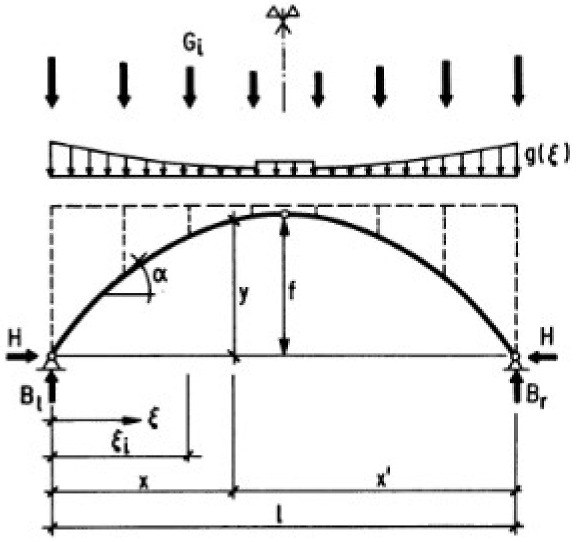

Figure 3.3: Pressure line configuration due to dead loads

The pressure line is calculated assuming the arch hinged at the springing lines and at the crown; moreover, the dead loads, *G* and *q*, the span length *L*, and rise *f* are given.

The moments produced are $M_0(x)$, the horizontal reaction component, H, is

obtained from moment equilibrium of one half of the three-hinged arch as:

$$H = \frac{M_0\left(\frac{L}{2}\right)}{f} \tag{3.1}$$

Then, the moments in the arch, M(x), are given by:

$$M(x) = M_0(x) - Hy \tag{3.2}$$

where y is the arch ordinate obtained by imposing M(x)=0:

$$y = \frac{M_0(x)}{H} = \frac{M_0(x)}{M_0\left(\frac{L}{2}\right)} f \tag{3.3}$$

The total weight of the system (arch, girder, columns) can be approximated to a uniform distributed load $\bar{q}$, so the corresponding horizontal reaction H is:

$$H(\bar{q}) = \frac{\bar{q}L^2}{8f} \tag{3.4}$$

Generally speaking, the moments are shared by girder and arch when the system is flexible, and they can be evaluated as distributed ones for both the limit cases (deck-stiffened arch and stiff arch) as:

$$M^G = M \frac{I^G}{I^G + I^{A,C}} \ (girder) \tag{3.5}$$

$$M^A = M \frac{I^{A,C}}{I^G + I^{A,C}} \ (arch\, crown) \tag{3.6}$$

In Fig.3.4 and Fig.3.5 the maximum moments at the springings, kidneys, and crown for the preliminary design and the respective diagrams are reported due to partial live load configurations. At the springing lines, the flexible system moment will be resisted essentially by the arch alone: $EI^G \approx EI^{A,C}$.

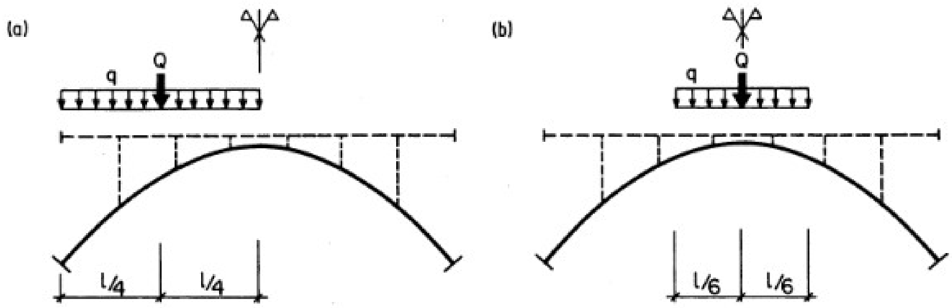

Figure 3.4: Partial live load arrangements: a) half span; b) span middle third

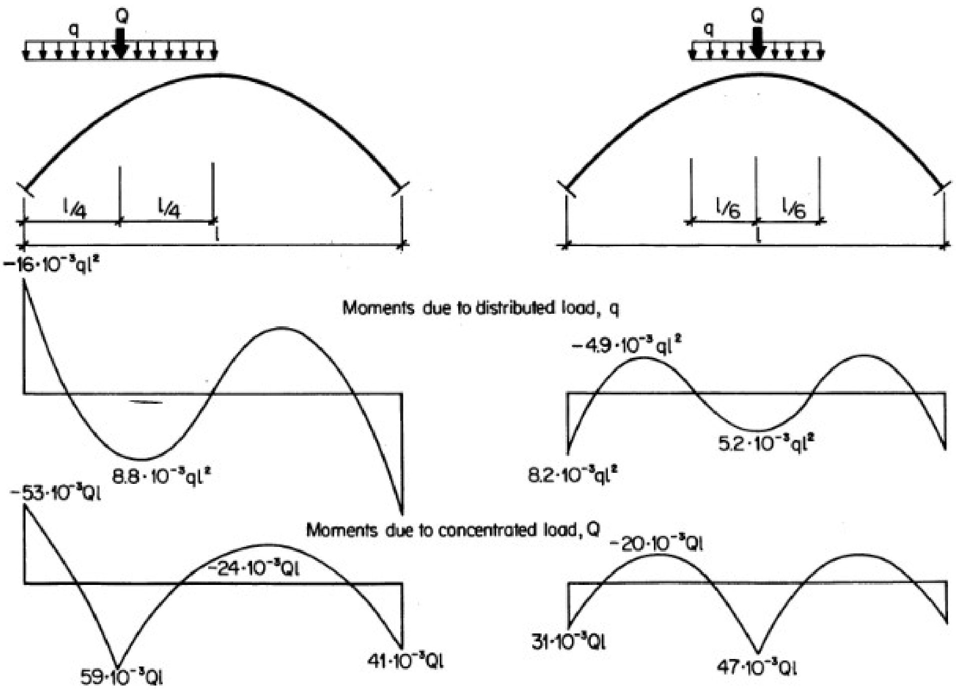

Figure 3.5: Frame system moments due to partial live load

3.2 Leonhardt recommendation about arch bridges

Also, Leonhardt in its book "Bridges, Part VI" analyzed the arch bridges, proposing some span-to-depth ratio values (*L/f*), which provide a logical basis for the definition of the most representative ones. That is, because designers rely on *L/f* recommended by standard texts such as Menn and Leonhardt or other sources to size the structural members in a preliminary design stage due to their considerable importance in the primary dimensions often chosen on this basis only.

Concrete arch bridges, as already specified in the Section 2.1, are sensitive to creep, shrinkage, temperature change, and support displacements which increase increasing *L/f*. It can be said that the concrete affects the type of arch to be built: arch with three hinges, two hinges, one hinge or embedded. For each one of these cases, Leonhardt proposed a different span-to-rise ratio to ensure the arch shape to be adapted to the line of pressure (Leonhardt, 1979).

- Arch with three hinges, *L/f* from 5 up to 12m;

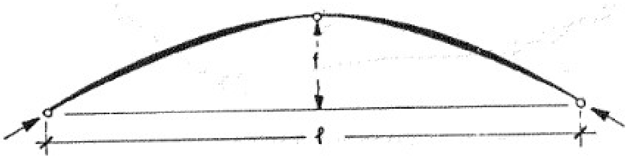

Figure 3.6: Three-hinged arch bridge

- Arch with two hinges, *L/f* from 4 up to 12m;

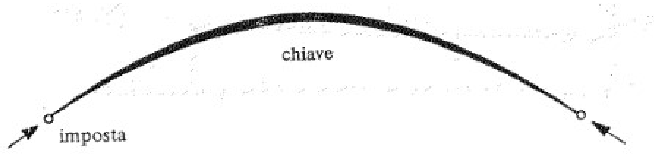

Figure 3.7: Two-hinged arch bridge

- Arch with one hinge, not suitable for bridges due to the high cost of their foundations;
- Embedded arch, *L/f* from 2 up to 10m with a width greater at the springing lines rather that in crown.

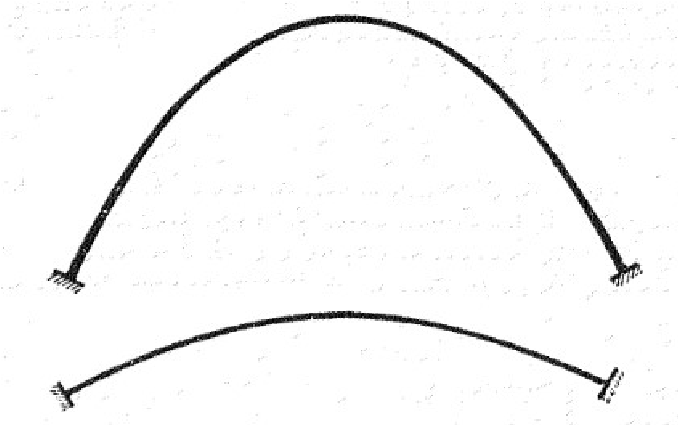
Figure 3.8: Embedded arch bridge

Leonhardt also stated that, for span greater than 50m, the three-hinged arch shape geometry developed by the swiss engineer A. Maillart is particularly economical, having a small column span ratio with respect to the arch span length (Fig.3.9). The arch starts at the springing lines with a flat shape, then at the kidneys it presents a U-shape transversal section to resist to the great bending moments and finally at the crown it is joined to the girder (Leonhardt, 1979).

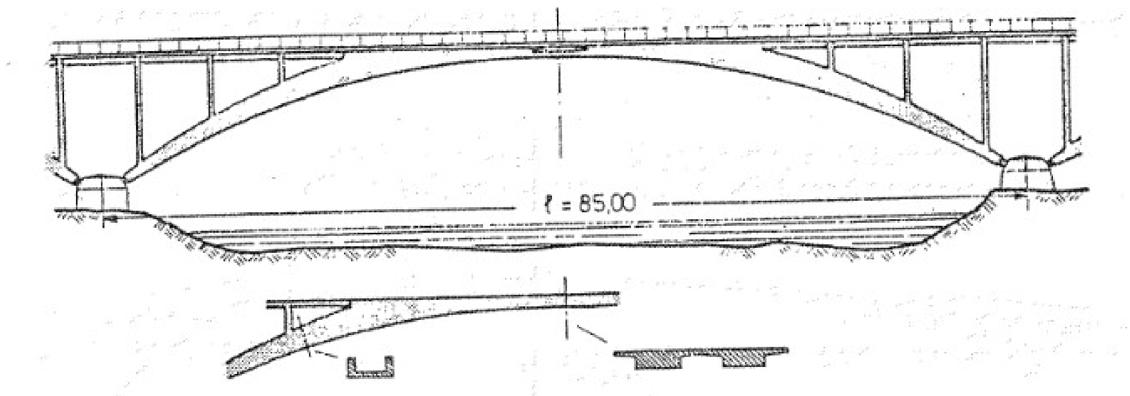

Figure 3.9: Maillart arch shape geometry

3.3 Arch bridges analysis proposed by Manterola

Since the coming out of prestressing, which allows the construction of straight bridges of great light, and the cable-stayed bridge, which covers easily lights from 200 to 500m up to 1000m, the arch bridge, in general, and in particular concrete, has experienced a prolonged stop (Manterola, 2006). The use of large falsework was the most important difficulty in the construction process of these bridges, generally located in areas of hard access, large valleys, or important waterways. However, the application to the arches of the cantilever construction method, it has relaunched again the presence of this type of concrete or metallic bridges for spans ranging between 100 and 400m for concrete bridges like the Krk bridge in Croatia (L=390m), or up to 530m as New River George Bridge in USA (L=518.5m) in the case of metal bridges (Manterola, 2006).

Manterola also proposed the classification for the arch bridges according to the position of the deck:

- deck arch bridges;
- through arch bridges;
- half-through arch bridges.

3.3.1 Deck arch bridges

There are several parameters which can affect the different variants of this type of bridges:

- Material. Steel, concrete, and a mixed of both for the construction of the arch, piers and girder.
- Joints. Bi-embedded arch, bi-articulated arch, or tri-articulated arch.

- Cross section of the arch. Box section with one or more cells. Solid rectangular section, tube sections, lattices, etc.
- Girder section. Box sections. Solid or lightened slab, “T or double T” beam sections.
- Arch-deck relation. Pillars, tympanum, etc.
- Stiffness distribution between arch and deck. Rigid arch and flexible girder, or flexible arch and rigid girder.
- Plan director guideline of the arch. Flat and space arch.

According to Manterola, generally, an arch bridge with a top deck is a bi-embedded arch bridge. Joints are expensive items of questionable preservation, avoided whenever possible. They introduce great deformability in the arch and are only compulsory in case of large turns at the foundations, a situation difficult to find, since the arch must be located on terrain with good resistance (Manterola, 2006).

Manterola also proposed a database of deck arch bridges, that it has been consulted for the present work development. He established the most important characteristics of “classic” arch bridges since they have been built starting from 30s and are still being built today without major changes. Almost all the large concrete arch bridges belong to this family. This collection of information from different authors, allowed bridge designers, which are often inspired by existing structures, to carry a first structural and geometrical definition of a new bridge; therefore, a comprehensive collection of existing structures maybe very useful from the designer perspective (Manterola, 2006).

As initial boundary condition, it can be stated that in most of the cases this type of arch bridge is bi-embedded, as previously said. The director guideline of the arch must follow the anti-funicular curve of the permanent loads of the bridge, arch + deck + piers, which leads to curves close to a 2nd order parabola. The rise to be used should be, in principle, the largest possible, to minimize the stresses on the concrete and the loads on the foundation, in addition to control as much as possible the effects produced by the imposed deformations and the sitting of the supports. However, the concept of using the largest possible rise is very clear in bridges over rivers, in which, normally, the distance between the slope and the shore is not very high. For bridges of the first half of the century, the downgrades were of the order of L/8 to L/10, since at that time there was no prestressing to make a straight bridge. On the other hand, in a bridge over a valley type of configuration, the problem is that the rise depends also on other types of concepts. If the rise is too big, the arch is too short and little used. If it is very small, the arch is more expensive and very vulnerable to horizontal movements of the foundation. A frequent ratio is L/4, which produces good arches. Increasing the lowering, the arch becomes visually more tense and fuller (Manterola, 2006).

About the arch cross-section, the most common one in arch bridges is the box section, with one, two or three cells. These sections are lightweight and have an excellent turning radius. The compression, therefore, can eliminate the tractions produced by bending due to overload. For example, the Panamata Bridge cross section of the arch is made up of four boxes, practically independent, attached one next to the other and without joining reinforcement. The reason for this solution was the reduction in the size of the formwork, which was reused four times, once per each arch, and the subdivision of the total weight into light and manageable segments. When the arch span is not very large, smaller than 150m, the box section, mono or multicellular, can change from two boxes to "U" sections, as in the Seniers-sur-ain bridge, or to two simple solid rectangular sections (Fig.3.10) (Manterola, 2006).

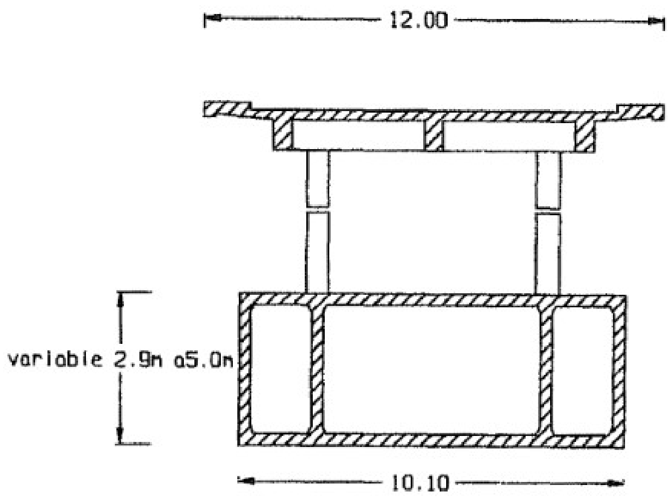

PUENTE DE SANDO L=264.0M (1943)

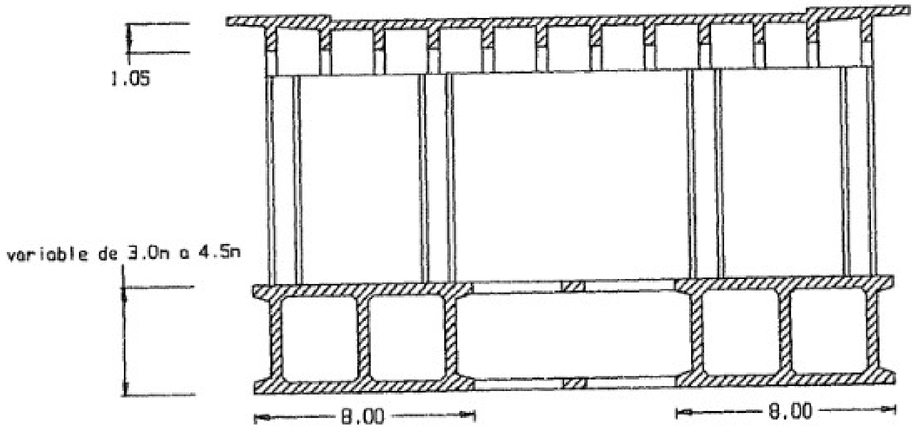

PUENTE ARRABIDA L=270.0M (1963)

Figure 3.10: Examples of arch typical configurations

Regarding the deck, it rests on the arch, through the pillars, and accompanies it in its formation. When this occurs, the arch and deck are re-aligned with the effect of non-symmetrical loads in the longitudinal direction, but the amount of the contribution of each of them to this distribution depends on the respective stiffness. The greater the span of the bridge, the inertia of the arch predominates, therefore it receives practically all the effect of the non-symmetric loads and the deck receives the effect of the direct loads and the bending corresponding to the differential sittings that occur between its supports, due to the rise of the arch. Its shape will depend on the construction process used for the girder, depending on whether it is construction "in situ" on falsework, or if a self-supporting and self-launching falsework is used, or if the type of support bridges is used (Manterola, 2006).

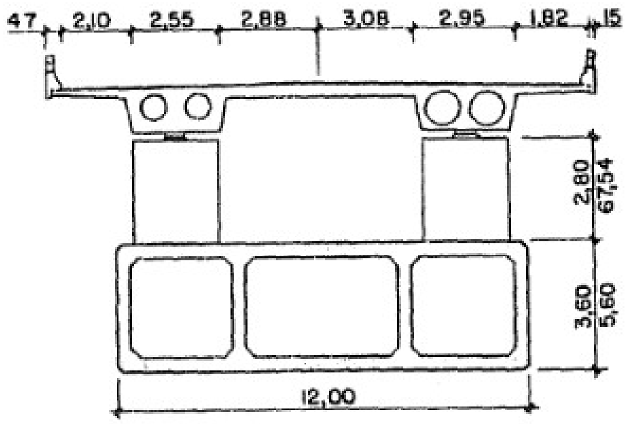

PUENTE BROUKLAUS L = 270.0 M (1985)

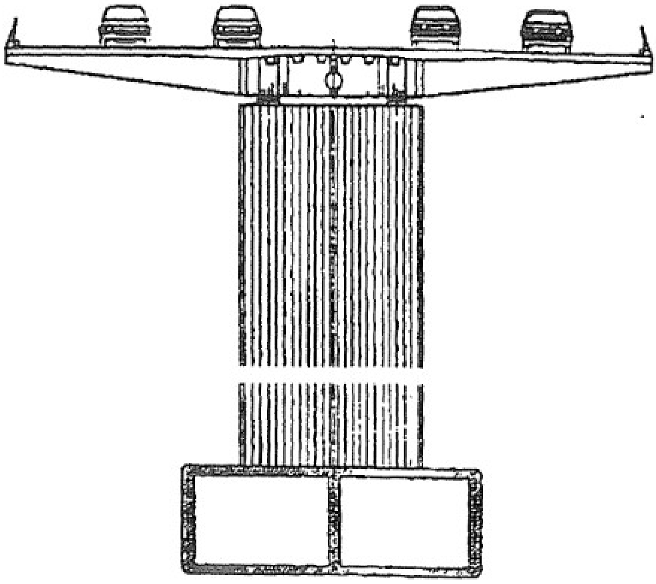

PUENTE DE LA REGENTA L= 194.0 M (1995)

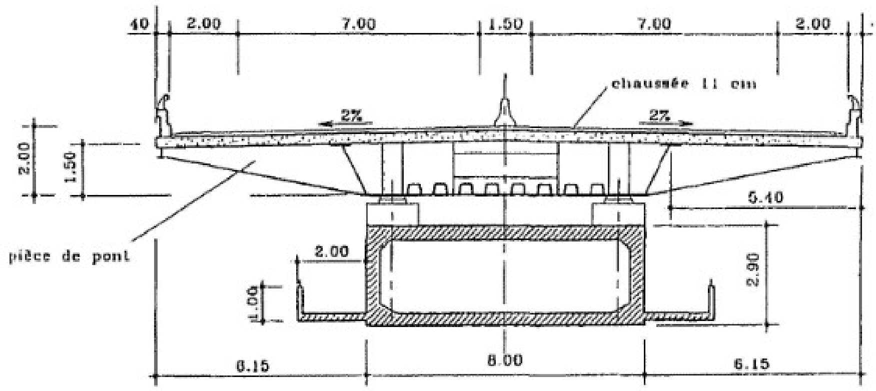

PUENTE SOBRE LA ROCHE BERNARD L = 200.0M (1996)

Figure 3.11: Examples of girder section types

With respect to the arch-deck relationship, it occurs by means of vertical pillars. Their separation is, at least, the division of the arch into 8 equal parts, with 10 or 12 parts being more frequent, or the odd parts in between, which occur when a pillar is not arranged in the arch key. Regarding the connections of the columns with the arch and the deck, several procedures can be established. The continuous girder floats on the pillars, supported by means of sliding supports. In this case the pillars are always embedded in the arch and a joint is arranged in the deck, on the end pillar of the arch (Fig.3.12(a)).

However, this arrangement, although it is common, is not very good. On one side, it has the advantage that the arch sittings, differential ones in the girder, are eliminated by the arrangement of the joint. But, on the other hand, it has the disadvantage that the transverse wind over the girder does not move to the abutment of the deck, which produces, on many occasions, the need to make special pillars at the end of the arch to transmit the wind forces acting on the girder. Secondly, the deck is formed by openings supported on the pillars. In this case, the girder does not transmit the loads to the arch through the columns. The pillars are embedded in the arch and have two supports for each of the girder spans that are supported on them. Thirdly, the pillars are embedded in the arch and deck, except for those close to the keystone, which are very short in length, and which can undergo significant bending due to different temperature deformations, creep and shrinkage in the arch and deck and due to twists overload. In these cases, the short columns must be converted into connecting rods or provided with sliding supports (Fig.3.12(b1)). When the arch and the deck are embedded in crown, the deformability of the deck is equal to the one of the arches forming an all one. The deck can be easily expanded or shortened as the high pillars at the ends, due to their great flexibility, hardly constrain a deformation that grows from the crown of the arch (Fig.3.12(b2)). From an aesthetic point of view, the relative position of the arch and the girder in crown has a significant importance. Menn recommended that, when the arch and deck have the same width, the axis of the arch should coincide with the bottom of the girder (Fig.3.12(b3)).

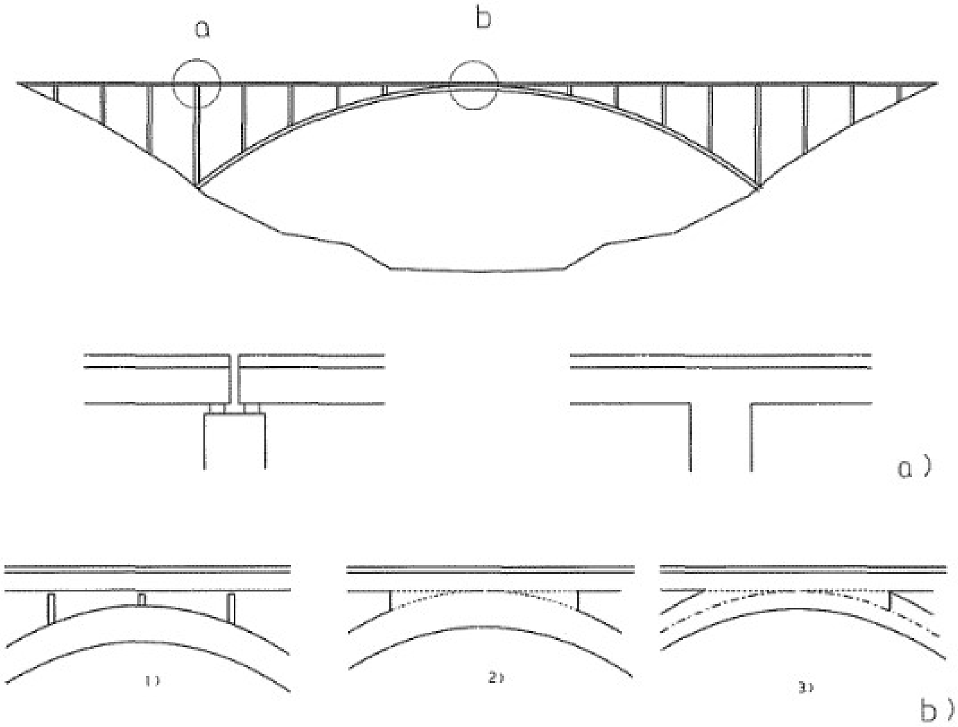

Figure 3.12: Arch-deck relationship

4 DATABASE ASSEMBLY

The realization of the database for this work has been inspired by the research on concrete arch bridges performed by Salonga and Gauvreau, where a comparative study of 55 worldwide bridges, built during the 20th century, is presented (Salonga & Gauvreau, 2014).

The present dataset is constituted by geometrical and mechanical information of 58 Spanish concrete arch bridges, of which 38 roadways and 20 railways. These data together with the ones collected by Salonga and Gauvreau are employed to investigate the correlation between parameters with the goal of defining a reliable source for carrying a preliminary sizing of such bridges, topic that will be developed in the following chapters of this work (Salonga & Gauvreau, 2014).

Bridge designers are often inspired by existing structures to carry a first structural and geometrical definition of a new bridge; therefore, a comprehensive collection of existing structures maybe very useful from the designer perspective. This efficient process is based on the satisfaction of a given set of requirements, such as some empirical trends of flatness, arch depth and girder depth, bending stiffness, slenderness and shallowness of completed bridges that satisfy similar requirements, needed for the realization of an exhaustive dataset which can be used as a starting point for de pre-design process. These trends can be used for evaluating the feasibility of concrete arch bridges, initial proportioning, and validation. In addition, it has to be underlined that the previously mentioned ratios do not provide any implication of deviating from the recommended values, providing a logical basis for the definition of representative ones and the implications in switching from them. For example, designers rely on span-to-depth ratios recommended by standard texts such as Menn and Leonhardt or other sources to size the structural members in a preliminary design stage due to their considerable importance in the primary dimensions often chosen on this basis only (Menn, 1990) (Leonhardt, 1979).

The sample bridges are concrete deck arches with three-hinged, two-hinged and fixed supports in Spain, widely used in modern and ancient engineering permitting to transfer loads from the superstructure to the foundations with low structural weight; moreover, if properly shaped, they become an optimal solution to cross large spans and transfer high loads.

4.1 Database assembly

As a starting point, the primary objectives of this study are:

- characterize the state of art of the concrete deck arch bridges by compiling an inclusive database;
- identify and describe the most relevant geometrical trends among the set of bridges taken into consideration.

In this chapter of the thesis, the construction and assembly of the database used to perform the analysis on deck arch bridges in Spain has been treated. The main scope of the database is to be a source of documented information that could be used for quantitative analysis in the predesign process, providing engineers actual values of structural characteristics taken from individual bridges within a representative sample set. The dataset assembled for this work is based on the description of each structure from both the qualitative and quantitative points of view. The collected information concerns the geometry of the bridge in its entirety, as well as each of its single component: deck, arch, and columns. The data collected have to be reliable, so a deep research based on the knowledge of previously completed works have been conducted. This description, together with the selected empirical trends among the system parameters, can be used for the preliminary assessment of a certain design concept as a guide for the designers, aspect that will be more deeply analyzed in the following chapters.

The database has been assembled by selecting roadway and railway bridges consisting of a concrete arch supporting the deck from below, allowing the selection of a suitable number of structures to perform as much as possible an exhaustive source of documented information to enable a quantitative analysis. All these bridges are located in Spain. Concrete arch footbridges and aqueducts are out of the scope of this thesis. Moreover, it was necessary to ensure that, for every bridge in the database, numerical values could be defined for the set of geometrical properties selected in this work. For these reasons, an extensive research on the web (*Structurae*), in several books (e.g. *Puentes de fabrica y Hormigon armado* (1930) y Eugenio Ribera), conference proceedings and journals as *Hormigón y Acero* and *Revista de Obras Publicas* (Ribera, 1930),.

The criteria used to skim all the arch bridges were:

- Location: Spain
- Material: reinforced concrete for arch and girder
- Position of the deck: below the arch
- Traffic type: roadway and railway

To start populating the dataset, a deep and long research on the website *Structurae* has been conducted to individuate the bridges satisfying the previously mentioned criteria. This research leads at a starting database of 100 bridges. After filtering, only the structures with relevant information have been selected for the final database presented in this work. Specifically, the following information have been considered mandatory: complete geometrical definition (elevation and main cross-sections), materials, typology of arch and girder. Therefore, 58 structures (38 roadways and 20 railways) have been finally considered in this study. The found sources cannot be considered fully exhaustive, but in any case, it is expected that this set of structures will provide a reasonably suitable overview of the state of the art of concrete deck arch bridge design (Salonga & Gauvreau, 2014). In the following chapters will be explained all the empirical trends arising from the database with rational considerations and the chosen preliminary design procedure.

4.2 Database contents

All the bridges satisfying the criteria mentioned above have been included into the database. In the Fig.4.1, Fig.4.2 and Fig.4.3 illustrate the elevations and the representative cross-sections of roadway and railway bridges. For reader's convenience, all the drawings have been drawn to the same scale. All the structures reported are identified by name and ID numbers assigned in increasing order of span length and divided by traffic type. All the cross-sections of the representative sections reported are composed by the girder, a spandrel column, and the arch. For columns with a thickness equal or greater than 1.5m, if not specified differently, they are assumed to be hollow with a wall thickness of 0.3m (Salonga & Gauvreau, 2014).

For the arch cross-sections the reported dimensions are: the one at crown and the one at the springing lines in case of non-uniformity. Tab.4.1 and Tab.4.2 report, for all the collected bridges, the year of completion, the region of Spain in which the structure is placed, the span, the rise, the number of interior spans, the number of hinges, the traffic type (roadway or railway) and all the data obtained from the references. In addition, the Tables include the computed section properties for the girder, the arch, and the columns.

Then, descriptive and topographic information are reported (Tab.4.1 and Tab.4.2) specifying the designer, the construction company, and the region of Spain where the structure is placed. After this first general overview, more technical data have been included:

- span length and rise, which are generally the first two dimensions to be determined in the design process;
- construction method, which for deck arch bridges has been identified to be of the type: centering, effective truss cantilever, cable-stayed, blondin, rotation or temporary diagonals;
- number of interior spans in the main central arch, identified by the number of spandrel column present;
- number of hinges present at the springing lines and/or in crown if any, identifying a three-hinged arch, a two-hinged arch or a fixed-arch;
- the traffic type, roadway or railway.

This primary discretization allowed to find 42 roadway deck arch bridges and 20 railway ones as suitable structures, with respect to the 100 initially selected.

Then, a more detailed analysis based on the three typical sections of girder, arch and column have been performed. Typical sections include a transversal cross section through the girder, a transversal cross section through the arch and an elevation of a typical spandrel column. In particular, for each one of them, have been reported:

- the type of section: slab, n-cell box, T or rectangular;
- the characteristic compressive strength of the material;
- the number of arches and spandrel columns making up the bridge;
- the geometry in terms of width, depth, cantilever part for the girder, resisting area and span length for the spandrel columns;
- the inertia both in X and Y directions.

In compiling the information, some other assumptions have been used:

- for variable depth girders and arches, all the values reported into the references and not an average one for calculating the section properties have been considered;
- for the continuity of the girder, it has been taken into consideration if it spans between spandrel columns in a continuous way or as a simply supported beam;
- regarding the material characteristic compressive strength, for older bridges, a conversion table taken from the *Puentes de fabrica y Hormigon armado* (Ribera, 1930) by Eugenio Ribera has been consulted.

Next Tab.4.1, Tab.4.2 present the geometrical data gathered for, respectively, roadway and railway bridges. While Tab.4.3 and Tab.4.4 illustrate the system parameters for, respectively, roadway and railway bridges.

Bridges that do not satisfied the scope was excluded from the dataset based on any subjective criterion, yielding to a final set of 38 deck arch concrete roadway bridges and 20 railways.

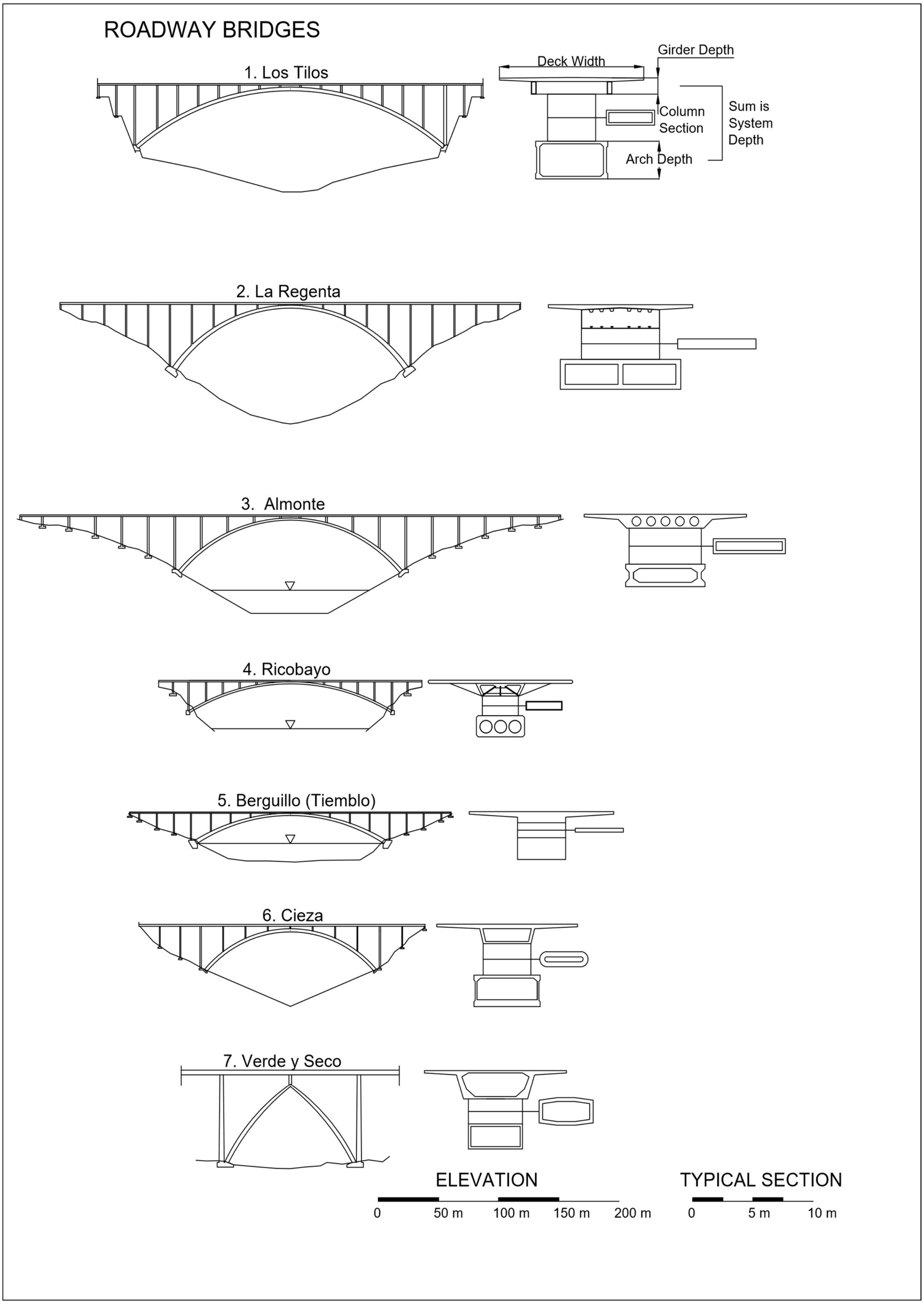

Figure 4.1: Elevation and cross section of roadway concrete arch bridges collected in the database (1)

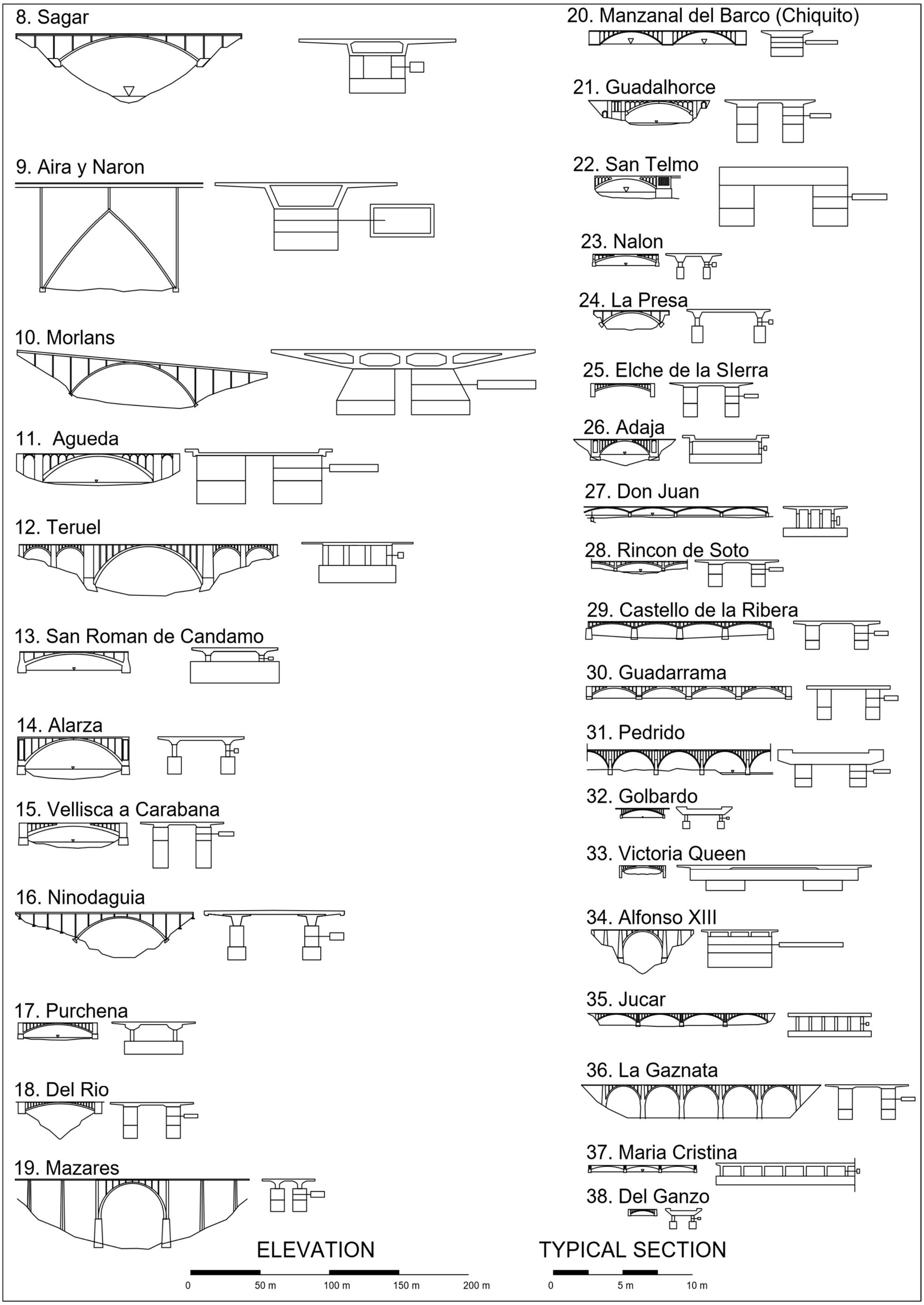

Figure 4.2: Elevation and cross section of roadway concrete arch bridges collected in the database (2)

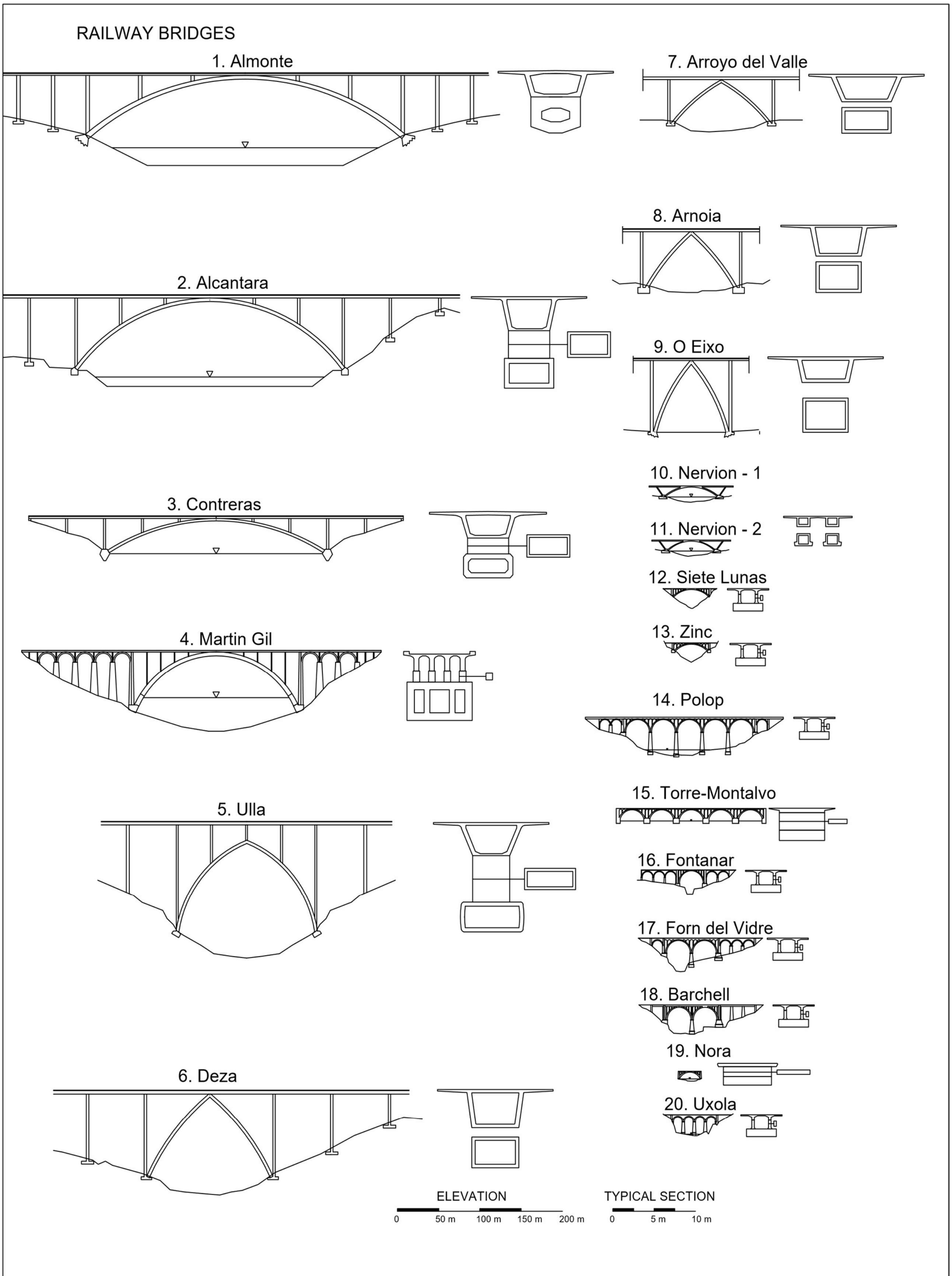

Figure 4.3: Elevation and cross section of railway concrete arch bridges collected in the database

ROADWAY BRIDGES																								
Bridges									**Girder Section**						**Arch Section**								**Column Section**	
ID	**Name**	**Year**	**Reg.**	**Span**	**Rise**	**Const. Met.**	**N. int sp.**	**N. hin.**	**Type**	**Width**	**Depth**	**Area**	**Inertia**	**Cont**	**Type**	**Width**	**Depth Spring**	**Depth Crown**	**Area Spring**	**Area Crown**	**Inertia Spring**	**Inertia Crown**	**Area**	**Inertia**
				[m]	**[m]**					**[m]**	**[m]**	**[m²]**	**[m⁴]**			**[m]**	**[m]**	**[m]**	**[m²]**	**[m²]**	**[m⁴]**	**[m⁴]**	**[m²]**	**[m⁴]**
1	Los Tilos	2004	I.C.	255,0	46,2	d	15	0	c	12,0	1,32	3,2+s	?	yes	1□	6,0	3,00	3,00	3,91	3,91	5,750	5,750	1,92	0,420
2	La Regenta	1996	Ast.	194,0	50,4	d	11	0	2□ c	12,0	1,65	3,9+s	?	no	2□	10,0	4,20	2,40	12,08	9,92	33,510	8,520	6,50	0,28; 0,54
3	Almonte	2005	Ext.	184,0	42,0	d	8	0	s	13,5	1,10	9,80	1,01	no	1□	6,0	3,00	1,80	6,71	5,87	9,400	2,650	4,80	0,26; 0,71; 1,23
4	Ricobayo	1999	C&L	168,0	23,0	d	12	0	c	12,0	1,25	6,89	0,84	yes	—	4,0	1,70	1,70	4,37	4,37	1,450	1,450	0,40	0,034; 0,091
5	Berguillo (Tiemblo)	1999	C&L	165,0	22,0	c.s.	10	0	s	12,0	0,90	6,17	0,39	yes	—	4,0	3,10	1,75	12,40	7,00	9,930	1,780	3,60	0,24; 0,009
6	Cieza	2004	Can.	141,0	32,0	d	8	0	1□	11,7	1,55	4,80	1,2	no	1□	5,5	2,52	2,52	5,02	5,02	4,720	4,720	3,30	0,055; 0,49
7	Verde y Seco	2009	And.	106,5	62,0	r	2	3	1□	11,8	2,3; 3,8	6,07; 7,08	4,57; 15,04	yes	1-2□	5,5	3,00	2,00	4,16	2,44	5,980	1,600	3,46	2,240
8	Sagar	2000	P.V.	100,0	17,0	ce	8	0	1□	11,3	1,15	4,08	0,6	no	—	4,0	1,50	1,00	6,00	4,00	1,120	0,330	1,40	0,02; 0,056
9	Aira y Naròn	2001	G.	95,0	55,0	ce	2	0	1□	13,1	1,83; 3,08	5,37; 7,5	2,27; 10,92	no	—	4,0	1,25	1,25	5,00	5,00	0,320	0,320	3,65	3,150
10	Morlans	1999	P.V.	90,0	25,0	ce	6	0	4□	19,0	1,32	11,13	2,01	yes	—	7,8	1,00	1,00	8,40	7,20	0,700	0,600	5,04	0,152
11	Agueda	1952	C&L	80,0	16,0	r	8	3	s	10,6	0,20	2,37	0,028	yes	—	7,0	2,60	1,60	18,20	11,20	10,260	2,400	3,50	0,072
12	Teruel (F. Huè)	1929	Ar.	79,0	26,5	ce	16	0	s	8,0	0,20	1,30	0,0042	yes	—	6,0	2,40	1,20	15,52	6,65	7,460	0,800	0,64	0,008
13	San Roman de Candamo	1924	Ast.	72,0	8,0	ce	8	0	T	6,2	0,75	2,00	0,071	yes	—	6,4	1,66	1,50	5,98	3,38	2,440	1,800	0,09	0,001
14	Alarza (Desaparecido)	1929	Ext.	70,0	17,0	ce	10	0	T	6,2	0,75	2,00	0,071	yes	—	2,0	2,00	1,20	4,00	2,40	1,340	0,280	0,18	0,001
15	Vellisca a Carabaña	1928	Ext.	66,0	6,6	t	16	0	s	6,0	0,36	1,38	0,013	yes	—	2,2	2,50	1,90	5,50	4,18	2,860	1,260	0,66	0,005
16	Niñodaguía	1989	G.	65,2	15,7	ce	7	0	s	10,3	1,10	4,06	0,26	yes	—	2,6	1,40	0,90	3,64	2,34	0,600	0,160	1,00	0,010
17	Purchena	1929	And.	50,0	6,3	ce	20	0	s	6,0	0,36	1,38	0,013	yes	—	4,2	0,96	0,90	4,03	3,78	0,310	0,260	0,13	0,001
18	Del Rio	1930	I.C.	50,0	5,0	t	18	0	s	6,0	0,18	1,27	0,0078	yes	—	2,0	1,00	1,00	2,40	1,80	0,280	0,122	0,50	0,003
19	Mazares	1935	C&L	47,0	25,0	b	10	0	s	3,8	0,66	0,91	0,029	yes	—	2,0	1,88	0,80	3,76	1,60	0,550	0,043	0,80	0,011

20	Manzanal del B. (Chiquito)	1928	C&L	45,0	9,0	b	8	0	s	3,6	0,80	2,26	0,12	yes	—	2,3	0,70	0,60	1,61	1,38	0,066	0,041	0,58	0,003
21	Guadalhorce	1936	And.	45,0	6,8	ce	10	0	T	6,5	0,50	2,21	0,44	yes	—	3,0	1,50	1,25	4,50	3,75	0,420	0,240	1,20	0,014
22	San Telmo	1931	And.	44,0	6,9	t	10	0	s	15,0	1,20	18,90	2,5	yes	—	5,0	1,26	1,26	6,30	6,30	0,420	0,420	2,00	0,026
23	Nalòn	1932	Ast.	44,0	4,4	ce	10	0	s	4,2	0,80	1,21	0,032	yes	—	1,0	1,30	0,80	0,65	0,40	0,092	0,021	0,09	0,009
24	La Presa	1916	P.V.	41,5	7,9	ce	6	0	T	6,0	0,60	1,56	0,031	yes	—	1,6	1,60	1,15	2,56	1,84	0,540	0,200	0,18	0,001
25	Elche de la Sierra	1927	C.M.	40,0	4,0	ce	14	0	s	6,0	0,29	1,21	0,0071	yes	—	2,0	1,08	0,94	2,16	1,88	0,100	0,069	0,50	0,026
26	Adaja	1924	C&L	36,0	9,0	ce	12	0	s	6,2	0,50	1,23	0,022	yes	—	5,1	0,95	0,60	4,85	3,06	0,360	0,092	0,12	0,001
27	Valencia de Don Juan	1910	V.	33,0	3,3	ce	16	0	s	6,5	0,20	1,10	0,017	yes	—	4,6	0,70	0,60	3,22	2,76	0,130	0,083	0,80	0,032
28	Rincon de Soto	1922	LaR.	32,8	3,3	t	10	0	s	6,0	0,18	1,27	0,0078	yes	—	2,0	1,00	0,85	2,00	1,70	0,166	0,102	0,50	0,003
29	Castellò de la Ribera	1930	V.	32,0	11,0	ce	10	0	s	6,2	0,36	1,38	0,0087	yes	—	2,0	0,82	0,62	1,64	1,24	0,046	0,019	0,60	0,002
30	Guadarrama	1936	C.M.	32,0	5,0	ce	8	0	s	6,0	0,25	1,50	0,0078	yes	—	2,0	1,05	0,85	2,10	1,70	0,096	0,051	0,64	0,003
31	Pedrido	1942	G.	31,0	12,4	ce	12	0	s	7,6	0,80	6,28	0,4	yes	—	2,4	0,60	0,60	1,44	1,44	0,022	0,022	0,60	0,002
32	Golbardo	1903	Can.	30,0	4,0	ce	20	0	s	4,0	0,40	1,60	0,032	yes	—	1,0	0,50	0,50	0,50	0,50	0,005	0,005	0,06	0,0001
33	Victoria Queen	1909	M.	30,0	3,0	ce	14	0	s	14,0	0,18	3,15	0,02	yes	—	5,6	0,90	0,70	5,04	3,92	0,340	0,160	4,20	0,032
34	Alfonso XIII	1909	I.C.	30,0	15,0	t	8	0	T	5,5	0,30	1,03	0,012	yes	—	4,6	1,50	1,00	6,90	4,60	1,290	0,380	1,38	0,010
35	Jucar	1917	V.	30,0	5,0	ce	15	0	s	6,0	0,25	1,50	0,0078	yes	—	6,0	1,00	0,40	6,00	2,40	0,500	0,032	0,24	0,001
36	La Gaznata	1915	C&L	25,0	12,5	t	14	0	s	6,0	0,30	1,27	0,0078	yes	—	2,0	1,00	1,00	1,40	1,40	0,056	0,056	0,50	0,003
37	Marìa Cristina	1982	P.V.	24,0	2,2	ce	0	0	T	20,0	0,20	5,11	0,064	yes	—	20,0	0,70	0,60	14,00	12,0	0,570	0,360	2,60	0,034
38	Del Ganzo	1903	Can.	17,4	2,3	t	12	0	s	2,6	0,34	0,79	0,012	yes	—	1,0	0,50	0,50	0,50	0,50	0,104	0,104	0,06	0,0001

I.C. Islas Canarias
Ast. Principado de Asturias
Ext. Extremadura
C&L Castilla y Leon
Can. Cantabria
And. Andalucia
P.V. Pais Vascos
G. Galicia
Ar. Aragon
C.M. Castilla y La Manca
V. Comunidad Valenciana
LaR. La Rioja
M. Madrid

ce centering
t cantilever using effective truss
r rotation
b blondin
c.s. cable-stayed
d temporary diagonals

— Rectangular section
n□ n-cell box section
T Tee section or similar
s Slab section
c Composite section

Table 4.1: Geometrical data recorded for roadway bridges considered in the present research

RAILWAY BRIDGES																								
Bridges									Girder Section						Arch Section								Column Section	
ID	Name	Year	Reg.	Span	Rise	Const. Met.	N. int sp.	N. hin.	Type	Width	Depth	Area	Inertia	Cont.	Type	Width	Depth Spring.	Depth Crown	Area Spring.	Area Crown	Inertia Spring.	Inertia Crown	Area	Inertia
				[m]	[m]					[m]	[m]	[m²]	[m⁴]			[m]	[m]	[m]	[m²]	[m²]	[m⁴]	[m⁴]	[m²]	[m⁴]
1	Almonte	2016	Ext.	384,0	69,2	c.s.	8	0	1□	14,0	3,10	10,34	13,44	no	—+1□	6,00	6,30	4,20	116,40	17,31	368,05	24,880	7,41	21,14; 13,92
2	Alcantara	2019	Ext.	324,0	80,7	c.s.	6	0	1□	14,0	4,00	9,31	19,95	no	1□	6,00	4,00	3,50	17,76	9,96	44,24	16,570	3,85	5,190
3	Contreras	2009	V.	261,0	36,9	c.s.	6	0	1□	14,2	3,00	9,96	11,3	no	1□	6,00	3,40	2,80	34,04	9,11	38,42	9,050	3,12	4,170
4	Martìn Gil	1942	C&L	192,4	60,0	b	12	0	T	8,7	1,98	6,80	2,78	yes	3□	8,50	5,50	4,50	35,55	22,87	115,92	52,280	3,26	0
5	Ulla	2011	G.	168,0	05,0	c.s.	6	0	1□	14,0	3,89	9,36	18,39	no	1□	7,70	3,50	3,50	9,88	9,88	18,04	18,040	5,60	5,400
6	Deza	2010	G.	150,0	96,0	r	2	3	1□	14,0	4,50	11,09	32,37	no	1□	5,70	3,60	3,60	6,80	6,80	13,20	13,200	/	/
7	Arroyo del Valle	2006	M.	120,0	50,4	r	2	3	1□	14; 17,6	3,2; 5	9,06; 16,88	13,14; 60,37	no	1□	6,00	3,00	3,00	6,56	6,56	8,88	8,880	/	/
8	Arnoia	2013	G.	110,0	66,4	r	2	3	1□	14,0	3,65	9,10	16,9	no	1□	5,50	3,60	3,60	6,64	6,64	12,79	12,790	/	/
9	O Eixo	2008	G.	88,0	82,0	r	2	0	1□	14,0	3; 4,5	9,5; 11,09	12,19; 32,37	no	1□	5,50	4,00	4,00	6,16	6,16	14,96	14,960	/	/
10	Nervìon: 1	2002	P.V.	63,0	11,0	r	2	3	s	8,3	1,20	3,08	0,56	yes	2□	3,20	1,40	1,40	2,56	2,56	0,32	0,320	/	/
11	Nervìon: 2	2002	P.V.	56,5	11,0	r	2	3	s	8,3	1,20	3,08	0,56	yes	2□	3,20	1,40	1,40	2,56	2,56	0,32	0,320	/	/
12	Siete Lunas	1929	V.	44,0	8,8	t	10	0	T	5,0	0,35	1,20	0,032	yes	—	3,60	1,40	0,80	5,04	2,88	0,82	0,220	0,36	0
13	Zinc	1929	V.	40,0	8,0	t	8	0	T	5,0	0,35	1,20	0,032	yes	—	3,60	1,40	0,80	5,04	2,88	0,82	0,220	0,36	0
14	Polop	1929	V.	30,0	15,0	c	6	0	T	5,0	0,35	1,20	0,032	yes	—	3,60	1,40	0,80	5,04	2,88	0,82	0,220	0,36	0
15	Torre-Montalvo	1926	P.V.	30,0	10,4	c	6	0	s	9,5	0,50	3,17	0,069	yes	—	7,00	1,80	1,20	12,60	8,40	3,40	1,000	3,50	0,073
16	Fontanar	1929	V.	30,0	15,0	c	8	0	T	5,0	0,35	1,20	0,032	yes	—	3,60	1,40	0,80	5,04	2,88	0,82	0,220	0,36	0
17	Forn del Vidre	1929	V.	30,0	15,0	c	6	0	T	5,0	0,35	1,20	0,032	yes	—	3,60	1,40	0,80	5,04	2,88	0,82	0,220	0,36	0

18	Barchell	1929	V.	30,0	15,0	c	8	0	T	5,0	0,35	1,20	0,032	yes	—	3,60	1,40	0,80	5,04	2,88	0,82	0,220	0,36	0
19	Nora	1924	Ast.	25,0	6,2	c	6	0	s	7,0	0,30	3,36	0,044	yes	—	7,00	1,85	1,00	12,95	7,00	1,60	0,580	3,50	0,073
20	Uxola	1929	V.	12,0	6,0	c	0	0	T	5,0	0,35	1,20	0,032	yes	—	3,60	1,40	0,80	5,04	2,88	0,82	0,220	/	0

I.C. Islas Canarias
Ast. Principado de Asturias
Ext. Extremadura
C&L Castilla y Leon
Can. Cantabria
And. Andalucia
P.V. Pais Vascos
G. Galicia
Ar. Aragon
C.M. Castilla y La Manca
V. Comunidad Valenciana
LaR. La Rioja
M. Madrid

ce centering
t cantilever using effective truss
r rotation
b blondin
c.s. cable-stayed
d temporary diagonals

— Rectangular section
n□ n-cell box section
T Tee section or similar
s Slab section
c Composite section

Table 4.2: Geometrical data recorded for railway bridges considered in the present research

ROADWAY BRIDGES													
ID	**Name**	**Year**	**Span/Rise**	**System Depth**	**Radius of Gyration**	**Span/Arch Depth**	**Span/System Depth**	**Slenderness Ratio**	**Shallowness Ratio**	**I_{arch}/I_{sys}**	**t_{eff}**	**d_{eff}**
			[-]	[m]	[m]	[-]	[-]	[-]	[10^{-3}]	[%]	[m]	[m]
1	Fadón et al. 2003	2004	5,52	4,32	1,21	85,00	59,03	79,88	13,12	?	0,59	1,79
2	Pantaleón et al 2008	1996	3,85	4,95	1,38	58,79	39,19	57,53	13,72	?	1,83	2,76
3	Siegrist Ridruejo 2006	2005	4,38	3,50	1,06	76,67	52,57	69,03	12,59	86	1,55	1,84
4	Pérez-Fadón and Herrero 1999	1999	7,30	2,95	0,72	98,82	56,95	85,23	15,74	63	0,41	1,32
5	Corres Peiretti et al. 2001	1999	7,50	3,33	0,80	68,04	49,62	75,34	18,24	94	1,51	1,84
6	Calvo Rodríguez et al. 2005	2004	4,41	4,07	1,09	55,95	34,64	51,45	16,97	80	1,18	1,82
7	Pozo Vindel et al. 2005	2009	1,72	5,55	2,03	42,60	19,19	26,37	16,37	28	1,21	2,40
8	Calvo Rodríguez et al. 2001	2000	5,88	2,40	0,51	80,00	41,67	73,11	15,14	55	0,92	1,12
9	Pozo Vindel et al. 2002	2001	1,73	3,71	1,18	76,00	25,64	40,72	10,69	5	1,28	1,85
10	Arenas de Pablo 1999	1999	3,60	2,32	0,58	90,00	38,79	64,43	11,68	24	1,33	1,19
11	Casado 1952	1952	5,00	2,30	0,66	38,10	34,78	46,98	20,55	100	2,05	1,93
12	Hué 1931	1929	2,98	2,00	0,61	43,89	39,50	57,83	11,52	100	2,16	1,84
13	Ribera 1930	1924	9,00	2,33	0,47	45,57	30,90	55,90	29,10	97	2,01	1,62
14	Ribera 1930	1929	4,12	2,35	0,52	43,75	29,79	53,72	15,43	92	0,96	1,19
15	Ribera 1930	1928	10,00	2,56	0,65	30,00	25,78	36,23	49,58	99	1,15	1,61
16	Arenas et al. 1990	1989	4,15	2,25	0,46	56,70	28,98	56,63	14,73	59	0,82	0,91
17	López Rodríguez 1930	1929	7,94	1,29	0,28	53,76	38,76	66,01	21,92	96	0,94	0,84
18	Pérez Fadón et al. 2005	1930	10,00	1,18	0,32	50,00	42,37	56,97	31,53	96	0,65	0,75
19	Díaz Burgos 1942	1935	1,88	2,00	0,35	35,07	23,50	110,10	0,00	91	1,92	1,01
20	Ribera 1930	1928	5,00	1,45	0,34	69,23	31,03	51,02	18,93	31	1,23	0,83
21	Villalba Granda 1936	1936	6,67	1,88	0,43	32,73	24,00	38,60	32,00	43	1,15	1,12
22	Ribera 1922	1931	6,38	2,46	0,68	34,92	17,89	24,08	49,33	14	1,82	1,33
23	Ovies 1934	1932	10,00	1,85	0,29	41,90	23,78	54,45	32,99	64	0,56	0,63
24	Peña Boeuf 1916	1916	5,24	1,98	0,43	30,18	21,01	37,24	26,95	92	0,68	0,93
25	Tanner and Bellod 2005	1927	10,00	1,30	0,21	39,60	30,77	67,48	26,62	92	0,61	0,57
26	Villalba 1924	1924	4,00	1,28	0,25	46,45	28,24	51,23	13,92	91	0,97	0,78

27	Ribera 1910	1910	10,00	0,85	0,20	50,77	38,82	58,33	30,79	86	0,75	0,61
28	Pozo Vindel et al. 2005	1922	10,00	1,11	0,28	35,46	29,68	42,56	42,20	94	0,57	0,66
29	Millanes Mato and Matute Rubio 1994	1930	2,91	1,08	0,17	44,44	29,63	85,42	7,69	79	0,70	0,43
30	Del Pino 1936	1936	6,40	1,20	0,21	33,68	26,67	57,60	20,69	90	0,66	0,55
31	Villalba Granda 1944	1942	2,50	1,40	0,54	51,67	22,14	27,72	21,83	5	1,29	0,87
32	Ribera 1903	1903	7,50	0,90	0,27	60,00	33,33	40,29	34,10	14	0,55	0,48
33	Ribera 1910	1909	10,00	0,98	0,25	37,50	30,61	67,73	0,00	93	0,78	0,61
34	Fernández Arroyo 1909	1909	2,00	1,55	0,38	24,00	19,35	42,97	12,79	99	2,39	1,23
35	Monfort 1917	1917	6,00	0,95	0,26	42,86	31,58	44,11	25,53	97	1,05	0,82
36	Ribera 1930	1915	2,00	1,30	0,21	25,00	19,23	64,38	8,54	88	0,89	0,50
37	Ribera 1904	1982	11,01	0,85	0,20	36,92	28,24	42,55	46,27	88	0,93	0,68
38	Gomendio 1903	1903	7,57	0,84	0,48	34,80	20,71	13,22	104,71	90	0,52	0,81

Table 4.3: System parameters of both roadway bridges collected in the present research based on geometrical data

RAILWAY BRIDGES													
ID	Name	Year	Span/Rise	System Depth	Radius of Gyration	Span/Arch Depth	Span/System Depth	Slenderness Ratio	Shallowness Ratio	I_{arch}/I_{sys}	t_{eff}	d_{eff}
			[-]	[m]	[m]	[-]	[-]	[-]	[10^{-3}]	[%]	[m]	[m]
1	Mazarracín 2020	2016	5,55	8,35	1,77	73,14	45,99	119,14	12,81	94	6,32	5,65
2	Manterola et al. 2015	2019	4,01	7,75	1,91	86,40	41,81	93,45	11,81	60	2,05	3,51
3	Manterola et al. 2012	2009	7,07	6,10	1,27	84,19	42,79	112,60	17,25	68	2,41	3,09
4	Castellon et al. 1942	1942	3,21	6,98	1,72	38,48	27,56	61,33	14,37	97	5,71	4,93
5	Del Valle Pérez et al. 2010	2011	1,60	7,39	1,92	48,00	22,73	74,21	0,00	50	2,52	3,15
6	De Vera Posada 2010	2010	1,56	8,10	2,59	41,67	18,52	31,86	13,48	29	1,46	3,39
7	Pozo Vindel et al. 2007	2006	2,38	7,10	2,64	40,00	16,90	25,01	26,17	19	1,41	3,26
8	Llombart et al. 2013	2013	1,66	7,25	2,11	30,56	15,17	28,60	15,92	43	1,32	2,94
9	Rodríguez et al. 2008	2008	1,07	7,75	2,46	22,00	11,35	30,36	0,00	40	1,26	3,17
10	Troyano and Muñoz 2004	2002	5,73	2,60	0,59	45,00	24,23	59,08	26,65	36	0,70	1,08
11	Troyano and Muñoz 2004	2002	5,14	2,60	0,59	40,36	21,73	52,98	26,65	36	0,71	1,08
12	Roselló 1924	1929	5,00	1,45	0,37	40,00	30,34	66,25	20,75	94	1,23	1,10
13	Roselló 1924	1929	5,00	1,45	1,16	36,36	27,59	18,99	72,38	94	1,15	1,10
14	Roselló 1924	1929	2,00	1,45	0,37	27,27	20,69	45,17	12,17	94	1,67	1,10
15	De Goytia 1926	1926	2,88	2,00	0,46	20,00	15,00	35,48	22,35	97	2,21	1,42
16	Roselló 1924	1929	2,00	1,45	0,61	27,27	20,69	26,94	20,41	94	1,70	1,10
17	Roselló 1924	1929	2,00	1,45	0,79	27,27	20,69	21,01	26,17	94	1,54	1,10
18	Roselló 1924	1929	2,00	1,45	0,93	27,27	20,69	17,81	30,88	94	1,70	1,10
19	Castellón 1924	1924	4,03	1,73	0,34	17,54	14,49	40,76	27,19	96	2,56	1,25
20	Roselló 1924	1929	2,00	1,45	1,05	10,91	8,28	6,29	87,38	94	1,56	1,10

Table 4.4: System parameters of both railway bridges collected in the present research based on geometrical data

In addition to the collected information, some empirical parameters based on the basic geometrical data are also reported into the database. These quantities, which characterize the bridges in terms of proportion, efficiency and system behavior will be defined and discuss more deeply in the following chapter of this work. Some additional consideration can be done in this section regarding the collected information.

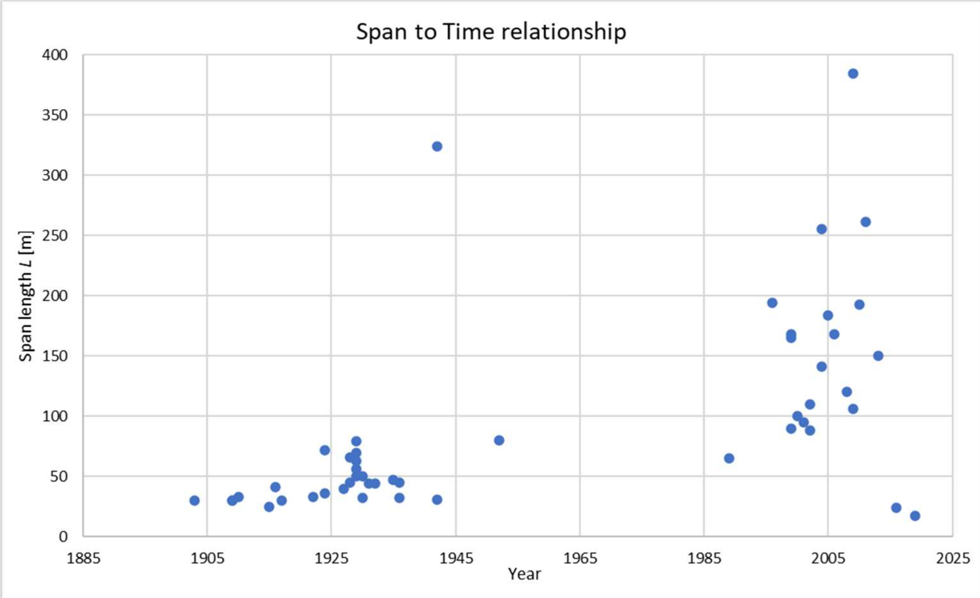

Figure 4.2 – Span length-to-Time relationship of all the bridges collected into the database

The sample bridges used to build the graph are concrete deck arches in Spain, widely used in modern and ancient engineering, as can be seen, permitting to transfer loads from the superstructure to the foundations with low structural weight; moreover, if properly shaped, they become an optimal solution to cross large spans and transfer high loads (Menn, 1990).

In the Fig.4.2, the span of the bridges contained into the database with respect to time have been plotted. During the 19th century, with the advent of the cement industry, for the arch bridges only few works were made of concrete, with spans as much as 36m in Spain (Martínez, 2005). At that time, the biggest problem in building concrete arch bridges were the construction method, in particular setting up the scaffolding (Martínez, 2005). With reinforced concrete arches development, scaffolding became a key issue due to the difficulty of assembly and the resulting costs. To avoid this problem, scaffolding was developed to be embedded in the final structure (Martínez, 2005). Due to these issues, the concrete arch bridge construction was employed mainly just for short spans where the topographic site conditions allowed it. With the passing of time, modern construction method and approaches have been developed, permitting to the construction to reach spans up to 380m. In Spain, the arch having the longest span is Los Tilos in the Canary Island of La Palma, with a span length of 255m.

It seems easy to say that arches with an average span between 125 and 250m will continue to be built considering that the three existing construction methods (cable-stayed, temporary diagonals and rotation) make them very competitive in this span range rather than other types, like suspended bridges or stay cable bridges. Even below this span range, arches will continue to be built for aesthetic reasons, as can be seen in the upper graph. Regarding the long spans, the structural limits of these arches, including the stability, could allow to build spans up to 1000m for single arches and up to 2000m for twin ones. The obstacles in realizing so long spans are the costs and the construction difficulties so that the limited recommended range has been set up to 300-500m resulting in a medium/low frequency solution, using other types of bridges like cable-stay or suspended ones for spans from 1000m up to 3500m.

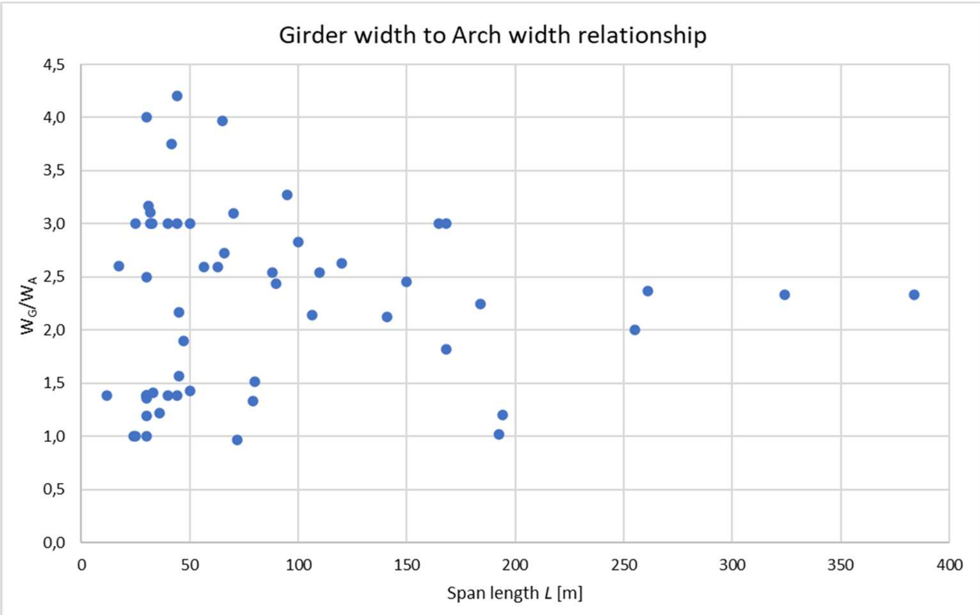

Figure 4.3: Girder/Arch width relation with respect to the span length of all the considered bridges

In this graph has been reported the ratio between the width of the girders W_G and the one of the arches W_A with respect to the span length L. In most of the cases, the designer known before the width of the bridge girder, because the number of lanes or the number of tracks is already known from the infrastructure. Therefore, this relation can help during the pre-design process in deciding the initial value of the arch width, from which also the type of section, if solid or hollow, is dependent as can be seen in Fig.4.4. Then, knowing the arch width as a function of the transversal rigidity of the girder width and of the span length, also the type of arch section can be deduced according to L. Further considerations have been done for the girder section type according to the girder depth and the column span length in the next chapters.

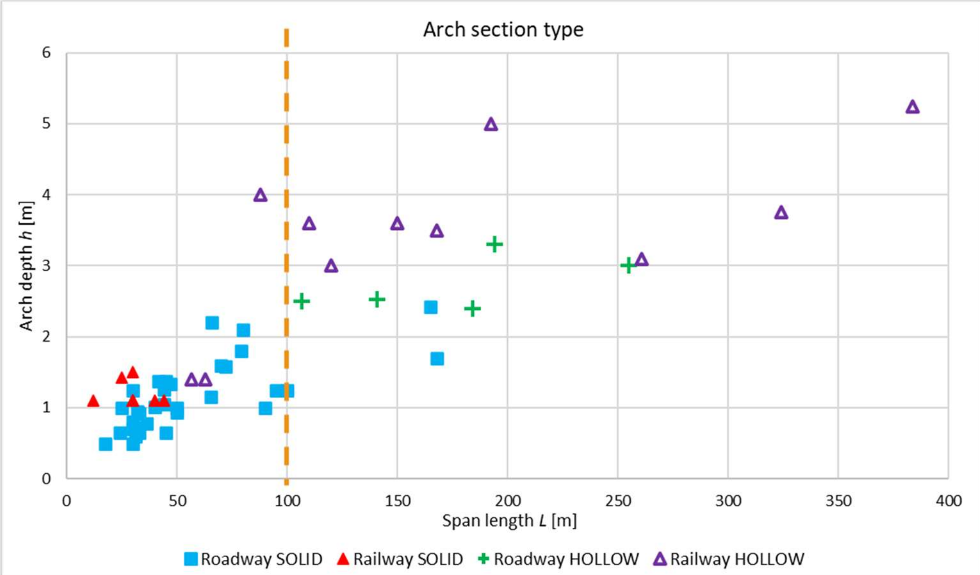

Figure 4.4: Arch section type with respect to the arch depth and span length of the bridges into the Present Research database

References of the Database

Aparicio, Carlos, Ruiz, Etsi, Gutiérrez. (2020). Introducción al viaducto sobre el río Almonte en la línea de alta velocidad ferroviaria Madrid-Extremadura. *Hormigon y Acero*.

Apia XXI. (1999). Puente de Morlans. Retrieved from http://www.arenasing.com/proyectos/puentes-urbanos/puente-de-morlans

Arenas, Alonso, Pantaleon. (1985). La reconstruccion del puente historico de Maria Cristina, de San Sebastian. *Hormigón y Acero*, *157*(591-2–181), 123–131.

Arenas, Alonso, Pantaleon. (1989). Puente sobre el barranco de Ninodaguia (Orense). *Hormigon y Acero*, *171*(591-2–211), 47–51.

Arenas, Miguel, Pereda, Martinez. (2016). Viaducto sobre el rio Almonte en el Embalse de Alcantara para la linea de alta velocidad Madrid-Extremadura. Talayuela-Caceres. *Hormigon y Acero*, 1–10.

Arenas. (1996). *XIII Congreso de la FIP y Expositores.* In *ACHE* (pp. 391–397).

Arenas. (1999). El Puente arco del Valle de Morlans en San Sebsatian. *ACHE*, (I Congredo de Puentes y Estructuras, Sevilla, Noviembre 1999), 1151–1152.

Armisén, Cutillas, Martínez. (2015). Puente sobre el río Tajo en el embalse de alcántara para ferrocarril de alta velocidad. *Revista de Obras Publicas*, *162*(3562), 83–92.

Arroyo. (1909). Viaducto de Alfonso XIII. *Revista de Obras Publicas*, 241–242.

Beneítez, Bajo, Palmero. (1930). Arco Del Rio. *ACHE*, 1–15.

Burgos. (1942). Puente para camino vecinal sobre el embalse de Esla en Manzanal del Barco (Zamora). *Revista de Obras Publicas*, *Tomo I* (2724–04), 182–184.

Camon. (1929). Construccion del puente sobre el Ebro, en Mequinenza (Zaragoza), en la carretera de Maella a Fraga. *Revista de Obras Publicas*, *Tomo I* (2520–01), 85–88.

Casado. (1952). *Carlos Fernandez Casado Vol.1*.

Castellon, Villalba, Salazar, Torroja. (1942). Viaducto Martin Gil. *Revista de Obras Publicas*, *Tomo I* (2730–03), 500–510.

Castellon. (1924). Sostitucion del puente metalico sobre el rio Nora, en el kilometro 143,811 de la linea de Leon a Gijon, por un arco de hormigon en masa. *Revista de Obras Publicas*, *Tomo I* (2398–05), 48–49.

Corres Peiretti, Martin, Caldentey, Herranz. (2001). Puente arco sobre el embalse de El Berguillo (Avila). Diseno y control de la ejecucion. *Hormigon y Acero*, *200*, 3–17.

Del Pino. (1936). Nuevo puente sobre el rio Guadarrama, en el Kilometro 66 de la linea de Madrid a Valencia de Alcantara. *Revista de Obras Publicas*, *Tomo I* (2704–02), 376–380.

Del, Torrealba, Santillana, Ramos, Dorado, & Martìn. (n.d.). Viaductos De Aira y Naròn Autovia Del Noroeste. *ACHE*, *II Congres*, 1–6.

Delgado, Peiretti, Caldentey, Martín, Ruiz Herranz. (2001). Puente arco sobre el embalse de El Burguillo (Ávila): diseño y control de la ejecución. *Hormigon y Acero*, (220), 3–17.

Estructuras. (2006). Ampliacion del puente de rincón de soto, 1–12.

Fhecor. (1999). Bridge over " El Burguillo " reservoir.

Florencio, Vindel. (2006). Viaducto Arroyo del Valle. *ACHE*.

Gomendio. (1903). Pruebas de los puentes de Golbardo y de Ganzo. *Revista de Obras Publicas*, *Tomo I* (119), 475–476.

Goytia. (1926). El nuevo puente de Torre Montalvo. *Revista de Obras Publicas*, 263–266.

Guijarro. (2011). La Alta Velocidad y el cruce del embalse de Contreras. Una obra singular. *Revista de Obras Publicas*, *158*(3522), 21–40.

Hué. (1931). El Viaducto de Teruel. *Revista de Obras Publicas*, 413–417.

Leyda. (1934). Puente de Aragon, sobre el Turia, en Valencia. *Revista de Obras Publicas*, *Tomo I*(2639–02), 66–72.

Los Ingenieros de Caminos. (1922). El puente de San Telmo sobre el Guadalquivir, en Sevilla. *Revista de Obras Publicas*, 25–28.

Los Ingenieros de Caminos. (1997). Viaducto de la Pena sobre la ria del Nervion. *Revista de Obras Publicas*, (3363), 64–65.

Los Ingenieros de Caminos. (2001). Punte Urbano de Morlans en San Sebastian. *Revista de Obras Publicas*, (3410), 82–85.

Manterola, Cutillas, Navarro, Martínez. (2020). Puente arco de ferrocarril sobre el embalse de Contreras en la línea de alta velocidad Madrid-Levante. *Hormigon y Acero*.

Marquina. (1923). Puentes de 72 metros de luz sobre el rio Nalon, en San Roman de Candamo, provincia de Oviedo. *Revista de Obras Publicas*, 209–215.

Marquina. (1924). Puentes de 72 metros de luz sobre el rio Nalon, en San Roman de Candamo, provincia de Asturias. *Revista de Obras Publicas*, 153–157.

Martínez, Herrero. (1999). Proyecto y construccion del Arco de Ricobayo. *Hormigon y Acero*.

Mediterráneo, & Bruna. (2009). Viaductos de la Cuesta, Verde y Seco. *ACHE*, 1–10.

Mermigas, & Wang. (2020). Comparative Study of the Proportions and Efficiency of Steel Arch Bridges. *Structural Integrity*, *11*, 280–288. doi: 10.1007/978-3-030-29227-0_28

Miguel. (2015). Puente arco de alta velocidad sobre el río almonte. *Revista de Obras Publicas*, *162*(3562), 73–82.

Monfort. (1917). Puente de hormigon armado sobre el rio Jucar (Valencia). *Revista de Obras Publicas*, *Tomo I* (2166–01), 149–154.

Muñoz, Troyano. (2004). Puentes Arco sobre el Rio Nervion en Bilbao para el ferrocarril Metropolitano de la Ciudad. *Revista de Obras Publicas*, (3445), 115–126.

Ovies. (1932). Puente del rio Nalon, en Valduno. *Revista de Obras Publicas*, *Tomo I* (2591–04), 90–93.

Pantaleon. (1996). *XIII Congreso de la FIP y Expositores*. In *ACHE* (pp. 428–436).

Pena Boeuf. (1916). Puente de la Presa (Navarra). *Revista de Obras Publicas*, *Tomo I*(2150–02), 629–636.

Perez, Lara, Munoz, Chico Lopez. (2020). Viaducto sobre el rìo Ulla. *Hormigon y Acero*.

Posada, Prieto. (2011). Viaductos sobre Rio Deza y Anzo 2. *Hormigón y Acero*, (259), 61–73.

Ribera. (1902). Puente De Golbardo.Pdf. *Revista de Obras Publicas*.

Ribera. (1904). Puente Monumental en San Sebastian (Maria Cristina). *Revista de Obras Publicas*, *Tomo I* (86), 309–311.

Ribera. (1910). El puente Victoria en Madrid. *Revista de Obras Publicas*, *Tomo I* (1807–01), 221–224.

Ribera. (1910). Puente de Valencia de Don Juan. *Revista de Obras Publicas*, *Tomo I* (1799–01), 121–122.

Ribera. (1930). *Puentes de fabrica y hormigon armado - Tomo III* (Vol. 3).

Ribera. (1931). Puente de San Telmo, en Sevilla, sobre el Guadalquivir. *Revista de Obras Publicas*, 372–377.

Ribera. (1934). Capitulo III. In *Puentes de Fabrica y Hormigon Armado*.

Ribera. (1934). Capitulo IV. In *Puentes de Fabrica y Hormigon Armado*.

Ridruejo. (2006). Arco de Almonte. Autovía de la Plata. Tramo Hinojal-Cáceres. *Hormigon y Acero*, (240), 5–29.

Rodriguez, De Asiaìn. (2013). Viaducto del Sagar. *Journal of Chemical Information and Modeling*, *53*(9), 1689–1699.

Rodriguez, Muller, Vega, De la Zabìa, Marquez, Palmero. (2005). Dos puentes arco de hormgon prefabricado sobre el rio Cieza. *Hormigon y Acero*, *235*, 3–16.

Rodriguez. (1930). Dos puentes sobre el rio Almanzora en la carretera de Baza a Huercal-Overa (Purchena). *Revista de Obras Publicasev*, *Tomo I* (2540–05), 17–18.

Rodriguez, Rivera, Puertas. (2010). *Realizaciones Espanolas 1998-2008*. ACHE.

Rosellò. (1929). El ferrocarril de Alicante a Alcoy y los grandes viaductos de hormigon armado. *Revista de Obras Publicas*, *Tomo I* (2533–01), 349–354.

Simon-Talero, Villar, del Valle. (2010). Viaduct for the High-Speed railway over the river Ulla (Spain), (figure 1), 1–12.

Sobotkova. (2016). Arch bridges Almonte river Viaduct. *E-Mosty*, (04), 9–41.

Tanner, Bellod. (2005). Widening of the Elche de la Sierra Arch Bridge, Spain. *Structural Engineering International: Journal of the International Association for Bridge and Structural Engineering (IABSE)*, *15*(3), 148–150. doi:10.2749/101686605777963017

Torijano, Martínez, Beneítez, Sánchez Ramírez. (2003). El H.A.P. en el Arco de los Tilos. *Hormigón y Acero*, (228), 57–66.

Villalba Granda. (1924). El puente de Adaja, en arco elìptico de hormigon armado. *Revista de Obras Publicas*, 167–171.

Villalba Granda. (1929). El puente sobre el rio Tajo, en Alarza. *Revista de Obras Publicas*, 107–112.

Villalba Granda. (1934). Un nuevo puente sobre el rio Tajo, Vellisca Carabana. *Revista de Obras Publicas*, 225–232.

Villalba Granda. (1936). El puente sobre el Rio Guadalhorce, en Pizarra, Malaga. *Revista de Obras Publicas*, *Tomo I* (2693–01), 185–190.

Villalba Granda. (1943). El Puente del Pedrido. *Revista de Obras Publicas*, *Tomo I* (2743–03), 500–513.

Villalba Granda. (1944). El puente del Pedrido - Segunda parte. *Revista de Obras Publicas*, *Tomo I* (2746–05), 75–88.

Villela. (2013). Viaducto sobre el rio Arnoia. *Journal of Chemical Information and Modeling*, *53*(9), 1689–1699.

5 GEOMETRICAL AND MECHANICAL TRENDS

The present work identifies some empirical trends from which it can be deduced that optimization is a key issue for a good design, searching optimal solutions in terms of material consuming, shape section and also from the architectural point of view (Salonga & Gauvreau, 2014).

Bridge designers rely on the knowledge of previously completed works to identify links to access new design conceptions. This efficient process is based on the satisfaction of a given set of requirements, such as some empirical trends of flatness, arch depth and girder depth, bending stiffness, slenderness, shallowness, and dimensionless axial force of completed bridges that satisfy similar requirements and for that reason can be used as a starting point (Salonga & Gauvreau, 2014). These trends can be used for the evaluation of feasibility of concrete arch bridges, initial proportioning and for validation. In addition, it has to be underlined that the previously mentioned ratios do not provide any implication of deviating from the recommended values, as already said in the previous chapter "Database assembly", providing a logical basis for the definition of representative ones and the implications in switching from them.

The database realized and described in the previous chapter of this work is based on the description of each structure from both the graphical and qualitative points of view. This description, together with the selected empirical trends performed among the system parameters and related to the proportions, flatness, stiffness, slenderness, shallowness, efficiency, and dimensionless axial force can be used for the preliminary assessment of a certain design concept as a guide for the designers (Salonga & Gauvreau, 2014). The found sources cannot be considered fully exhaustive, but in any case, it is expected that this set of structures will provide a reasonably suitable overview of the state of the art of concrete deck arch bridge design.

5.1 Empirical trends

This section presents all the empirical trends related to proportions, flatness, stiffness, slenderness, shallowness, efficiency, and dimensionless axial force. The influence of these parameters on the structural behavior on concrete arch bridges is briefly explained in the following paragraphs (Mermigas & Wang, 2020).

a. Flatness (span-to-rise ratio)

The first two dimensions determined in the design process are usually the span length L and the arch rise f, whose ratio provides a simple quantitative visual representation of the arch with respect also to the surroundings. Moreover, this relation plays an important role in influencing the structural behavior (Salonga & Gauvreau, 2014). The L/f is plotted as a function of the span length L for the bridges considered into the study in the Fig.5.1. The values of L/f range from 1.72 up to 11.01 for roadway bridges with a mean value of 5.95 and from 1.07 up to 7.07 for the railway ones with a mean of 3.29. From the graph it can be noticed that there is not a clear relation defining span-to-rise ratio versus span length, in fact the coefficients of determination R^2 are very low, respectively, 0.0367 for roadways and 0.1268 for railways. This finding is consistent with the same conclusion obtained by Salonga and Gauvreau (Salonga & Gauvreau, 2014). This lack of correlation could be attributed to the typography and environment constraints which always affect the selection of L/f for concrete arch bridges (Fig.5.2). However, the L/f ranges between 2 and 10 which is coherent with Menn recommendations for railways (Menn, 1990). A L/f below 2 would result in an awkward appearance and substantial increases in construction cost. On the other hands, the sensitivity of arches to creep, shrinkage, temperature variation and imposed displacements at supports increases with higher values of L/f. That is the reason when exceeding a value of 10, it may be necessary to reduce or eliminate redundancy due to restrained deformations providing hinges at the springing lines and at the crown. Similar considerations have been done also by Leonhardt (Leonhardt, 1979) who proposed the following ranges for L/f: 5-12 for three-hinged arches, 4-12 for two-hinged arches and 2-10 for fixed-end arches without internal hinges. Although these considerations, the highest span-to-rise ratio (L/f=11) for roadway bridges exceeds both the limitations proposed by the two authors for fixed-end arches, which means that practicable solutions can be developed out of these recommended ranges. However, the fact that just 1/38 roadway arch bridges analysed overcomes this threshold, highlights that designers generally do not exceed this limit. According to these considerations, for given profiles of roadway, railway, and terrain to be crossed, generally the choice of the arch span length is limited to a small set of possible rises. In conclusion, the selection of adequate L/f relations depends on several factors, especially topography which can guide in many cases the location of the springing lines.

By looking at Fig.5.1, the slope tends to decrease instead of increasing, which means that raising the span length L, the L/f ratio tends to decrease, leading to a general decreasing of the horizontal forces which is basically the principle of the arch which, if properly shaped, can become the optimal solution to cross large spans and transfer high loads.

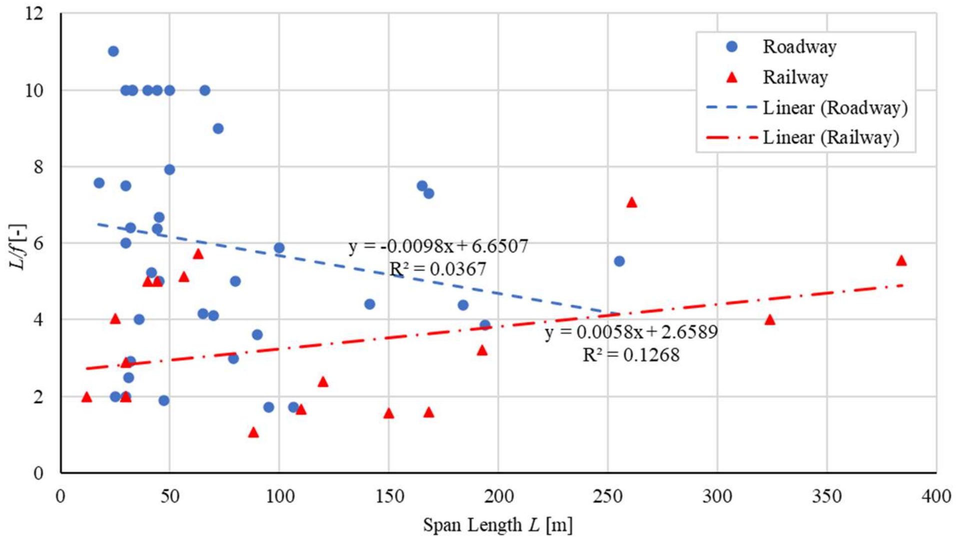

Figure 5.1: Span-to-Rise ratio L/f as a function of the span length L for the collected database roadway and railway bridges

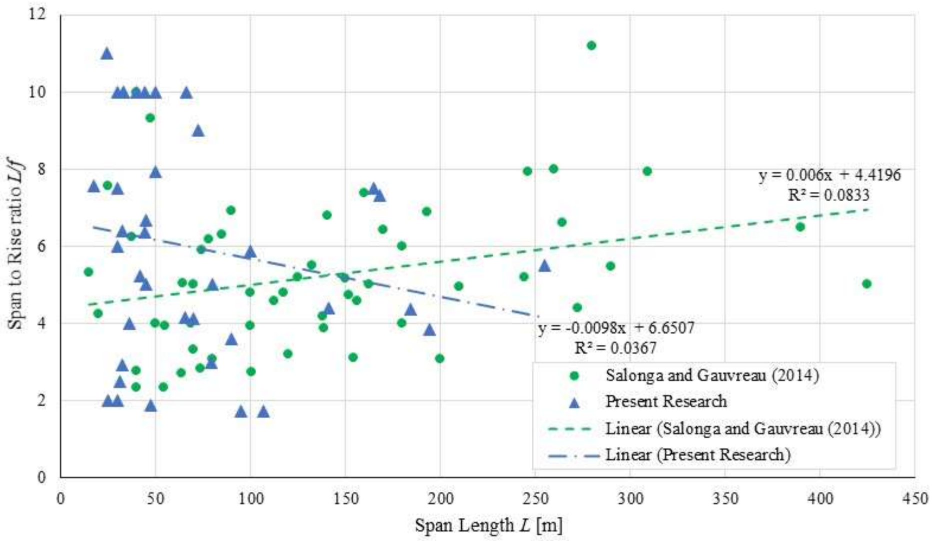

Figure 5.2: Span-to-Rise ratio L/f as a function of the span length L for the entire database roadway and railway bridges (present work and Salonga and Gauvreau (Salonga & Gauvreau, 2014)*)*

b. Girder and arch depths

In the design process, the arch and girder depths are chosen in the first steps, due to their significant aesthetic and structural relevancies (Mermigas & Wang, 2020). According to Menn, it is suggested that the girder depth should be constant for the entire length of the bridge; furthermore, the approach spans should be quite similar in length to the girder spans above the arch. The recommended span-to-depth ratio should be chosen between 12 (in the arch spans) and 15 (in the approach spans).

Regarding the arch depth, neither Menn nor Leonhardt specify any recommended range of values.

All the bridges into the database, both the roadways and railways, can be divided into two main subgroups: the first one is made of 51 out of 58 bridges which referred to deep-arch systems, with the arch depth greater than the girder one; the second group is constituted by the other 7 bridges which referred to deep-girder systems, those with girder depth greater than the arch one. In the Fig.5.3 and Fig.5.4, the arch and girder depths according to their span lengths L have been plotted dividing the deep-arch from the deep-girder case. It can be noticed that both the trends are similar although the bridge traffic type is different, both the linear regression lines tend to increase with the span length as a sign of the possible significance in summing the girder depth and the average arch depth as system depth d_{sys}. This parameter is plotted as a function of the span length L in Fig.5.5. The high values of coefficient of determination R^2 confirm a good fit of data with a linear trend. The strong empirical relation between d_{sys} and L helps the designers in the selection of the suitable system depth (d_{sys} ~ L/50) with a certain freedom between arch and girder depths. This correlation provides for the lack of relation between the L/f and L as it has been previously underlined. This consideration stands that, on the contrary to what was said in the previous paragraph for the L/f and L, the site-specific geometrical constraints have a small impact on the primary members' depth. System depth is used to further investigate the combined effect of girder depth and arch depth as d_{sys} gradually increases as span length increases (Salonga & Gauvreau, 2014).

A further consideration can be performed according to the arch depth definition. The Fig.5.6, Fig.5.7, Fig.5.8 and Fig.5.9 reports graphs in which the comparison between the real values of arch depth at crown and at springing lines have been plotted with respect to the ones obtained by the following empirical correlations:

$$h_{crown} = \frac{L}{100}\ [m] \tag{5.1}$$

$$h_{springings} = \frac{L}{50}\ [m] \tag{5.2}$$

The plots contain both the roadway and railway bridge types, and it can be easily noticed that in most of the cases the real and the approximated arch depth values are comparable. This observation suggests a preliminary method for the evaluation of the arch depth in the pre-design process, considering the goodness of the fittings. More accurate estimations of h_c and h_s will be treated in the chapter related to pre-design, where new empirical correlations will be extrapolated by looking at the slope of the linear regression line of the arch and girder depth plots using the entire database (present research and Salonga and Gauvreau (Salonga & Gauvreau, 2014).

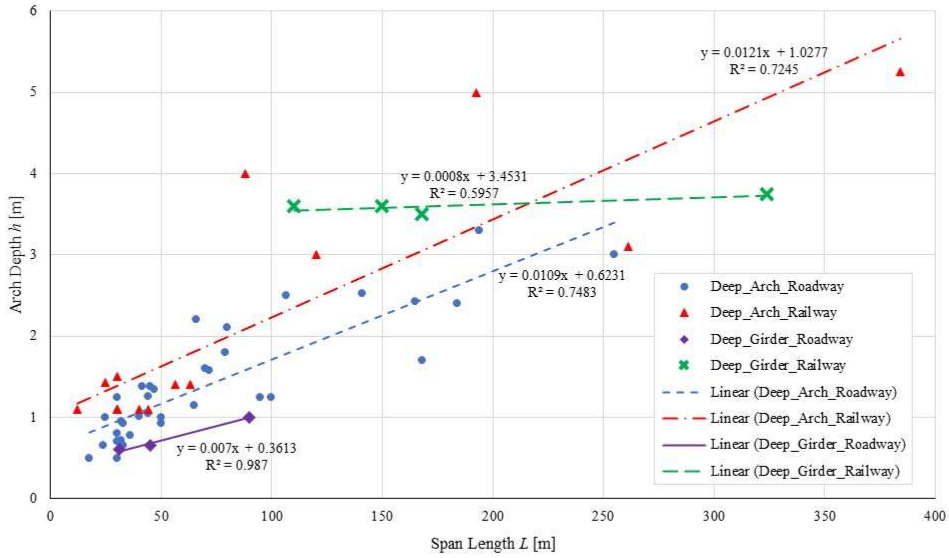

Figure 5.3: Arch depth h with respect to span length L of the present work database collected

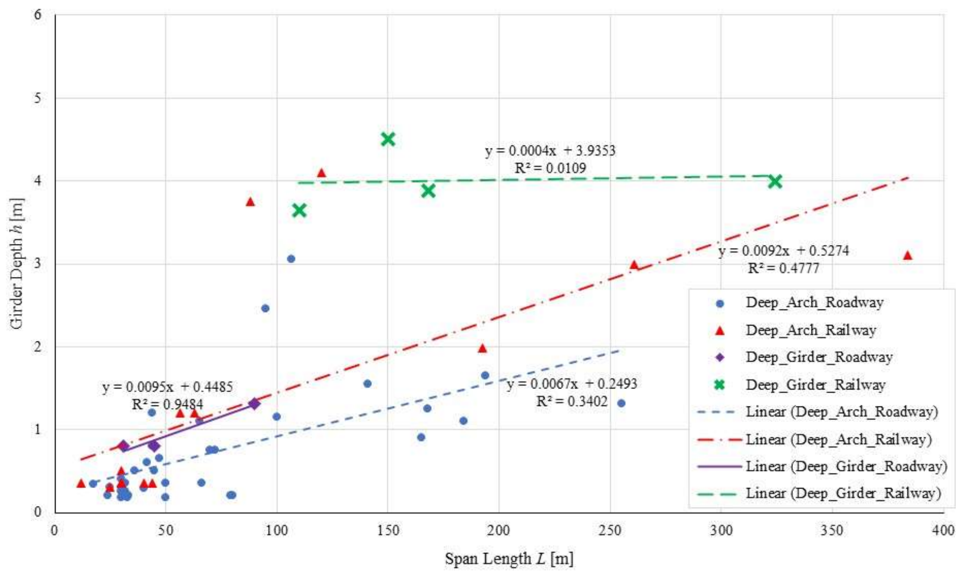

Figure 5.4: Girder depth h with respect to span length L of the present work database collected

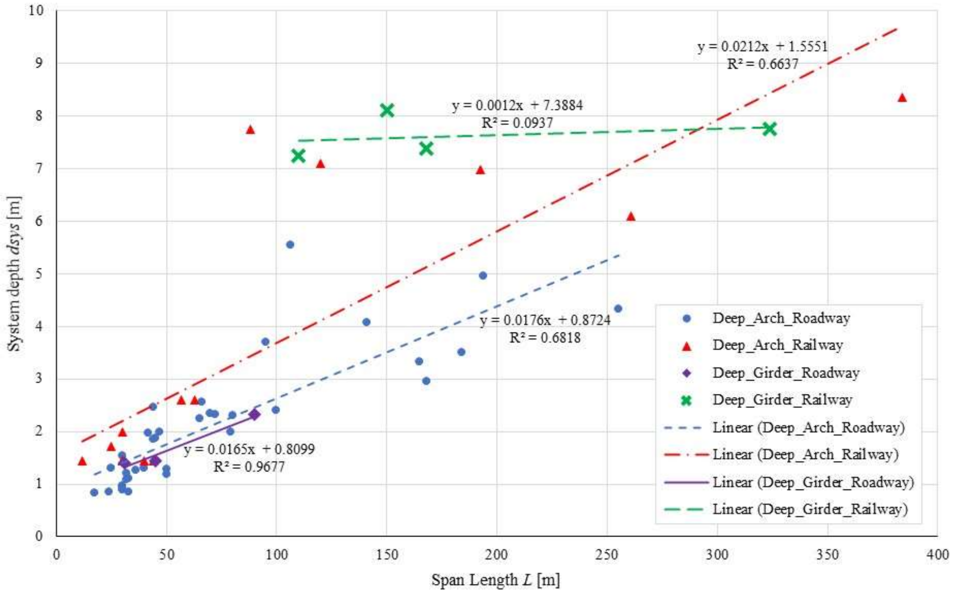

Figure 5.5: System depth (sum of arch and girder depths) d_{sys} with respect to span length L of the present work database collected

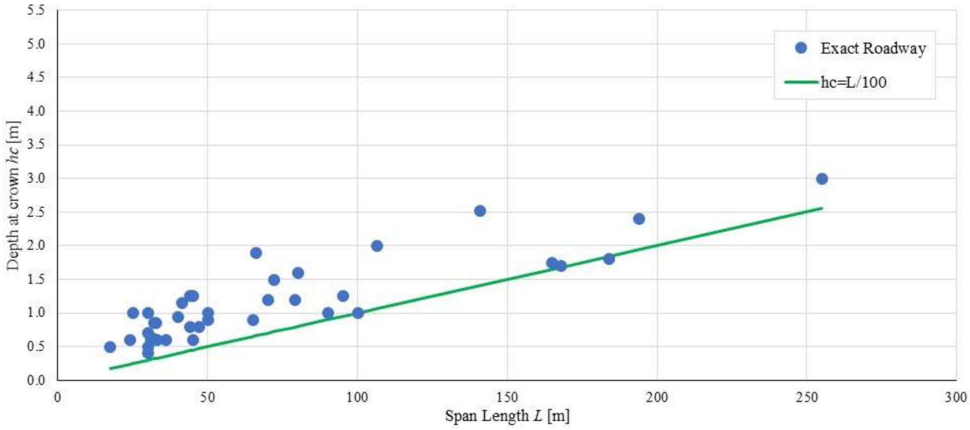

Figure 5.6: Arch depth at crown h_c with respect to the span length L for roadway bridges considering the exact values form the database and the approximated ones

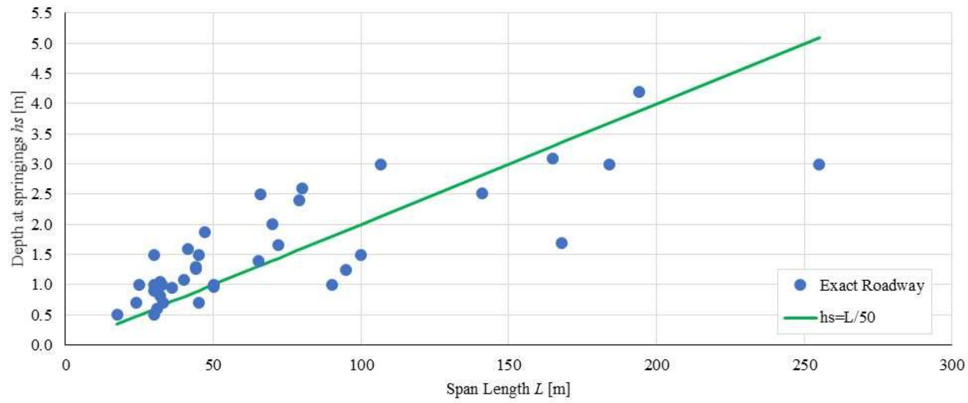

Figure 5.7: Arch depth at springing lines h_s with respect to the span length L for roadway bridges considering the exact values form the database and the approximated ones

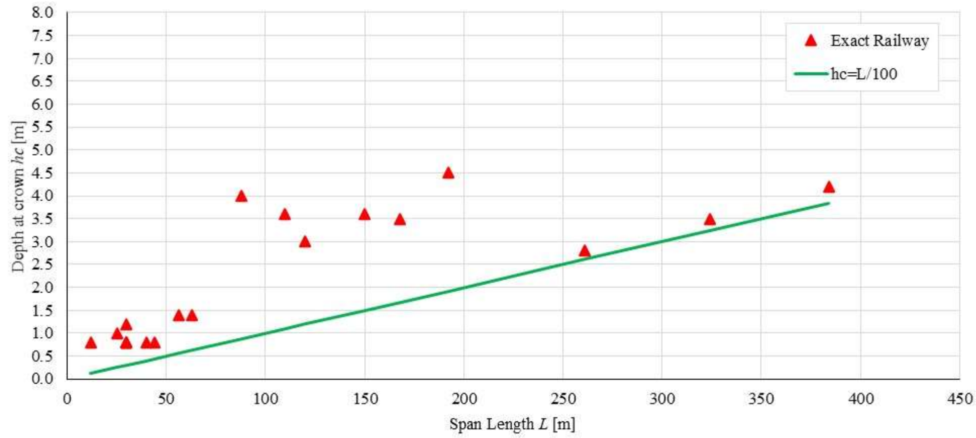

Figure 5.8: Arch depth at crown h_c with respect to the span length L for railway bridges considering the exact values from the database and the approximated ones

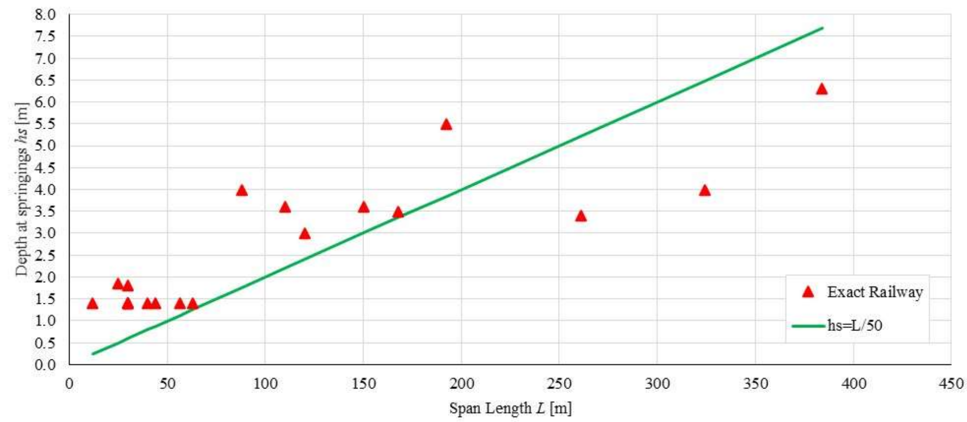

Figure 5.9: Arch depth at springing lines h_s with respect to the span length L for railway bridges considering the exact values form the database and the approximated ones

c. Bending Stiffness

The arch/girder bridge system's response to load is affected by member stiffness which plays an important role into the determination of the structural response. The global response of the bridge, and, consequently, the distribution of internal actions due to non-uniform distributed live loads depends on the relative stiffness between arch and girder. According to Maillart, the bending moment of girder (M_{girder}) is estimated as a function of the total bending moment (M_{tot}) due to non-uniform distributed live load with the proportion of its own moment of inertia I_{girder} over the system moment of inertia I_{sys} (Equation 5.3) (Billington, 1973). The I_{sys} is defined as sum of the girder inertia (I_{girder}) and the arch inertia at crown (I_{arch}). This simplified evaluation is based on the assumption that the modulus of elasticity of concrete is the same for both the girder and the arch (Billington, 1973). Generally speaking, bridges with I_{arch}/I_{sys} close to 0 are defined as deck-stiffened arches; on the contrary, the ones with I_{arch}/I_{sys} close to 1 are instead known as self-stiffened arches. The bending moment of the arch can be obtained in an analogue way (Equation 5.4).

$$M_{girder} = M_{tot} \frac{I_{girder}}{I_{sys}} \; [kNm] \tag{5.3}$$

$$M_{arch} = M_{tot} \frac{I_{arch}}{I_{sys}} \; [kNm] \tag{5.4}$$

Similar considerations have been done by Menn. He states that in general, moments in the flexible system are shared by girder and arch. They can be calculated approximately by distributing the moments M obtained from either a deck-stiffened arch or a stiff arch to girder and arch according to their respective stiffnesses (Menn, 1990).

For a given value of M_{tot}, the Equations 5.3 and 5.4 are independent from the arch span. This implies that, at least regarding the load path for live load, there is essentially no restriction on the relative bending stiffness of arch and girder for any given value of arch span. That means that the values of I_{arch}/I_{sys} should be properly distributed between deck-stiffened and self-stiffened arches over the full range of possible span length, but as can be seen in the Fig.5.10, that it is not completely true. In any case, the measures seem to be quite well distributed for both railway and roadway traffic types between the extreme possibilities: deck-stiffened arch bridge (i.e., I_{arch}/I_{sys} =0) and self-stiffened arch bridge (i.e., I_{arch}/I_{sys} =1); nevertheless, there is not a clear tendency of higher I_{arch}/I_{sys} with the increasing of the span length values.

The parameter I_{sys} depends only on the depths of arch and girder; consequently, two cross-sections of identical depth can have large difference in the member's moment of inertia depending on the section, if solid or not. For that reason, as an alternative, it is possible referring to a total bending stiffness of the system characterized by an inertia equal to I_{sys} from which the effective stiffness depth d_{eff}, can be calculated assuming a depth of a solid rectangle with a width equal to the bridge deck (Equation 5.5):

$$d_{eff} = \sqrt[3]{12I_{sys}/b_{deck}}\ [m] \tag{5.5}$$

This new parameter d_{eff} is plotted as a function of the span length (Fig.5.11) for the bridges collected in this research. The fact that there is a quasi-linear trend in the data, does not depend on the linear relationship between d_{sys} and the span length L (as observed in Fig.5.5), in fact, systems with identical system depth d_{sys} can have significant different values of effective stiffness depth d_{eff}.

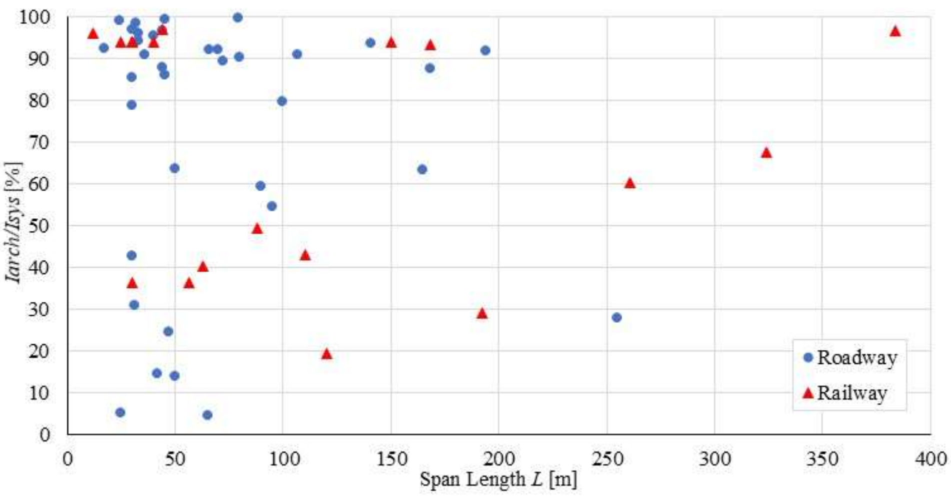

Figure 5.10: Ratio of arch moment of inertia I_{arch} to system moment of inertia I_{sys} as a function of the span length L for both roadway and railway bridges collected in the present work

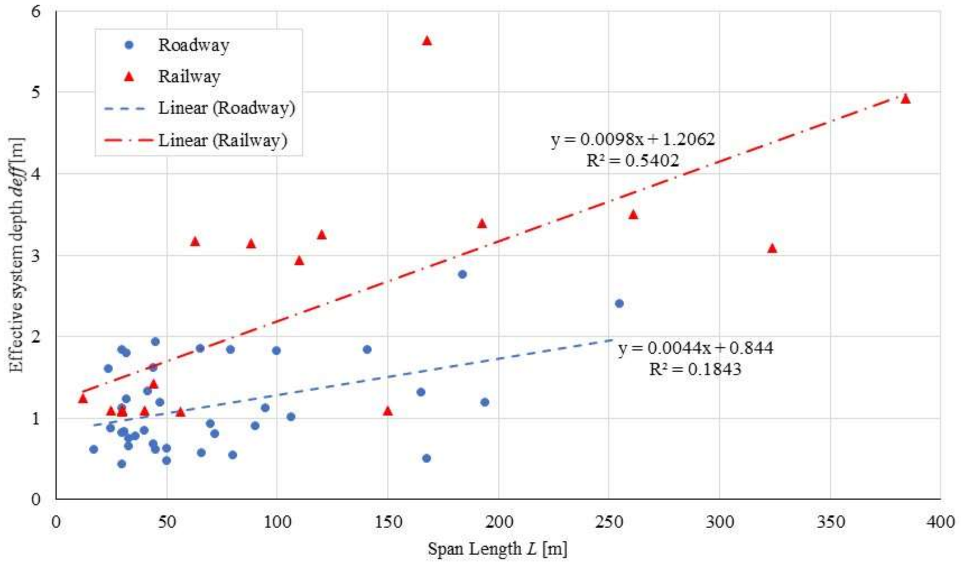

Figure 5.11: Effective stiffness depth d_{eff} as a function of the span length L for both roadway and railway bridges collected in the present work

d. <u>Slenderness</u>

Arch structures under the combined action of permanent and live loads are subjected to second-order effects (Menn, 1990), which can be related to buckling through the slenderness ratio obtained as illustrated in Equation 4 (Galambos, 1998):

$$\lambda = kS/r_{sys} \tag{5.6}$$

where k is the effective arch length factor, S is the arch length and r_{sys} is the system radius of gyration. Austin proposed the following values for *k*: 0.35 for fixed arches, 0.50 for two-hinged arches and 0.54 for three-hinged arches (Austin, 1971); while the system radius of gyration r_{sys} can be calculated as follows (Equation 5.7):

$$r_{sys} = \sqrt{I_{sys}/A_{arch}} \tag{5.7}$$

where A_{arch} is the cross-sectional area of the arch, taken as an average between the crown and the springing line (this assumption implies that the girder does not resist axial compression). In the following Fig.5.12 and Fig.5.13, both the radius of gyration r_{sys} and the slenderness ratio λ have been plotted according to the span length L for the bridges in the database. In Fig.5.12, roadway bridges with span length of 25 to 50m have a system of radius of gyration around 0.3 and the railway ones with L of 30m have a r_{sys} which ranges from 0.37 to 0.93. The system slenderness ratio λ is plotted in Fig.5.13 and it can be noticed that for railway bridge there are some outliers, where λ reaches the maximum value of 119. For short spans, observed values of λ are quite well distributed between the minimum of 13 and the maximum of 85 for the Ricobayo arch bridge (roadways) and from 74 up to 119 for the Rio Almonte viaduct (railways). According to the logarithm regression lines plotted for both the bridge subsets, an average value of 51 for the roadways and 47 for the railways have been found. The Spanish concrete deck arch bridges have generally a smaller span length rather than the other concrete arch bridges in the world. The graph reveals that, although arches of considerable slenderness have been built (up to λ=120), designers of long-span arches have looked at structures of more modest slenderness (λ=60). The relatively broad distribution of λ for short-span arches implies that this parameter is not a key aspect to be considered in the preliminary design of such bridges.

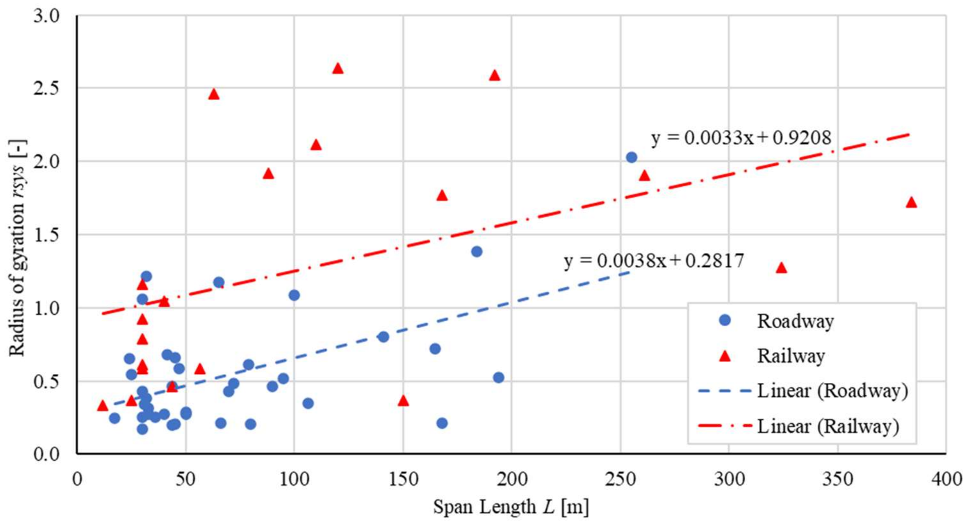

Figure 5.12: System radius of gyration r_{sys} as function of span length L for both roadways and railways of the database presented for this work

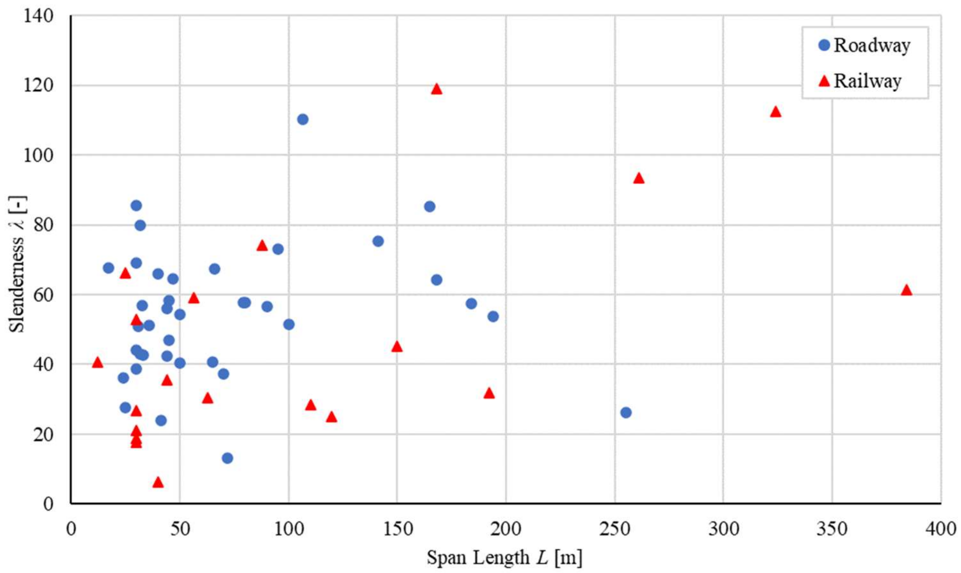

Figure 5.13 – System slenderness ratio λ as function of span length L for both roadways and railways of the database presented for this work

e. <u>Shallowness</u>

While earlier arches were designed based on true arch behavior, the more recent designs must also consider beam behavior (Kindij, 2008). With high span-to-rise ratios, beam action increases the bending stresses on the section and can cause the structure to become inefficient, which can be avoided respecting the threshold values for *L/f* ratios. Although the design of arch bridges could be challenging in a certain way, shallow reinforced concrete arches can be an effective solution to overcome some difficulties. A shallow arch is defined as an arch that is subject to axial deformations, implying compression forces which induce compressive strains in the arch, so crown deflection downward occurred. The second effect is that axial shortening causes redundant moments at fixed supports in statically indeterminate systems, which results in a transition from true arch behavior towards beam one. Using a force method approach on a fixed arch system, Salonga and Gauvreau proposed a dimensionless relation governed by the parameter, β defined as the shallowness ratio for an arch (Salonga & Gauvreau, 2014):

$$\beta = r_{sys}/(\eta f) \tag{5.8}$$

where η is a fixity factor that accounts for the support conditions of the arch which for fixed arches is assumed equal to 2, for two-hinged arches equal to $\sqrt{24}$ and for three-

hinged ones due to their determinacy do not develop redundant forces so β is equal to 0; f is the arch rise and r_{sys} is the system radius of gyration. In the Fig.5.14 have been plotted both the roadway and railway arch bridges collected in the database of the present research with respect to the span length. Moreover, Salonga and Gauvreau observed that systems with shallowness ratios less than $50 \cdot 10^{-3}$ generally can be considered true arches, because they satisfy the condition that at least 90% of the dead load is supported by the arch in compression (Salonga & Gauvreau, 2014). Increasing the shallowness ratio above the suggested threshold will cause a rapidly lose in the system of ability to carry permanent loads in pure axial compression increasing the tendency of behaving like a curved, fixed-end beam. So, it will result into an inefficient arch design. A greater proportion of arch action, which corresponds to smaller value of β, is what is expected increasing the f, decreasing the I_{sys} and increasing A_{arch}.
It can be also noticed from Fig.5.14 that, for the set of Spanish bridges chosen, just two overcome the recommended threshold of $50 \cdot 10^{-3}$ as a confirmation of no need to consider the shallowness if the arches have been designed with the conventional proportions.
Salonga and Gauvreau proposed then to combine the shallowness threshold with data coming from existing bridges to determine a curve for efficient arch behavior based on span-to-rise (Fig.5.15) (Salonga & Gauvreau, 2014). A linear regression of the data resulted in empirical equations to obtain the system radius which, substituted into the equation for shallowness ratio, leads to the following relation:

$$\frac{L}{f} < 16.1 \cdot \frac{L}{L + 48.4} \tag{5.9}$$

In this equation, L is the span length and f is the rise of the structure. Fig.5.15 is a plot of the efficiency threshold curve based on the conservative high estimate trend line for the studied concrete arch bridges based on span-to-rise ratio. For a given span length, a span-to-rise ratio curve will result in an efficient design. As the span length increases, the threshold ratio for efficient arch behavior increases before flattening around 300m.

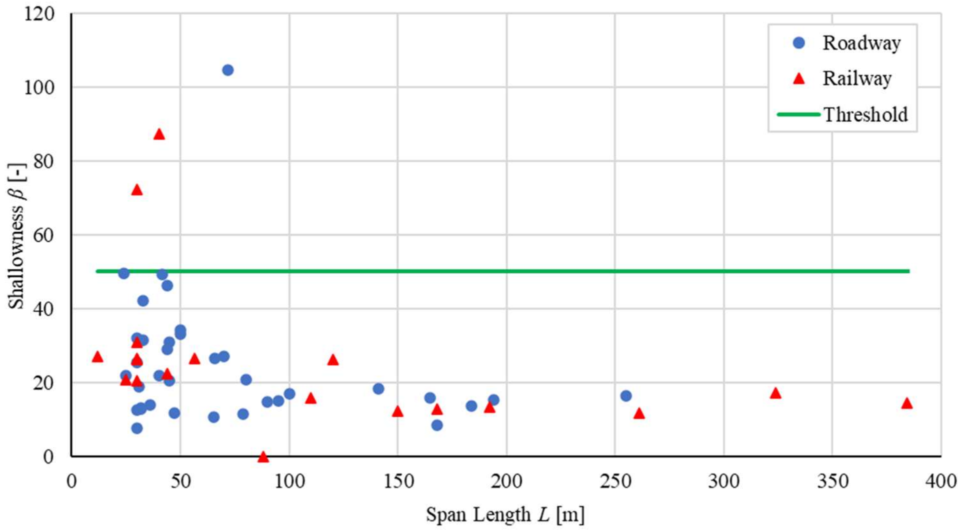

Figure 5.14: Shallowness ratio β as a function of span length L for both roadway and railway bridges collected in the present work compared with the suggested threshold by Salonga and Gauvreau (Salonga & Gauvreau, 2014)

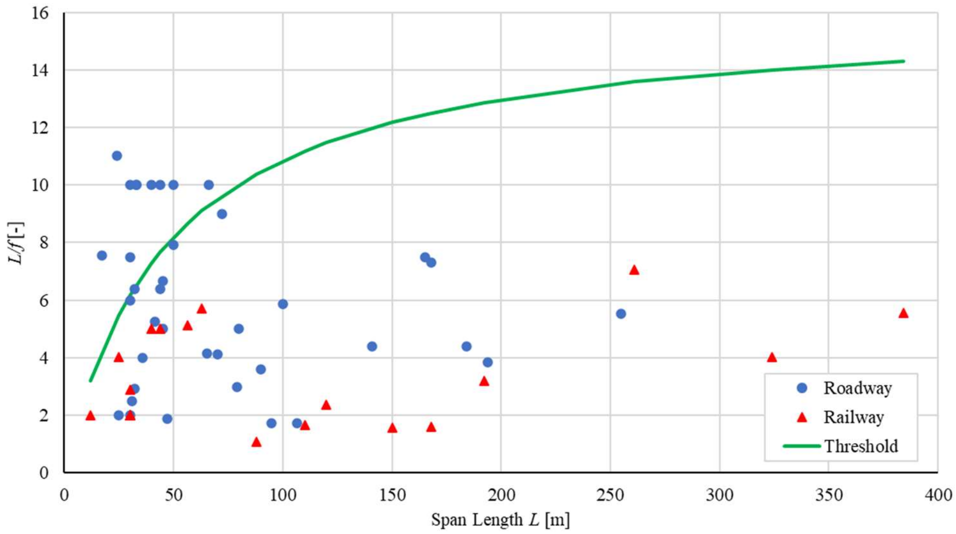

Figure 5.15: Linear regression of the data resulted in empirical equations to obtain the system radius in the present research

f. <u>Effective Slab Thickness</u>

For concrete arch bridges is quite common to express the quantity of concrete in the superstructure, which is important for economical consideration, according to the effective slab thickness t_{eff} expressed as shown in Equation 5.10:

$$t_{eff} = V/(L \cdot b_{deck}) \quad (5.10)$$

where V is the total volume of concrete in the superstructure (arch, girder, and spandrel columns), b_{deck} is the deck width and L is the arch span length. This parameter can be considered as a good tool for the comparison between consumption of concrete in bridges with different span lengths and widths. A similar expression has been provided before by Menn for the effective slab thickness evaluation in the case of posttensioned concrete girder bridges (Menn, 1990):

$$t_{eff} = 0.35 + 0.0045L \tag{5.11}$$

where L is the girder span length.

In Fig.5.16 it can be noticed the best linear regression which, although it has a low R^2 (29%), provides the following expression: $t_{eff} = 0.84 + 0.0071L$, which is somehow like the relation provided by Menn for posttensioned concrete girder bridges (Equation 5.11) (Menn, 1990). Both equations provide a very simplified method to quantify the concrete consumption, and their expressions are quite similar. This would suggest that the cost of both structural typologies is similar, with a light cost-saving of posttensioned concrete girder bridges respect to arch bridges especially for short spans.

The comparison between the Menn's formula and the one obtained from the data collected in the present work, although most of the arch points stay above the continuous line, it underlines that just two of them lie below (Menn, 1990). This implies that, although it is possible to design concrete arch bridges that consume less concrete than girder ones, most of them consume significantly more concrete than girder bridges.

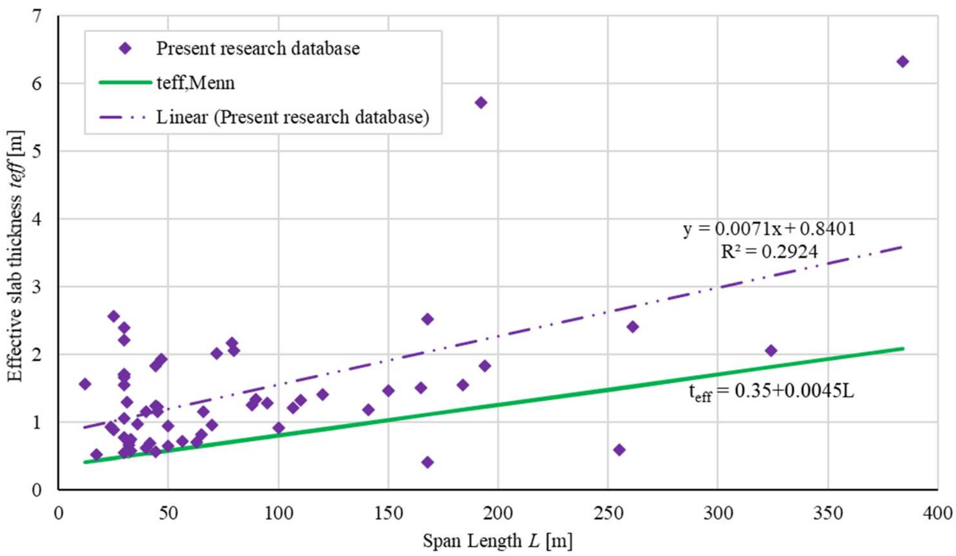

Figure 5.16: Effective slab thickness t_{eff} as a function of span length L of bridges contained into the present database compared with the Menn's formula (Menn, 1990) for concrete girder bridges

g. Dimensionless axial force

Another parameter used for the preliminary design of the arch is the dimensionless axial force *ν*, calculated as N_{Ed}/N_{Rd} where N_{Ed} is the axial force at the Ultimate Limit State and N_{Rd} is the design axial resistance. This coefficient could be used to perform a sound preliminary sizing of the arch cross section.

This parameter also guarantees the reliability of the suggested empirical formulas and relations to be followed in the preliminary design procedure. Next Fig.5.17 shows the *ν* calculated at springings for all the 38 roadway bridges collected in this work. The mean value of *ν* is 0.28, with a minimum and a maximum value of, respectively, 0.06 and 0.77, with a variation coefficient of 57%. It is worth mentioning that, considering the interaction domain (N-M) of a rectangular cross section with a continuous perimetral reinforcement, the highest bending strength is achieved for a value closed to 0.4. If the same analysis is performed at SLS, the following results of *ν* are obtained: 0.13 as mean value, 0.03 and 0.37 as, respectively, minimum, and maximum values. The variation coefficient is almost the same (58%). In addition, although is not graphically shown in a plot, the authors have investigated a possible relation between *ν* and the span length: as expected, there is a not a trend between these two parameters.

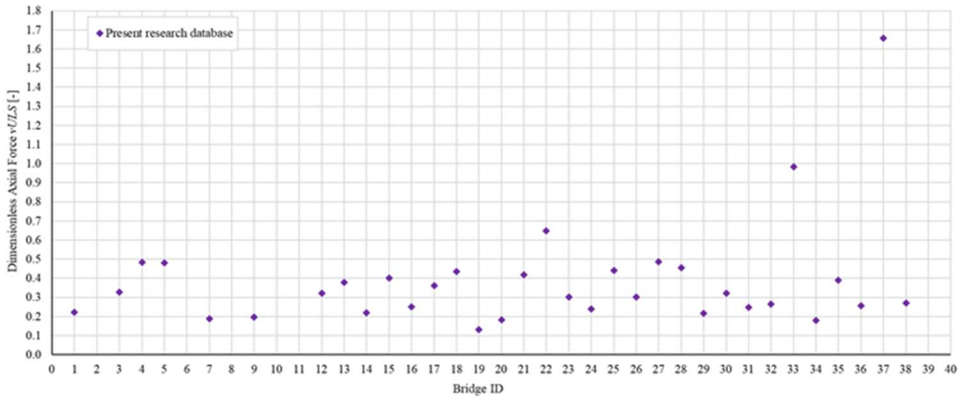

Figure 5.17: Dimensionless axial force ν at springing lines at ULS combination vs. bridge ID for roadway bridges collected in the present research database

5.2 Conclusions

This research presents the collection of descriptive and quantitative data about 58 concrete arch bridges located in Spain. These bridges cover a large span range from 12 to 384m and different traffic type, in fact 38 bridges are roadways, while the remaining 20 are railways. This information has been used to study fundamental parameters that define the structural behavior of such bridges. In most of the cases, these variables have been plotted with respect to the span length *L* to analyze possible trends which can be helpful in guiding the designer through the preliminary stage of the design process. In order to get a more global overview and a source of comparison, the data collected in this research have been joined with the data gathered on a similar work by Salonga and Gauvreau which refer to bridges located worldwide. The complete database, obtained as merging of both works, includes 112 reinforced concrete arch bridges (Salonga & Gauvreau, 2014).

The main findings of this research are summarized as follows:

a. <u>Flatness (span-to-rise ratio)</u>

The distribution of the *L/f* with respect to the span length *L* is not uniform; on the contrary the data seem to be quite spread which means that the choice of the span-to-rise ratio is defined by topographic site conditions rather than structural requirements. In addition, 8 out of 58 bridges present a value of *L/f* which is out of the recommended range of 2-10 as indicated by Menn or 3-8 as suggested by Leonhardt (Menn, 1990)(Leonhardt, 1979). In addition, the mean value of flatness of Spanish bridges is higher than bridges located in the rest of the world.

b. <u>Arch and girder depth</u>

From the database can be deduced that a significant number of deep-arch systems rather than deep-girder ones has been included. For roadway bridges, both arch and girder depths increase with the arch span length: the h_c=L/50 and h_s=L/100. More specifically, as will be explained in the "Bridge preliminary design" chapter, the h_c=L/50 and h_s=L/67 have been obtained as mean values for estimating such depths. In both cases, the coefficient of determination is around 90%, indicating a good fit between the data and the linear trend. In addition, also the system depth, obtained as sum of arch and girder depths, reveals a strong relationship with the arch span length.

c. <u>Bending Stiffness</u>

There is not a clear tendency between I_{arch}/I_{sys} and the span length *L*. This result is in contrast with the conclusion of Salonga and Gauvreau where, to higher spans (especially from values greater than 170m) correspond almost only self-stiffened arch bridges (I_{arch}/I_{sys} =1) (Salonga & Gauvreau, 2014). In addition, it can be noticed some outliers, which confirm that the full range of I_{arch}/I_{sys} can be indeed used for relatively long spans. The mathematical independency between the distribution of system bending stiffness and the span length implies a self-stiffened tendency with the increasing values of L, which can be explained by the needed for long-span arch bridges of flexural strength to resist nonuniform loads during construction.

d. Slenderness

For short span arches, the recorded values of system slenderness ratio λ are quite well distributed between 6 and 85. Increasing the value of span length, the trend tends to flatten a bit toward a value of λ equal to 70 for the roadway bridges, instead it cannot be recognized clearly for the railway case. This behavior cannot be deduced directly form the parameters used to evaluate the slenderness ratio like the arc length S or the system radius of gyration r_{sys}, so there is no indication whether slender arches would be possible to realize for long spans. Furthermore, the relatively broad distribution of λ for short-span arches implies that this parameter is not a relevant aspect to be considered in the preliminary design of such bridges.

e. Shallowness

From the plot of shallowness ratio β, it can be observed that just 1 roadway arch bridges and 2 railway arch bridges overcome the suggested threshold of $50 \cdot 10^{-3}$ beyond which arches are not capable to carry permanent loads in pure compression. So, for arches with standard geometrical properties, the shallowness can be neglected, allowing the realization of arches for greater span-to-rise ratios.

f. Effective Slab Thickness

This value considers the quantity of concrete in girder, columns, and arch. When it is plotted respect to the span length L, the best linear regression (although as a R^2 =29%), provides the following expression: $t_{eff} = 0.84 + 0.0071L$. It is somehow similar to the relation provided by Menn for posttensioned concrete girder bridges: $t_{eff} = 0.35 + 0.0045L$ (Menn, 1990). Both equations provide a very simplified method to quantify the concrete consumption, and their expressions are quite similar. This would suggest that the cost of both structural typologies is similar, with a light cost-saving of posttensioned concrete girder bridges respect to arch bridges especially for short spans.

g. <u>Dimensionless axial force</u>

The mean value of v obtained for bridges collected in the database is 0.28 (with a minimum and a maximum value of, respectively, 0.06 and 0.77, and a variation coefficient of 57%). This value is slightly lower than the optimal v obtained considering the interaction domain (N-M) of a rectangular cross section with a continuous perimetral reinforcement. If the same analysis is performed at SLS, the following results of v are obtained: 0.13 as mean value, 0.03 and 0.37 as, respectively, minimum, and maximum values. The variation coefficient is almost the same (58%). Finally, there is no evidence of a relation between v and the span length L. Taking advantage of the data collected in the dataset and the trends analyzed through this research, a preliminary design method of roadway arch bridges with fixed supports will be proposed in the following chapter. It will be based on very simple relation between geometrical parameters.

6 ANALYSIS OF THE STRUCTURAL SYSTEM

The arch built following the pressure line due to dead load is the most suitable type of bearing structure for construction materials with high compression strength, as concrete and masonry, together with a soil able to bear horizontal load with economical footings.

In order to study and better understand the main structural behavior in terms of resisting response of arch bridges, the "Tiemblo" bridge situated in Avila, Spain, designed by Fhecor in 1999 has been selected. The opportunity to visualize the executive drawings given by the designers of the Bridge Prof. Hugo Corres Peiretti, Prof. Alejandro Pérez Caldentey together with the co-supervisor Prof. Leonardo Todisco was the reason of the choice.

Initially, a brief introduction about the general arch response system will be presented. Then, more detailed analysis will be performed on "Tiemblo" bridge through a FE model built with SAP2000. Axial load and bending moment interaction will be studied with the goal to find out the stresses on the critical sections.

6.1 Static schemes

Generally, arch bridges with superior decks are fixed arches. Hinges are expensive elements which introduce great deformabilities reasonable only if settlements of the footings are expected, in contrast with the choice to adopt arch bridges. Last, they need maintenance, therefore is suggested to avoid them (Manterola, 2006). However, here there are introduced the possible static schemes configurations:

- Three hinged arches, with isostatic restrain, where *l / f=5 to 12*, possibly formed by the pressure line, with variable depth because of live loads;
- Two hinged arches, one-time hyperstatic, where *l / f=4 to 12*, generally with greater section toward the crown because of higher moments there;
- One hinged arches, with the hinge at crown, not recommended for bridges because of their high-cost foundations due to high moments at the springing lines;
- Fixed arches, three times hyperstatic, where *l / f=2 to 10* (Leonhardt, 1979).

Let’s now introduce the reactions at supports of a typical symmetric arch structure of span length *l* and rise *f*, loaded by a symmetric uniform distributed load q, adopting an isostatic scheme of a three hinged arch reported in *Fig.4.1*.

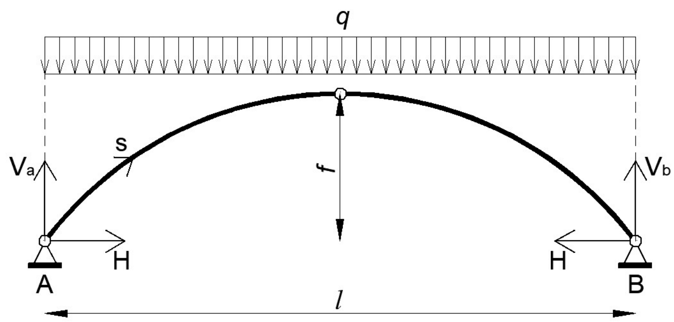

Figure 6.1: Isostatic scheme of a three hinged arch

Solving the equilibrium equations in the vertical direction and the moment equation around one of the two external constrains, the reactions found are:

$$V_a = V_b = \frac{q \cdot l}{2} \quad (6.1)$$

$$H_a = H_b = H = \frac{q \cdot l^2}{8 \cdot f} \quad (6.2)$$

As a first observation, it can be noticed that the horizontal thrust is inversely proportioned to the arch’s rise. Therefore, for lowered arch structures, high strength soil must be available.

6.2 Tiemblo bridge

The Bridge is located over the El Berguillo Reservoir, in Avila (Spain), and it comprises a reinforced concrete arch 165 m in span with a reinforced concrete upper deck 287 m in total length. The rise at the crown is 22 m, thus, the span to rise relation is 7.5 resulting in a very lowered arch. The site location of the structure is an ideal example for the realization of an arch. The slopes are very steep until they submerge inside the reservoir. Moreover, the geotechnical conditions are very good.

6.2.1 Materials

The whole structure is built by reinforced concrete. In particular, it has been used different concrete mix as C25 for footings and abutments, C35 for arch, piers and deck. For passive reinforcement steel, AEH-500N has been used. In order to have qualitative idea about the amount of materials involved in this bridge, here below is reported a table resuming all the concrete and reinforcement quantities:

	Unit	Measured	Quantity	
[m^3]	Concrete in deck	1794.94	0.56	[m^3/m^2]
[m^3]	Concrete in arch	1607.81	0.50	[m^3/m^2]
[m^3]	Concrete in pillars	480.77	0.15	[m^3/m^2]
[m^3]	Concrete in foundations	1609.26	0.50	[m^3/m^2]
[m^3]	Provisional concrete	176.40	0.05	[m^3/m^2]
[kg]	Steel in arch	195074.28	121.33	[kg/m^3]
[kg]	Steel in deck	290833.72	162.03	[kg/m^3]
[kg]	Steel to prestress	22384.60	6.96	[kg/m^2]
[kg]	Steel in columns	61917.42	128.79	[kg/m^3]
[kg]	Steel in foundations	109429.95	68.00	[kg/m^3]
[kg]	Steel in provisional cable-stay	56140.01	3.00	[kg/m^2]

Table 6.1: Main quantities of the bridge

6.2.2 Geometry

The arch is a solid cross-section of a constant 4.00m width and a variable depth starting from 3.10m at the abutments to 1.75m at the crown. The deck is a solid slender 0.90m deep section with 4.00m wide central core, coinciding with the width of the arch, and two large variable depth cantilevers each 4.00m in width. The deck is rigidly supported on the piers of the approach viaducts and on the piers upon the arch which are spaced 13.75m apart. This column span allows the realization of the deck in reinforced concrete together with minimum prestressing tendons in order to minimize the cracks openings. The piers are a constant 4.00m wide, as the arch, and their depth varies with height from 0.90m to 0.35m at the lowest piers (Fhecor, 1999).

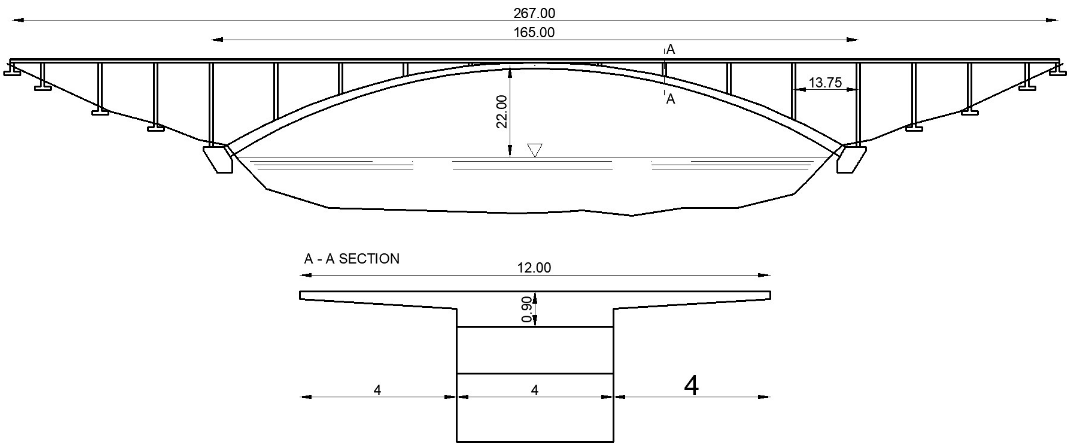

Figure 6.2: Elevation of the bridge and typical transversal section. All measurements are in m.

In the following table there are reported the main dimensions of the elements. In particular, regarding the resisting areas of columns and arch, according to their variable geometries, mean values have been evaluated.

Element	Width [m]	Depth [m]	Area [m^2]
Deck	12.00	0.90	6.17
Columns	4.00	0.9; 0.6; 0.4; 0.35; 0.3	2.04
Arch	4.00	3.1; 1.75	9.70

Table 6.2: Geometrical dimensions of Tiemblo bridge

In the following, there are reported some images taken from the executive drawings kindly shown by the designer of the bridge. There is reported the cross section of the arch, in its first segment of the construction (3.1x4m) with the longitudinal and transversal reinforcements, Fig. 6.3, a detail of the connection between spandrel columns and deck establishing an hinge connection inf Fig. 6.4, finally, a cross section of the first column of the arch, the greatest one (0.9x4m) in Fig. 6.5.

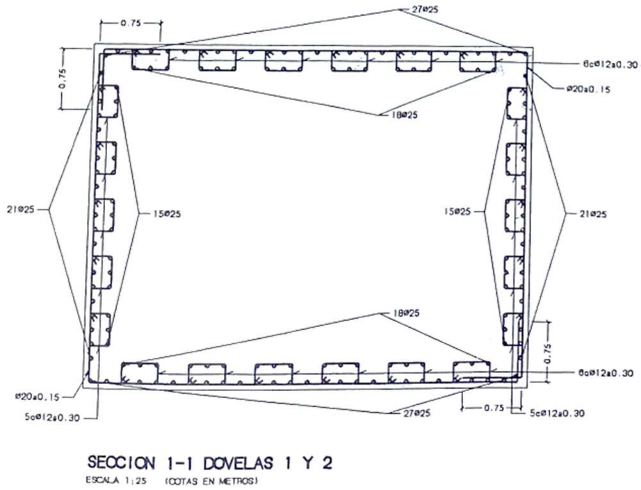

Figure 6.3: Section 1-1 of the Tiemblo arch

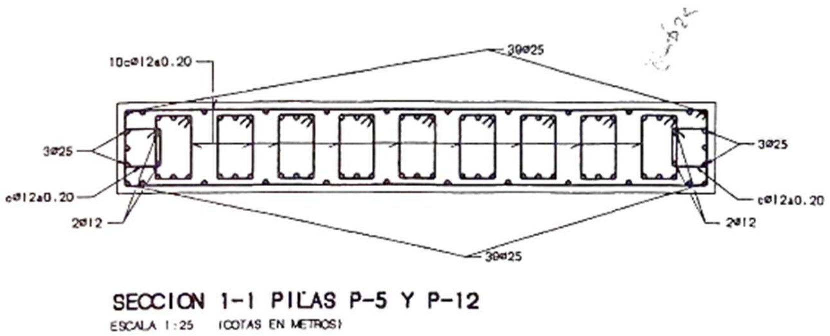

Figure 6.4: Section 1-1 of the piles P-5 and P-12

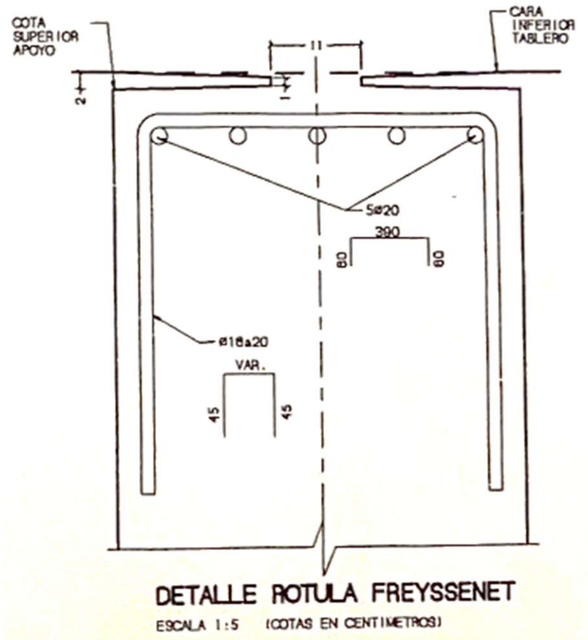

Figure 6.5: Detail of the Freyssenet connection

6.2.3 Loads

The actions taken into consideration for the purpose to build the M-N interaction domain are only vertical actions as permanent and live loads, applying some useful simplification to make easier the problem.

G_1 Self-weight of structural elements (arch, columns and deck)

G_2 Permanent non-structural elements (pavement and barriers)

Q Traffic load (highway type)

In the following list there are reported the evaluation of the loads:

- Deck, is a solid slender section, 12.00m wide and 0.90m deep in the central core, with two cantilevers of 4.00m wide each. Five vehicles restrain systems are present, whose load is considered $5\ kN/m$. The concrete pavement is 0.10m height. Finally concerning the traffic load, a representative value of $4\ kN/m^2$ has been adopted:

Deck

self-weight	$A \cdot \gamma_{cls} = 6.17\, m^2 \cdot 25\, kN/m^3 = 154.25\, kN/m$	G1 [kN/m]	154.25
pavement	$h \cdot \gamma_{cls} = 0.10\, m \cdot 25\, kN/m^3 = 2.5\ kN/m$	G2 [kN/m]	27.50
barriers	$5\, kN/m \cdot n_{barr} = 5\, kN/m \cdot 5 = 25\ kN/m$		
traffic	$4\, kN/m^2 \cdot W = 4\, kN/m^2 \cdot 12\, m = 48\ kN/m$	Q [kN/m]	48.00

Table 6.3: Load analysis of the deck

- Arch, is a solid cross section, 4.00m wide constant over the span, and variable depth from 3.10m at the footings to 1.75m at the crown. An average value of its self-weight has been evaluated as:

Arch

self-weight	$A \cdot \gamma_{cls} = 9.70\, m^2 \cdot 25\, kN/m^3 = 242.5\, kN/m$	G1 [kN/m]	242.50

Table 6.4: Load analysis of the arch

- Columns are solid cross sections, 4.00m wide with variable depth. Their self-weight has been considered as uniform distributed load according to the column span length of 13.75m. Moreover, a mean height equal to half of the rise of the bridge has been adopted.

Columns

self-weight	$A \cdot \frac{f/2}{l} \cdot \gamma_{cls} = 2.04\, m^2 \cdot \frac{22/2}{13.75} \cdot 25\, kN/m^3 = 40.80\ \frac{kN}{m}$	G1 [kN/m]	40.80

Table 6.5: Load analysis of columns

Finally, the loads involved can be summarized as:

G1 [kN/m]	437.55
G2 [kN/m]	27.50
Q [kN/m]	48.00

Table 6.6: Load values obtained by the load analysis

6.2.4 Load arrangement

Recalling the aim of this chapter, which is to study the axial load - bending moment interaction domain, three load arrangements have been investigated in order to find out the most critical situations for the cross sections at springing line, crown and at quarter span length. The shear is not relevant for this type of structures.

- Arrangement 1: maximum absolute value in compression of axial load (N_{min})

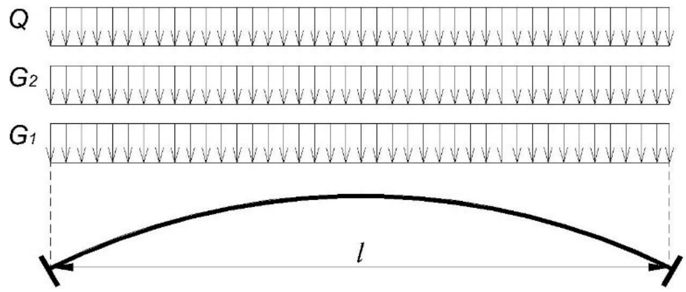

Figure 6.6: Load arrangement 1

- Arrangement 2: maximum value of bending moment at springing (M_{max})

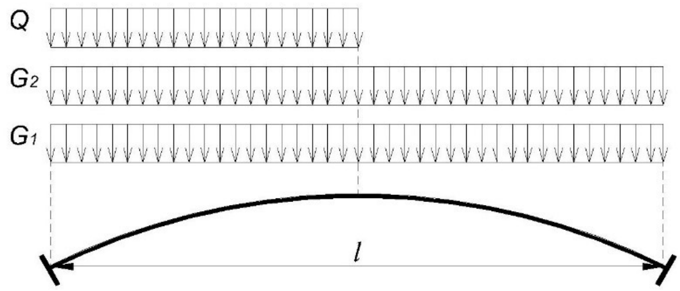

Figure 6.7: Load arrangement 2

- Arrangement 3: minimum value of bending moment at the crown (M_{min})

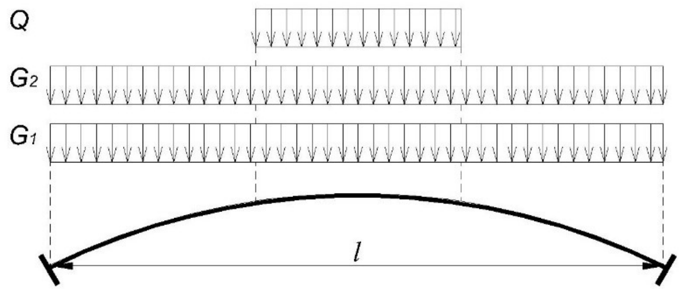

Figure 6.8: Load arrangement 3

6.2.5 FE model

In order to solve the structure, a FE model of the arch has been created using the software SAP2000. The process followed to set the model is:

- Definition of the material: Concrete C30/35 for all the elements;
- Definition of the sections: 18 different sections as reported in the executive drawings describing, in this way, the depth variation of the arch from the footings to crown and differences in steel reinforcements. Moreover, infinite axial stiffness multiplier has been assigned to each section.

SectionName	Material	Shape	Depth (3)	Wdth (2)	Area	TorsConst	$I_X(3)$	$I_Y(2)$	$I_{XY}(23)$	Axial Multiplier
-	-	-	[m]	[m]	[m^2]	[m^4]	[m^4]	[m^4]	[m^4]	-
Arch Section 1	HA-35	Rectangular	3.1	4	12.4	20.91	9.93	16.53	0	99999
Arch section 2	HA-35	Rectangular	3.02	4	12.08	19.73	9.18	16.11	0	99999
Arch section 3	HA-35	Rectangular	2.94	4	11.76	18.58	8.47	15.68	0	99999
Arch section 4	HA-35	Rectangular	2.86	4	11.44	17.45	7.80	15.25	0	99999
Arch section 5	HA-35	Rectangular	2.78	4	11.12	16.35	7.16	14.83	0	99999
Arch section 6	HA-35	Rectangular	2.7	4	10.8	15.28	6.56	14.40	0	99999
Arch section 7	HA-35	Rectangular	2.62	4	10.48	14.24	5.99	13.97	0	99999
Arch section 8	HA-35	Rectangular	2.54	4	10.16	13.23	5.46	13.55	0	99999
Arch section 9	HA-35	Rectangular	2.46	4	9.84	12.25	4.96	13.12	0	99999
Arch section 10	HA-35	Rectangular	2.38	4	9.52	11.31	4.49	12.69	0	99999
Arch section 11	HA-35	Rectangular	2.3	4	9.2	10.40	4.06	12.27	0	99999
Arch section 12	HA-35	Rectangular	2.22	4	8.88	9.53	3.65	11.84	0	99999
Arch section 13	HA-35	Rectangular	2.14	4	8.56	8.69	3.27	11.41	0	99999
Arch section 14	HA-35	Rectangular	2.06	4	8.24	7.90	2.91	10.99	0	99999
Arch section 15	HA-35	Rectangular	1.98	4	7.92	7.14	2.59	10.56	0	99999
Arch section 16	HA-35	Rectangular	1.9	4	7.6	6.42	2.29	10.13	0	99999
Arch section 17	HA-35	Rectangular	1.82	4	7.28	5.74	2.01	9.71	0	99999
Arch section 18	HA-35	Rectangular	1.75	4	7	5.18	1.79	9.33	0	99999

TABLE: Frame Section Properties 01 - General

Table 6.7: Frame section properties

- Definition of the element's typologies: frame elements
- Definition of the constrains: clamped nodes at the start and end of the arch
- Definition of load assignments: uniform distributed load applied on the Z projected axis;
- Definition of the analysis: linear static analysis

In Fig.6.9, there are reported two qualitative images of the model extrapolated by SAP2000 used, where it is possible to see the position of each node representing a different cross section of the real arch, and an extrude view where the depth variation is visible.

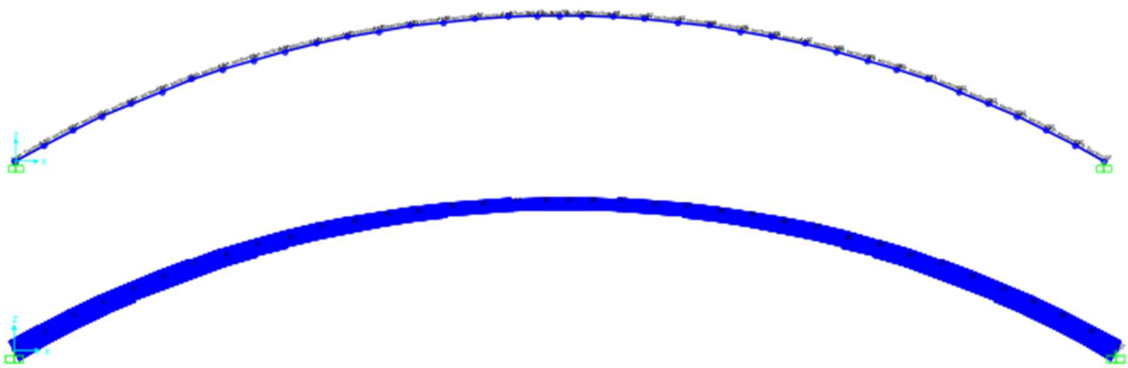

Figure 6.9: Qualitative images of the model from SAP2000, frame view above and extrude view below

In Fig.6.10, there is reported the assignment of loads, where particular attention was made in order to assign the load to the span length and not to the arc length of the arch, except made for the dead load of the arch itself that has been left along the gravity direction as dead load. This was achieved by assigning the loads to the frames along the Z projection axis instead of Z, where Z is defined positive upwards along the vertical and X is defined positive toward right in the horizontal direction.

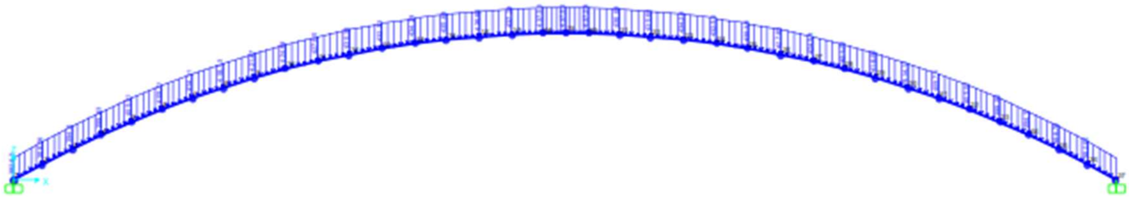

Figure 6.10: Assignment of loads on the arch

6.2.6 Results

In order to validate the model, a comparison between hand-made calculation of the reactions, applying formulas *(1)* and *(2),* with the values from the analysis of the model is done. For the purpose, load arrangement 1 (Fig. 6.6) is considered with the uniform distributed load q:

$$q = Q \left[\frac{kN}{m}\right] = 48.00 \left[\frac{kN}{m}\right]$$

thus, the reactions found are:

	Hand calculation	SAP2000
Va [kN]	3960.00	3960.01
Vb [kN]	3960.00	3959.99
H [kN]	7425.00	7548.13

Figure 6.11: Reactions coming from the uniform distribution load q

Despite the low difference in the horizontal reactions, the model is assumed correct, therefore, further analysis will be run on it.

6.2.7 Vertical deflections

First of all, vertical deflections have been studied for the three load arrangements. An interesting observation can be done by looking at the deflection from the dead load of the arch that is greater than the one from the real load configuration (arrangement 1). This is reasonable because it means that after the realization of the deck and columns, the internal actions reduce as the pressure line approaches to the axis of the arch, that is the key-point of the designing arch structures.

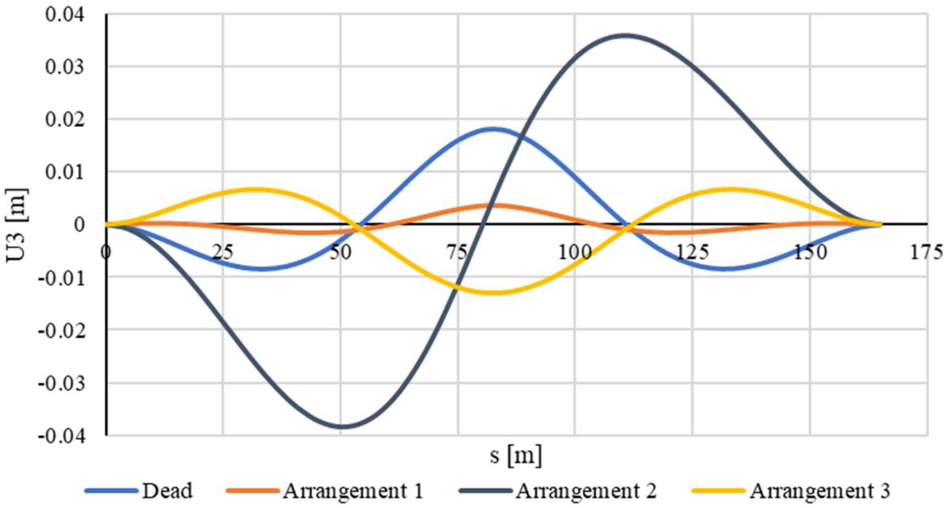

Figure 6.12: Vertical deflections plot due to dead load and the three load arrangements

At this point, seems natural to ask if a uniform depth section of the arch would lead to different results. Therefore, it has been assigned the average arch dimensions (4.00m x 2.42m) to the model and the load arrangement 1 has been performed. Results are reported in Fig. 6.13. The advantage of the variable section is evident, the deflections compared to the uniform section are one order of magnitude lower resulting in a better design choice.

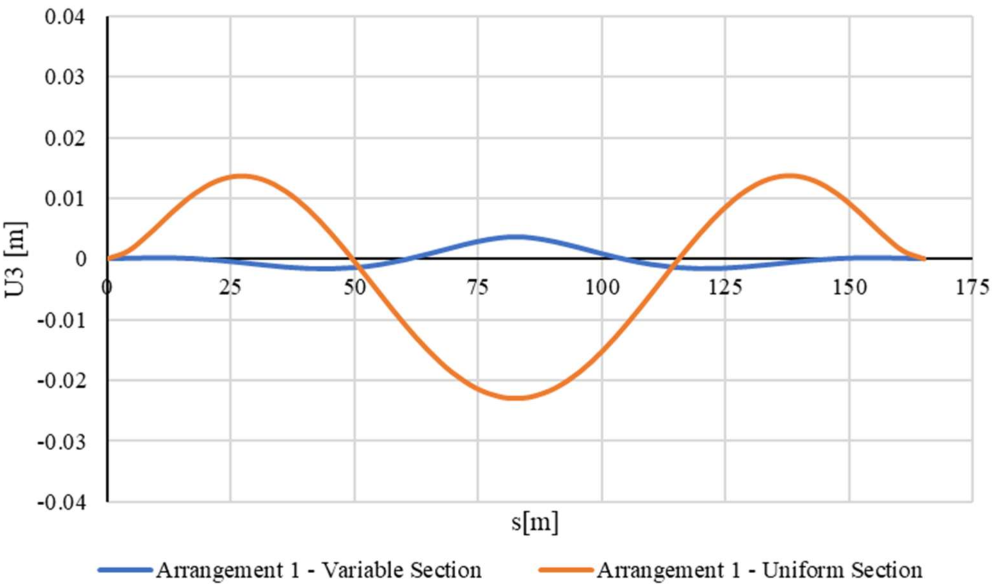

Figure 6.13: Vertical deflections plot due to dead load and the load arrangement 1 for both variable and uniform sections

6.2.8 Bending moments

Let's now consider the three load arrangements reported in Fig. 6.6-8 and evaluate the bending moments behavior, trying to validate the expected previsions.

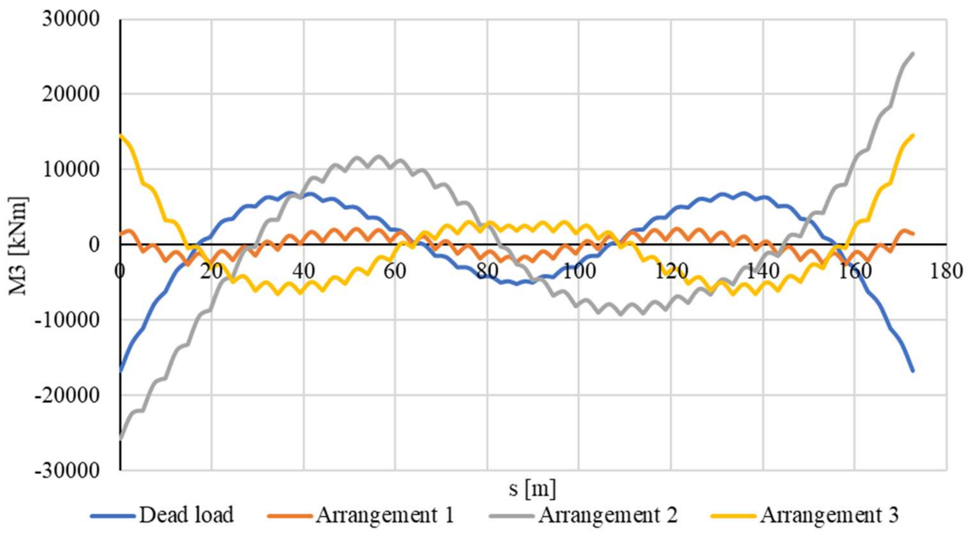

Figure 6.14: Bending moments due to dead load and the three load arrangements

As can be seen from the graph the bending moment induced by the dead load of the arch is quite high, it reaches values of -16661 kNm at the footings and 3458 kNm at quarter point, but, considering the load arrangement 1 where all the other self-weight of the structure are included as the deck and columns both with permanent non-structural elements and live load, the bending moment's values become practically null. This important result asserts the correct design process in which the shape of the arch follows the pressure line derived by the application of dead loads. According to this last observation, it can be noticed that every load applied with the same shape of the one of the dead loads will not give peak moments. Moreover, arrangements 2 and 3 have been investigated. In Tab. 6.8, there are reported the values of bending moments in the three load arrangements plus the dead load ones. As expected from the arrangement 2, the minimum bending moment has been found at the springing section (-25658 kNm), moreover, the maximum positive value at crown has been obtained from arrangement 3, despite a greater value in absolute terms from dead load configuration which can have a relevant role during the construction process, if the load configuration would be that.

	Section	Dead Load	Arrangement 1	Arrangement 2	Arrangement 3
Springings	x=0	-16661	1454	-25658	14500
Quarter span	x=l/4	3548	1967	11738	-1630
Crown	x=l/2	-5135	-2282	-2535	1908

Bending Moments [kNm]

Table 6.8: Bending moments due to dead load and the three load arrangements at crown, quarter span and springings

6.2.9 Axial force

Regarding the axial force induced by the three load arrangements, the most severe condition expected is from arrangement 1, where all the loads are present, and they are uniformly distributed all over the arch. Actually, Fig. 6.15 shows exactly this behavior, moreover, the most critical loaded sections are the springing's one, as can be obtained from theoretical resolution:

$$N_{crown} = H = \frac{q \cdot l^2}{8 \cdot f} \tag{6.3}$$

$$N_{springings} = \sqrt{V_a^2 + H^2} = \sqrt{\left(\frac{q \cdot l}{2}\right)^2 + \left(\frac{q \cdot l^2}{8 \cdot f}\right)^2} \tag{6.4}$$

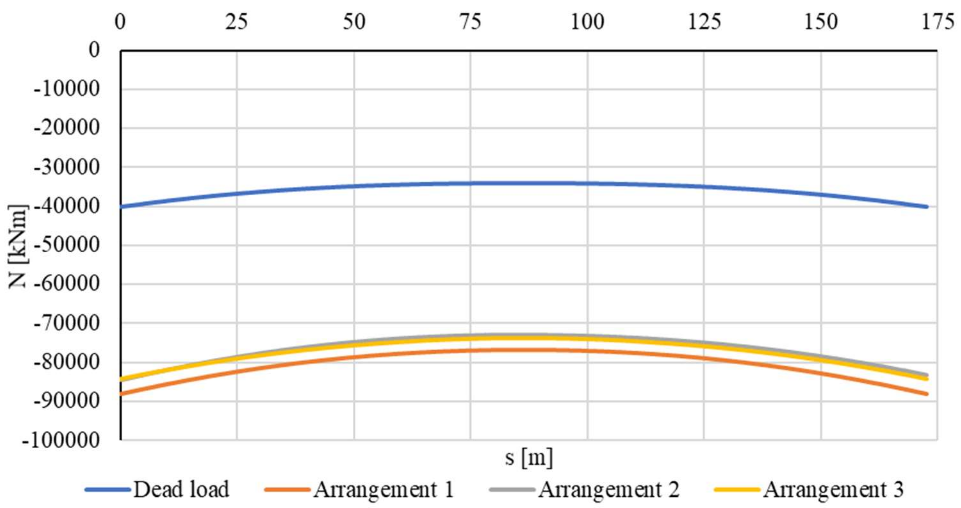

Figure 6.15: Axial force along the arch due to the dead load and the three load arrangements

Results at the most critical section are summarized in Tab. 6.9:

Axial Force [kN]

	Section	Dead Load	Arrangement 1	Arrangement 2	Arrangement 3
Springings	x=0	-40056	-88087	-84457	-84266
Quarter span	x=l/4	-34658	-77961	-74126	-75084
Crown	x=l/2	-34147	-76689	-72922	-73785

Table 6.9: Axial force at springings, quarter span and crown due to dead load from the three load arrangements

Moreover, it can be observed that the variation of axial load from its lower value at crown to its greatest value at the springing lines, is not high, that is explainable by the low rise of the arch. Therefore, for high rise arches, a much lower horizontal thrust is expected despite a bigger variation of axial load toward the footings, on the contrary, for low rise arches, a high horizontal thrust is transmitted to the footings with more stressed sections trough lower variation of axial load.

In Fig. 6.16 there is reported the comparison in terms of axial load between two arch rise situations, in order to study the variation of the horizontal thrust if varying the rise. Thus, the rise of Tiemblo (22m) has been raised up to half of its span length (82.50m) to obtain a semi-circular arch. The graph is plotted versus the develop of the arch on the horizontal direction and the load configuration selected is the self-weight of the arch assumed with the same sections (average Tiemblo section 4.00m x 2.42m).

The choice of the rise is not always free to the designer, moreover, the horizontal load transmitted to the footings is a relevant consequence.

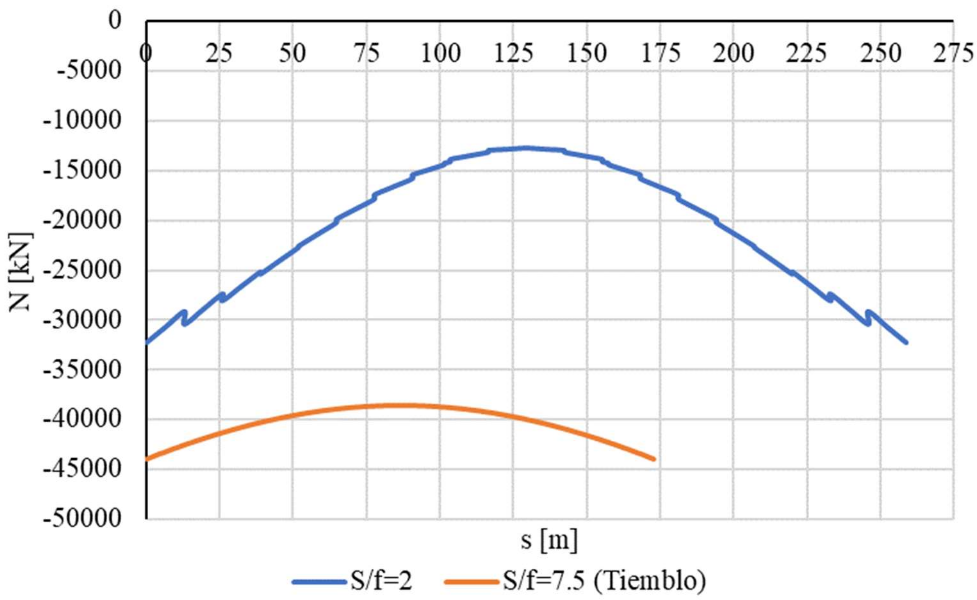

Figure 6.16: Comparison of axial forces along the arch under arch self-weight for two S/f configurations

6.2.10 Ultimate Limit State - M-N interaction domain

For the purpose of the study, a quick evaluation of the bending moment – axial force interaction domain is presented, with the aim to investigate the level of stress of the most critical section: at springing line (x=0), at quarter point (x=L/4) and at crown (x=L/2).

The assessment has been run in the Ultimate Limit State following the current Eurocode 0 – Tab. A1.2(B)(*Eurocode 0 - Basis of Structural Design*, 1990) with the partial safety factors:

$\gamma_{Gj,sup} = 1.35$ if the total resulting action effect is unfavorable

$\gamma_{Gj,inf} = 1.00$ if the total resulting action effect is favorable

$\gamma_{Q} = 1.50$ where unfavorable (0 where favorable)

In order to study the most critical situation concerning M-N assessment, the three load arrangements reported in Fig. 6.6-8 are investigated with their partial safety factors:

- Arrangement 1, maximum compression value of axial force (N<0 for compression);
- Arrangement 2, maximum bending moment at springing section;
- Arrangement 3, maximum bending moment at crown section;

The self-weights of the structure and permanent non-structural load act always on the structure by their nature, therefore, they will be multiplied by unfavorable coefficients where the structure must be loaded as usually done with live loads.

The reason of the load arrangements has to deal with the seek of maximizing and minimizing the solicitations on the arch, through the application of influence lines.

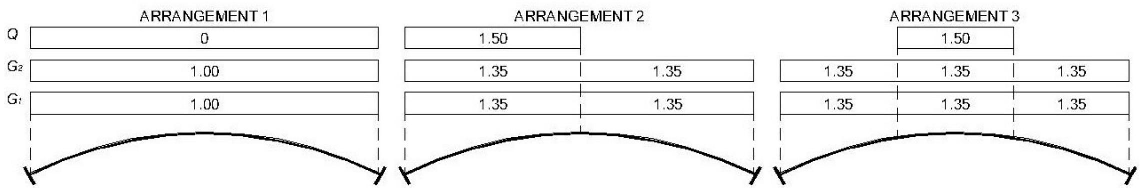

Figure 6.17: Load arrangement configurations

Results are reported in Tab. 6.9:

Arrangement 1			
	x=0	x=l/4	x=l/2
N_{Ed} [kN]	**-79566**	**-71405**	**-69141**

Arrangement 2			
	x=0	x=l/4	x=l/2
M_{Ed} [kNm]	**-32392**	**10869**	-1586

Arrangement 3			
	x=0	x=l/4	x=l/2
M_{Ed} [kNm]	22014	-8620	**3280**

Table 6.10: Results obtained from three load arrangements

After having identified the N_{Ed}-M_{Ed} couples (Tab. 6.10, bold values) it is now possible to compute the M-N interaction domain and verify the assessment of the three sections. The resisting domain has been obtained by VCASlu by Prof. Gelfi, which results as an output after having defined the properties of the sections. These sections are different both in terms of external dimensions, the depth varies, either in longitudinal and transversal reinforcement, therefore, it is expected to obtain a smaller resisting domain moving toward the crown where the section is smaller.

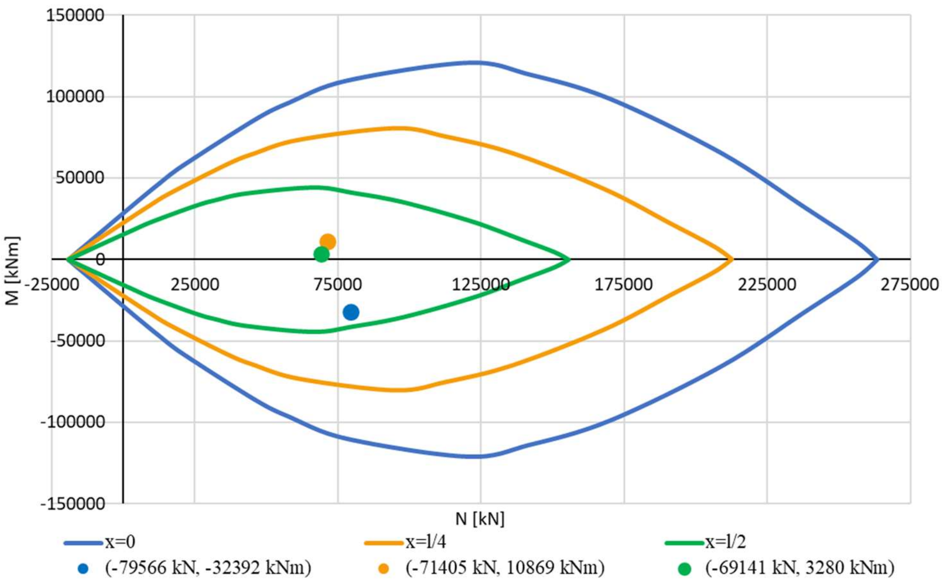

Figure 6.18: M-N interaction domain at springings, quarter span and crown for reinforced sections

Each N_{Ed}-M_{Ed} couple lies inside its resisting M-N domain, therefore the sections pass the assessment. Observing more in detail the domains, the states of stresses are quite far from their resisting boundaries, so perhaps, a lower concrete area could be use. This important consideration will be a key point of the proposed preliminary design method, in the next chapters. In order to have an idea about how far the couples actions are from the resisting boundary, there are reported the safety coefficient evaluated as M_{Rd}/M_{Ed} assuming a constant axial force:

	Reinforcement	
	YES	NO
Section	M_{Rd}/M_{Ed}	M_{Rd}/M_{Ed}
x=0	3.40	2.54
x=l/4	6.76	4.95
x=l/2	13.52	7.48

Table 6.11: Safety factors for bending moments assuming a constant axial load path

In the above table there are reported the results for both conditions with reinforcement and without reinforcement. The arch works mostly in compression, therefore, the expected amount of longitudinal reinforcement is quite low, resulting in a quite useless contribution at springings where the axial force is greater and becomes more important at crown, where axial force is lower and the resisting area of the cross-section is lower too. Here below there is reported the M-N interaction diagram with the resisting domains obtained without any reinforcement. As expected, the action couples N_{Ed}-M_{Ed} are inside each cross-section resisting domain.

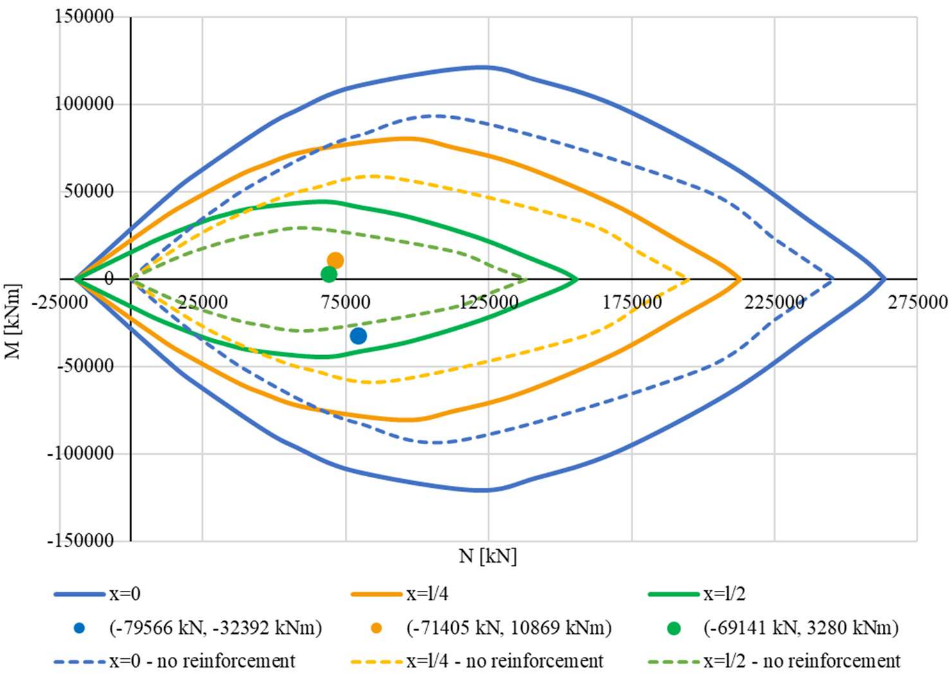

Figure 6.19: M-N interaction domain with the resisting domain obtained without reinforcement in the sections (dot lines)

Actually, the designer H. Corres Peiretti explained the choice to use such a great solid section compared for example with a hollow one because of its simplicity during construction stages and of its lower execution cost. Moreover, the Tiemblo bridge is indeed a singular case in the overview of Spain bridges, as it is very common to find ones with a lower span length built with a hollow arch cross section.

6.3 Reinforcements

As briefly said before, no great amount of reinforcement is needed in the arch as it is an element mostly subjected to compression. However, the use of steel reduces creep and gives a minimum tensile strength (Nettleton & Torkelson, 1977). Let's now evaluate the amount of percentage of reinforcing steel among the 17 segments that has been cast during the construction of the arch. As an example, there is reported the reinforcing steel distribution of the section 1-1 of the first segment:

Reinforcement

Longitudinal					Transversal				
Position	Layer	Quantity	Area [mm^2]	Tot [mm^2]	Position	Layer	Quantity	Area [mm^2]	Tot [mm^2]
Top	1	27φ25	13254	22089	Lateral left	1	φ20a0,15	314	628
	2	18φ25	8836		Lateral right	1	φ20a0,15	314	
Bottom	1	27φ25	13254	22089					
	2	18φ25	8836						
Lateral left	1	21φ25	10308	17671					
	2	15φ25	7363		Overlapping left (btw segments)	1.50	[m]		
Lateral right	1	21φ25	10308	17671	Overlapping right (btw segments)	1.50	[m]		
	2	15φ25	7363						
Total				79522					

Table 6.12: Reinforcement amount of the section at springing lines

The reinforcement percentages with respect to the concrete cross sections are evaluated now for each section in the following table:

Section [-]	Segment length [m]	Depth [m]	Width [m]	Long [mm^2]	Transv [mm^2]	ρ [-]
1	4.90	3.10	4.00	79522	628	0.6%
2	4.90	3.02	4.00	79522	628	0.7%
3	4.90	2.94	4.00	79522	628	0.7%
4	4.90	2.86	4.00	75595	628	0.7%
5	4.90	2.78	4.00	75595	628	0.7%
6	4.90	2.70	4.00	73631	628	0.7%
7	4.90	2.62	4.00	73631	628	0.7%
8	4.90	2.54	4.00	71668	628	0.7%
9	4.90	2.46	4.00	71668	628	0.7%
10	4.90	2.38	4.00	69704	628	0.7%
11	4.90	2.30	4.00	69704	628	0.8%
12	4.90	2.22	4.00	47615	628	0.5%
13	4.90	2.14	4.00	69704	628	0.8%
14	4.90	2.06	4.00	69704	628	0.8%
15	4.90	1.98	4.00	69704	628	0.9%
16	4.90	1.90	4.00	47615	628	0.6%
17	4.90	1.82	4.00	69704	628	1.0%
18	4.90	1.74	4.00	69704	628	1.0%

Table 6.13: Percentage amount of reinforcement in each section of the 17 construction segments

As can be seen from the above table, the amount of steel is very low with respect to the concrete cross section. The greatest percentage of reinforcement is observed at crown where the cross section is smaller.

The typical reinforcement arrangement of the cross section is like the one reported in Fig. 6.20, where it can be seen the distribution in layers all over each side of the arch.

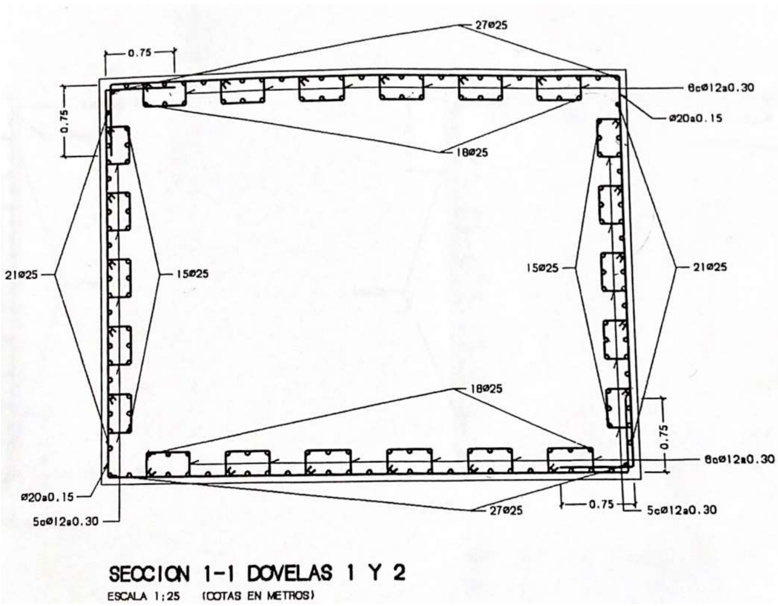

Figure 6.20: Typical arch cross section reinforcement arrangement

Finally, there are reported also the reinforcement quantities in the other structural member of the arch bridge:

6.4 C. Menn formulations

In front of this type of structures, one of the most reliable authors that have deal with its design process is Christiann Menn in his book: "Prestressed Concrete Bridges" edit by Birkhäuser and traduced by Paul Gauvreau in 1990. The Author first explain the way to approach the axis of the arch as close as possible to the pressure line due to dead load and then, he suggests some simple empirical formulation to evaluate bending moment at crown, quarter-point and at springing line to complete the preliminary design process.

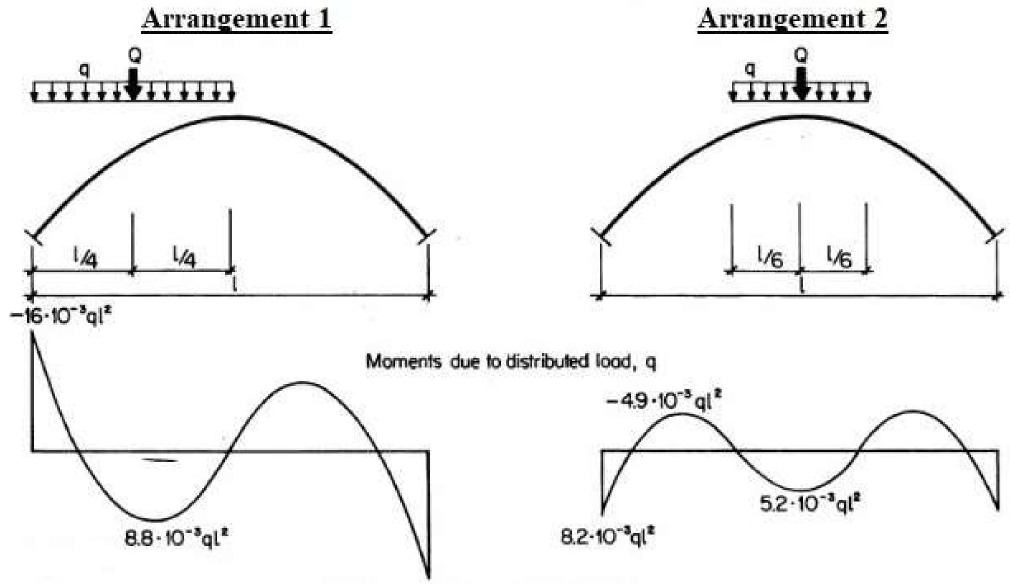

Figure 6.21: Preliminary design formulations for springins and crown sections suggested by C.Menn (1990)

Despite this, by looking at these formulas more deeply, is evident that no references can be found to their applicability (i.e. the rise of the arch, bending stiffnesses ratio between arch and girder, or number of spandrel columns), they depend only to load *Q* and span length *l*. Therefore, the aim of this paragraph is to find out if these common preliminary design rules suggested by *C. Menn* for arch bridges provide close results with those obtained by a FE model, taking as reference the Tiemblo bridge, exploiting their limits of applicability. In particular, the study has been run varying the following relevant parameters of an arch bridge structure:

- Variation of the arch rise;
- Variation of the number of spandrel columns;
- Variation of bending stiffness ratio between arch and girder;

The results will be shown in tables by comparing, in terms of percentages of errors, values obtained applying C. Menn formulations with the same two load configurations as reported in Fig. 6.21, and values obtained by the models in different study cases under the same load conditions. The load configurations consist of applying a distributed load q as: $q = 48.00 \left[\frac{kN}{m}\right]$.

FE models created with SAP2000 have been used for the purpose with the following assumptions:

- Definition of the material: Concrete C30/35 for all the elements;
- Definition of the sections: 1 uniform average section with real axial stiffness

TABLE: Frame Section Properties 01 - General

SectionName	Material	Shape	Depth (3)	Wdth (2)	Area	TorsConst	$I_X(3)$	$I_Y(2)$	$I_{XY}(23)$
-	-	-	[m]	[m]	[m^2]	[m^4]	[m^4]	[m^4]	[m^4]
Average Section	HA-35	Rectangular	2.425	4	9.7	11.83	4.75	12.93	0

Table 6.14: Frame section properties of an average section

- Definition of the element's typologies: frame elements
- Definition of the constrains: clamped nodes at the start and end of the arch
- Definition of load assignments: uniform distributed load applied on the Z projected axis;

6.4.1 Variation of the arch rise

The first parameter investigated is the rise (*f*) of the arch varying it with respect to the span length (*S*), knowing that the structural response changes significantly according to this parameter, three different cases are shown:

- S/f=10, is the configuration of a very low arch rise;
- S/f=5, is the configuration of a high arch rise;
- S/f=2, is the configuration of a very high arch rise, the round arch;

A FE model of the arch for each configuration has been built, without the superstructure, keeping the geometrical characteristics of Tiemblo as in terms of span length (S), arch section dimensions and material.

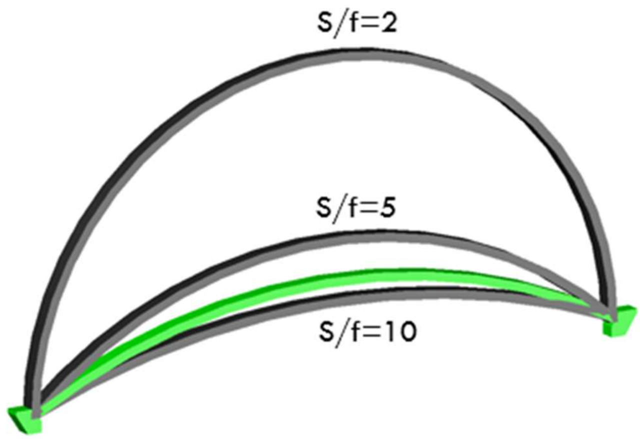

Figure 6.22: Arch rise variation representation, in green the Tiemblo's shape

In green is highlighted the real Tiemblo configuration where its S/f is 7.5.

Load Arrangement	Section	C. Menn	SAP2000							
			S/f =7.5		S/f =10		S/f =5		S/f =2	
		M [kNm]	M [kNm]	Δ [%]	M [kNm]	Δ [%]	M [kNm]	Δ [%]	M [kNm]	Δ [%]
1	x=0	-20909	-19077	8.8%	-19503	6.7%	-16383	21.6%	4488	78.5%
	x=l/4	11500	9733	15.4%	10069	12.4%	10545	8.3%	13133	14.2%
2	x=0	10715	11115	3.7%	11086	3.5%	12631	17.9%	21970	105.0%
	x=l/4	-6403	-6666	4.1%	-6103	4.7%	-6147	4.0%	-5815	9.2%
	x=l/2	6795	7181	5.7%	7081	4.2%	8495	25.0%	17680	160.2%

Table 6.15: Results comparison by changing S/f. In green the real case of Tiemblo

The values obtained by the FE models are very close to those predicted by Menn in case of low arch rise as in the case of Tiemblo and for S/f=10, the errors are practically null, less than 10% in most of the sections. The situation is worst for high rise arches where the errors become higher finding a limit of the formulations.

6.4.2 Variation of the number of spandrel columns

Let's now introduce the interaction between deck and girder. *C. Menn* identifies two type of systems: i) deck-stiffened arch, in which the stiffness of the deck is much greater compared to the one of the arch; ii) stiff arch, in which the stiffness of the arch prevail the whole system stiffness. Moreover, the Author suggests an approximate expression to distribute the moments obtained from either a deck stiffened arch or a stiff arch according to their respective stiffnesses:

$$M^G = M \frac{I^G}{I^G + I^{A,C}} \text{ (girder)} \quad (6.5)$$

$$M^A = M \frac{I^A}{I^G + I^{A,C}} \text{ (arch)} \quad (6.6)$$

Where I^G is the stiffness of the girder, and I^A the one of the arch at crown, according to the same elastic modulus E.

For the purpose, columns and girder have been added to the models according to the executive drawings of the bridge and assuming average sections for arch and columns.

TABLE: Frame Section Properties 01 - General

SectionName	Material	Shape	Depth (3)	Wdth (2)	Area	TorsConst	$I_X(3)$	$I_Y(2)$	$I_{XY}(23)$	Axial Multiplier
-	-	-	[m]	[m]	[m^2]	[m^4]	[m^4]	[m^4]	[m^4]	-
Average Arch Section	HA-35	Rectangular	2.425	4	9.7	11.83	4.75	12.93	0	99999
Girder	HA-35	PC Conc I Girder	0.9	12	6.2	0.97	0.39	44.53	0	99999
Average Column Section	HA-35	Rectangular	0.6	4	2.4	0.26	0.07	3.20	0	99999

Table 6.16: Frame section properties of girder, average arch and column sections

In order to model the union between the arch and the girder at crown, it has been decided, after several attempts, to add columns at the start, quarter, middle and at the end of the union in order to create a solid region as much as faithful to the reality, resulting of 13 columns with a column-span length of 13.75 m.

A representation of half-bridge model is reported below:

Figure 6.23: Half-bridge representation model

The columns are clamped both to the arch and to the girder.

The aim is to investigate if the number of columns affects the reliability of the expression 6.5 and 6.6 proposed by *C. Menn*, in particular, two extreme situations have been considered:

- The number of columns is increased to 23 obtaining a column-span length of 6.9 m;
- The number of columns is decreased to 9 obtaining a column-span length of 20.6 m;

Let's now apply the two load arrangements with the distributed load q as shown in Fig. 6.21, applying it at the girder level. The results reported below refers to the evaluation of the moment of the arch (M^A):

Load Arrangement	Section	C. Menn	SAP2000					
			13 columns		25 columns		9 columns	
		M^A [kNm]	M^A [kNm]	Δ [%]	M^A [kNm]	Δ [%]	M^A [kNm]	Δ [%]
1	x=0	-19322	-17947	7.1%	-17691	8.4%	-16547	14.4%
	x=l/4	10627	9315	12.3%	8259	22.3%	6997	34.2%
2	x=0	9902	10588	6.9%	10708	8.1%	9965	0.6%
	x=l/4	-5917	-5741	3.0%	-5394	8.8%	-5469	7.6%
	x=l/2	6280	6815	8.5%	6682	6.4%	6923	10.2%

Table 6.17: Results of the arch moment varying the number of spandrel columns

In green is highlighted the real case which shows the best results among the cases investigated. Quite good results are obtained in the two other situations confirming the reliability of the formulas despite the different degree of connection between arch and girder. The greater errors are found in the last case, load arrangement 1, where the transferring of the load from deck to arch through a low number of columns lead to more high and concentrated loads resulting in a vectoral composition of forces that is far away from the shape of the arch, unless a constant term.

6.4.3 Variation of the arch-girder stiffnesses ratios

The last check regards the influence of the distribution of the stiffness between arch and girder. The aim is to apply Menn's formulation (6.5 and 6.6) to systems with a girder much stiffer than the arch and check if the distribution of the moments between the two elements relies on those formulation. There are now reported the stiffnesses of Tiemblo bridge elements:

	Stiffnesses						
Arch	$I_{A,crown}$	1.78	[m^4]	→	$I_{A,avg}$	4.75	[m^4]
	$I_{A,springings}$	9.93	[m^4]				
Deck	I_{girder}	0.39	[m^4]				

Table 6.18: Stiffness of the arch and girder

As can be seen from Tab. 6.15, the dominant element that is expected to take the bending moment of the system is the arch, which result with its inertia (I_A) in one order of magnitude greater than the girder one (I_G). Therefore, let's now see what happens to the arch moment (M^A) distribution in presence of a stiffer deck:

- Deck with equal stiffness of the arch;
- Deck with stiffness 5 times of the arch;

First of all, approximated moment formulas from Fig. 6.21 and then distribution of moments (formulas 6.5 and 6.6) among arch and girder have been applied, the results are reported in table below:

Load Arrangement	Section	$I_G/I_{A,avg}$ = 0.08			$I_G/I_{A,avg}$ = 1.00			$I_G/I_{A,avg}$ = 5.00		
		M^A_{Menn}	M^A_{SAP} [kNm]	Δ [%]	M^A_{Menn}	M^A_{SAP} [kNm]	Δ [%]	M^A_{Menn}	M^A_{SAP} [kNm]	Δ [%]
1	x=0	-19322	-17947	7.1%	-10454	-16117	54.2%	-3485	-10298	195.5%
	x=l/4	10627	-9315	12.3%	5750	5867	2.0%	1917	-2583	34.8%
2	x=0	9902	10588	6.9%	5358	8365	56.1%	1786	-4237	137.2%
	x=l/4	-5917	-5741	3.0%	-3202	-3380	5.6%	-1067	-1238	16.0%
	x=l/2	6280	6815	8.5%	3398	4178	23.0%	1133	1665	47.0%

Table 6.19: Results of the moments distribution among the girder and the arch changing their stiffness relation

In green is highlighted the real case of the Bridge which shows the best results among the cases investigated, moreover, the error become higher when moving toward a stiffer girder. A great example of this limit case is Infante bridge designed by Architect Adao de Fonseca in Oporto inaugurated in 2003, which present a $I_G/I_A = 14.00$ due to its very thin arch and stiff high girder. Further consideration will be done in Chap. 7.

Figure 6.24: Infante bridge. It can be observed the slenderness of the arch and the great thickness of the girder

6.5 Deck-arch relation under eccentric vertical loads

The aim of this section is to understand the structural response of the deck-arch system when subjected to longitudinal torsion. A distributed live load of $4kN/m^2$ is applied to half width of the deck as shown in figure below.

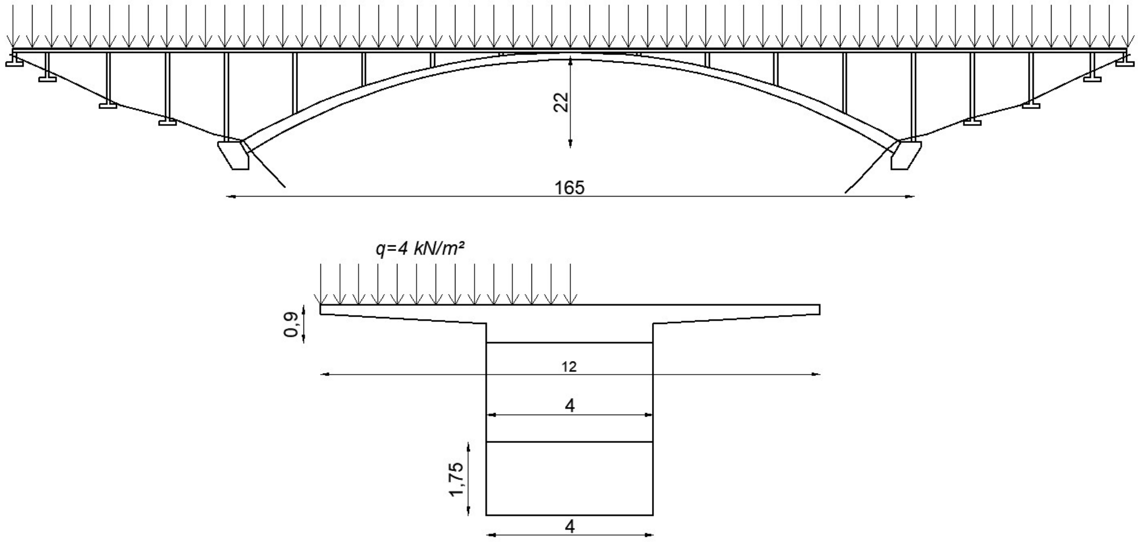

Figure 6.25: Scheme of the vertical eccentric load applied on Tiemblo. Above there is the elevation and below the typical cross section

Neglecting the distortion of the deck, it is possible to focus on the response of the arch system under the eccentric load. Which means to study the interaction between deck and arch for longitudinal torsion. As a first approximation, it can be observed that the exterior torsion M_T is taken by a couple of forces F acting on the deck and on the arch and two torsional moments M_A and M_D acting respectively on the arch and on the deck. In Fig. 6.26 there is reported a representation of the Tiemblo structure where the actions are shown. The quantity of each contribution depends on the respective rigidities and by the following aspects:

- Type of constraints between deck and the access columns;
- Type of constraints of the abutments;
- Presence of expansion joints;
- Type of constraint at the footing of the arch.

Moreover, from the transversal rigidity of the arch it will depend the flexibility of the vertical axis of each basic elements, therefore, the values of the forced F. In the same way, from the torsional rigidities of the arch and the deck it will depend the values of M_A and M_D.

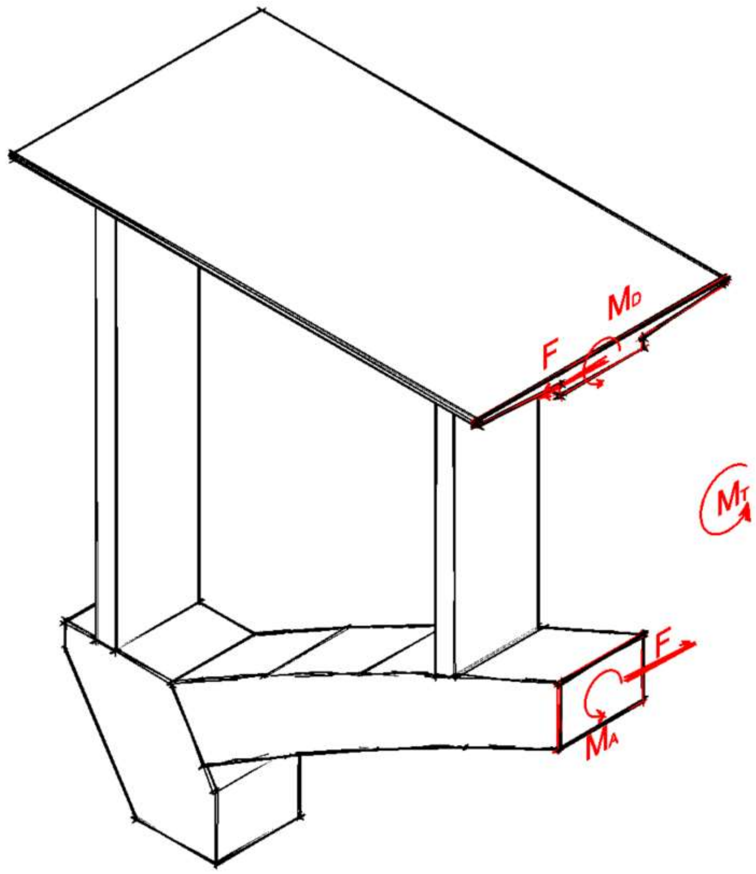

Figure 6.26: Structural response of Tiemblo deck-arch system under vertical eccentric load

As observed in the plot below, Fig. 6.27, the small torsional rigidity of the deck makes the moments law quite equal to those obtained in a girder bridge, with deck embedded on columns under eccentric vertical loads, so that deck moments depend only by the distance between the columns and not by the span of the bridge. Of course, the arch has greater torsional moments. This, together with the variation of the column's height from springings to crown provides an interesting effect. Firstly, the shears in the deck and arch, as shown in Fig. 6.28, are equal and opposite clearly responding to the torsional couple between arch and deck. Here, it happens that there is a sign inversion at quarter span length. The reason is that under eccentric vertical loads, the system deck-arch rotates in the direction of the eccentricity, both showing displacements in the same direction. Moreover, the rotation of the arch provides an additional displacement to the deck but, as a consequence of the variation of the distance between arch and deck from the footing to the crown, the forces F must change their sign in a specific point, so that the total transversal displacement of the deck due to the rotation of the arch can follow the transversal displacement of the arch at crown, where the columns are shorter.

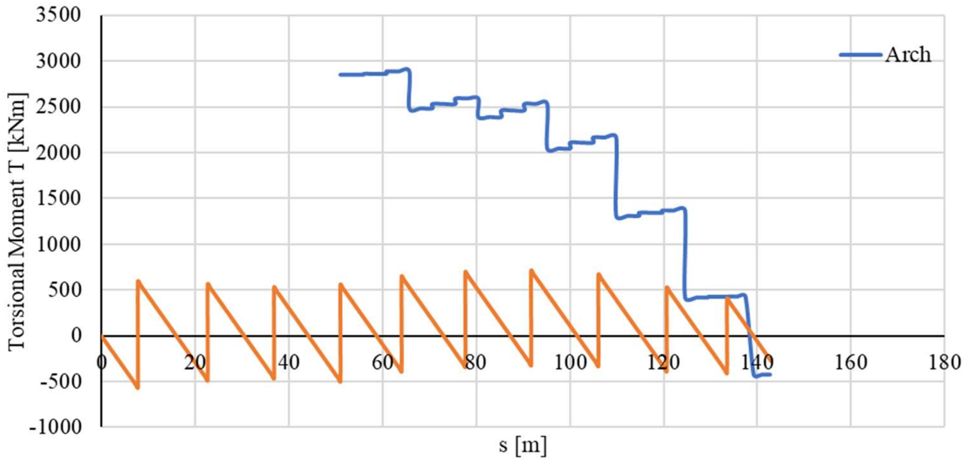

Figure 6.27: Torsional moments of Tiemblo bridge (half) under eccentric vertical load

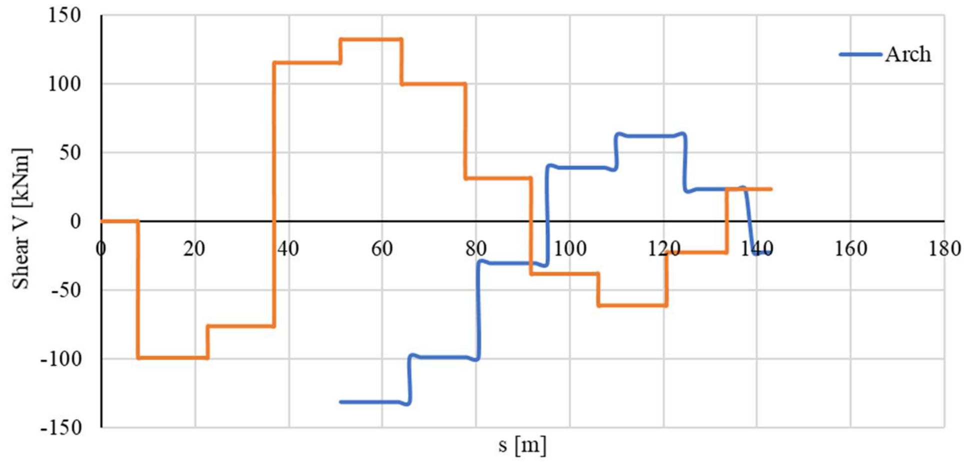

Figure 6.28: Shear forces of Tiemblo bridge (half) under eccentric vertical load

This phenomenon is clearly shown in Fig. 6.29 where the transversal displacements are plotted.

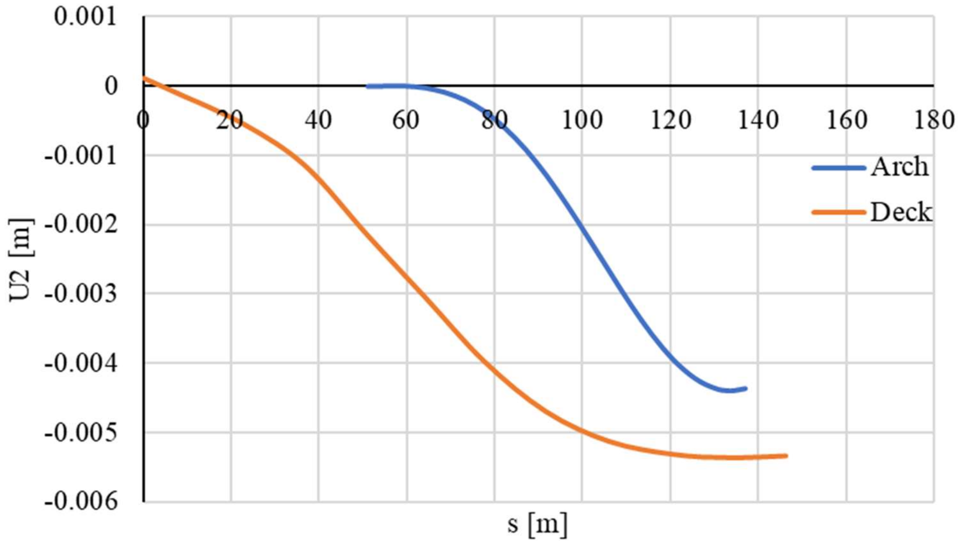

Figure 6.29: Transversal displacement of Tiemblo bridge (half) under eccentric vertical load

The displacements change sign of curvature. In the section between the springings and the quarter span length, the cruvatures are opposite, therefore the mechanical response is that of Fig. 6.26. Near the crown, the forces F change their sign and the torsional moment of the arch must increase rapidly because it has to contrast not only the exterior moment but also that coming from the couples F that acts in the same direction. When the forces F meet the torsional action at quarter span length, the torsional moment of the arch stops to increase. This effect is so important that, from the whole exterior torsional moment, only the 28% is taken by the arch and the rest 72% is taken by the couples F (Manterola, 2006).

6.6 Arch shape geometry

In order to achieve the best structural response from the arch, its axis should be located as close as possible to the pressure line due to dead load (*Menn, 1990*). A brief evaluation of the Tiemblo's pressure line is now presented trying to verify this rule. The process followed is:

- Estimation of dead loads, concentrated and distributed (deck, columns and arch);
- Evaluation of the moments $M_0(x)$ produced by dead loads to a simply supported beam of a length l equal to the span length (Fig. 6.30);
- Search for the horizontal reaction component H assuming the arch is hinged at the springing lines and at the crown;

- Evaluation of the arch ordinates as:

$$y = \frac{M_0(x)}{H} = \frac{M_0(x)}{M_0(l/2)} f \tag{6.7}$$

Here is reported a quick evaluation of the dead loads of Tiemblo bridge:

Deck	
G1 [kN/m]	181.75

Average section arch	
G1 [kN/m]	242.50

Spandrel columns				
	P5-P12	P6-P11	P7-P10	P8-P9
G1 [kN]	976.86	394.60	177.87	53.67

Table 6.20: Dead load of the deck, average section of the arch and of spandrel columns

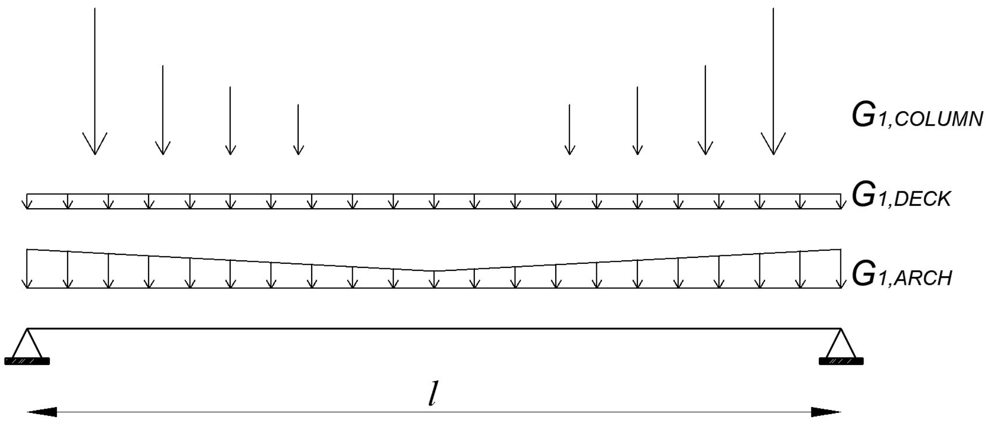

Figure 6.30: Evaluation of the moments produced by dead loads to a simply supported beam of a length l equal to the span length

Thus, the moments produced are:

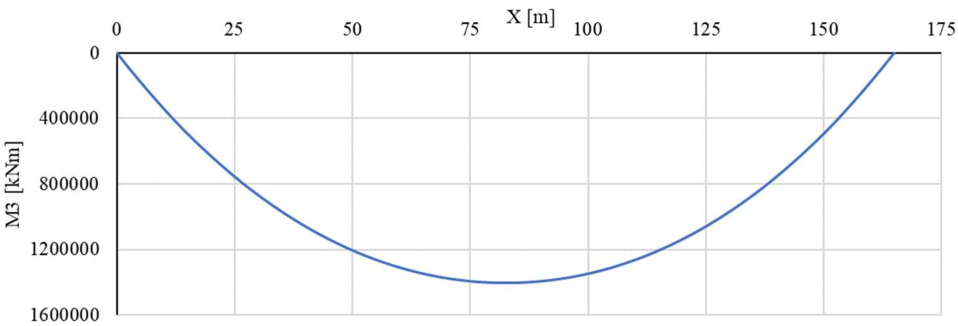

Figure 6.31: Moments in simply supported beam with span equal to Tiemblo's span

Knowing the rise of the bridge f, the horizontal thrust would be the one that respect the relation $y_{max} = f$ therefore, "goal seek" tool in Excel has been used to find it. Here below, there are plotted the axis obtained from the evaluation of the pressure line versus the real arch geometry.

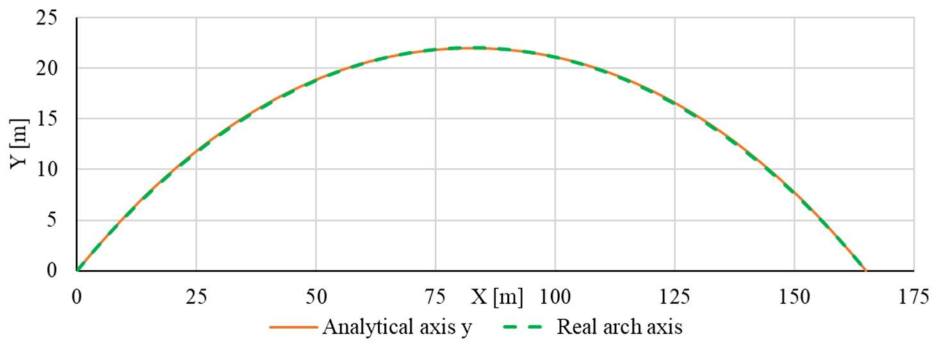

Figure 6.32: Axis comparison between the analytical and the real one

From the plot, is obvious that the real axis of the bridge follows the pressure line as suggested by Menn.

It is worth to mention that for bridges with long spans, the axis of the arch must be as close as possible to the anti-funicular shape due to dead loads as they are predominant against live loads. Vice versa, when live loads become comparable with permanent loads, which states for short span bridge, the actual shape of the arch would be in-between the anti-funicular and the parabola shape.

Regarding what has just been said, by analyzing the order of magnitudes of the loads, it is clear that, despite the simplified calculation of the live loads, dead loads are much greater, quasi 10 times, as reported below:

$G_{1Deck}+G_{1Arch}+G_{1Col}$:	454.20	[kN/m]
$Q_{Traffic}$	48.00	[kN/m]

Where $Q_{Traffic}$ is calculated assuming an average value of $4\ kN/m^2$ spread through the width of the deck (12 m).

For completeness, here there are applied the formulas suggested by Menn to estimate bending moments in the real flexible system, which means discarding the initial hypothesis of infinite axial stiffness useful for the determination of the arch axis. In fact, the axial force induced by dead loads provide axial deformation, which produce a vertical deflection at the crown, δ^C (Menn, 1990). Crown deflection can be approximated as:

$$\delta^C \cong \frac{H(\bar{g})}{EA^{A,C}} \cdot \frac{l(1+3(f/l)^2)}{4f/l} \tag{6.8}$$

Therefore, the moments induced by δ^C to the girder and to the arch are:

$$M^{G,C} = -\frac{1}{2} M^{G,S} \cong \frac{16EI^G}{l^2} \delta^c \quad (6.9)$$

$$M^{A,C} = -\frac{1}{2} M^{A,S} \cong \frac{16EI^A}{l^2} \delta^c \quad (6.10)$$

Concerning the girder, moments obtained by (6.9) have to be superimposed with those coming from dead loads; about the arch, moments obtained by dead loads are supposed to be null if the anti-funicular shape is followed, therefore (6.10) are the only redundant moments produced by the deflection at crown. Data and results are reported in Tab. X

E	35.00	GPa
$A^{A,C}$	7.00	[m^2]
$A^{A,S}$	12.40	[m^2]
$I^{A,C}$	1.78	[m^4]
$I^{A,S}$	9.93	[m^4]
$I^{G,C,S}$	0.39	[m^4]
δ^C	0.09	[m]

Arch		
$M^{A,C}$	3420	[kNm]
$M^{A,S}$	-38154	[kNm]

Girder		
$M^{G,C}$	746	[kNm]
$M^{G,S}$	-1492	[kNm]

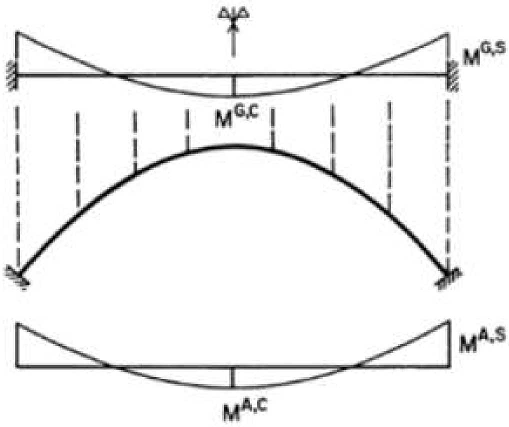

Table 6.21: Results of the bending moments due to vertical deflections at crown and representation of the moments on the right

In the next chapter, the engineering choice adopted for the design of Tiemblo bridge will be studied, in particular the influence of each choice to the structural response of the brige will be highlighted, such as the type of constraints, the difference in rigidity between deck and arch and more. Finally a brief description of the construction method will be shown.

7 ENGINEERING CHOICES OF TIEMBLO DESIGN

The aim of this section is to analyze and understand the most influencing choices that were made during the design of the reference bridge of this research, the Tiemblo. After a brief description of the influence of the type of constraints to the structural response under imposed deformation and concentrated loads, the analysis will be focus on the comparison between two opposite arch bridge structures. The Tiemblo's one, which is composed by a slender deck and a thick arch, and the Infante bridge, situated in Oporto, which comprises a slender arch and a thick deck. The scope of the comparison is to study the differences in terms of stresses and displacements among the two solutions suggesting to the designer the consequences in deciding one or the other type of structure.

7.1 External vinculation

The cross section of the Tiemblo's arch bridge is a solid concrete cross section. It is fixed to the foundation thanks to the high strength soil present in the El Berguillo Reservoir, Avila, where it is built. The aim of this section is now to understand the importance of the degree of constraint of such arch, studying the structural response under vertical loads and imposed deformations by making comparisons with a two-way hinged arch, although is not very common to build arch bridge with great span not fixed to the foundation.

In the longitudinal direction, the arch can be fixed to the foundation, two-way or three-way hinged, when adding a third hinge at the crown.

From the point of view of the internal actions, under permanent and antifunicular loads, the deformations due to the shortening of the concrete provide approximately the same axial force, independently to degree of vinculation.

On the contrary, the type of constraint affects deeply the law of bending moments as it increases with the degree of hiperstaticity of the arch.

7.1.1 Imposed deformation

The same behavior is found for the imposed deformations. In this case, an horizontal displacement of 1 cm is assign to the foundation, Fig. 7.1. Bending moments and axial force are clearly bigger in the case of fixed arch than for hinged arch, as expected, Fig.

7.2. Moreover, this last consideration is still valid for other imposed deformations such as temperature variation, fluage and shrinkage.

Therefore, at all these effects, the internal actions provided by the permanent load are the smaller the less hyperstatic the structure is.

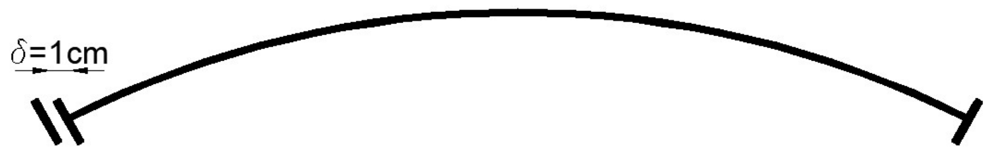

Figure 7.1: Imposed deformation to Tiemblo's arch

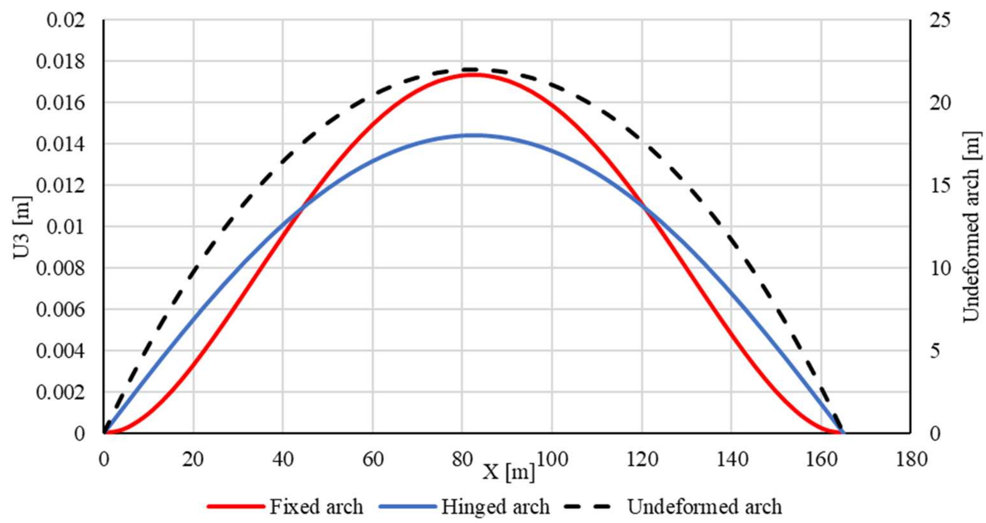

Figure 7.2: Deflections comparison between fixed and hinged arch under imposed deformation of 1cm applied on Tiemblo's arch

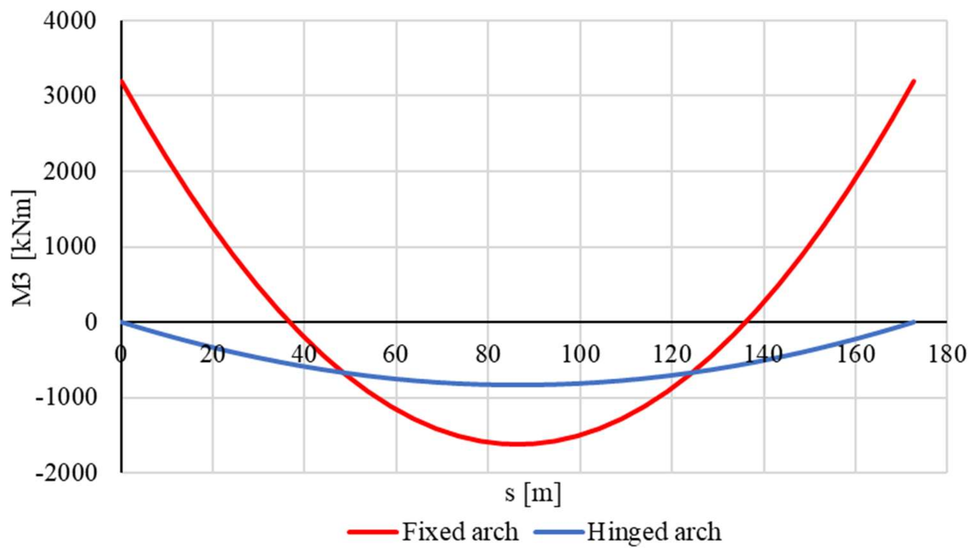

Figure 7.3: Bending moments comparison between fixed and hinged arch under imposed deformation of 1cm applied on Tiemblo's arch

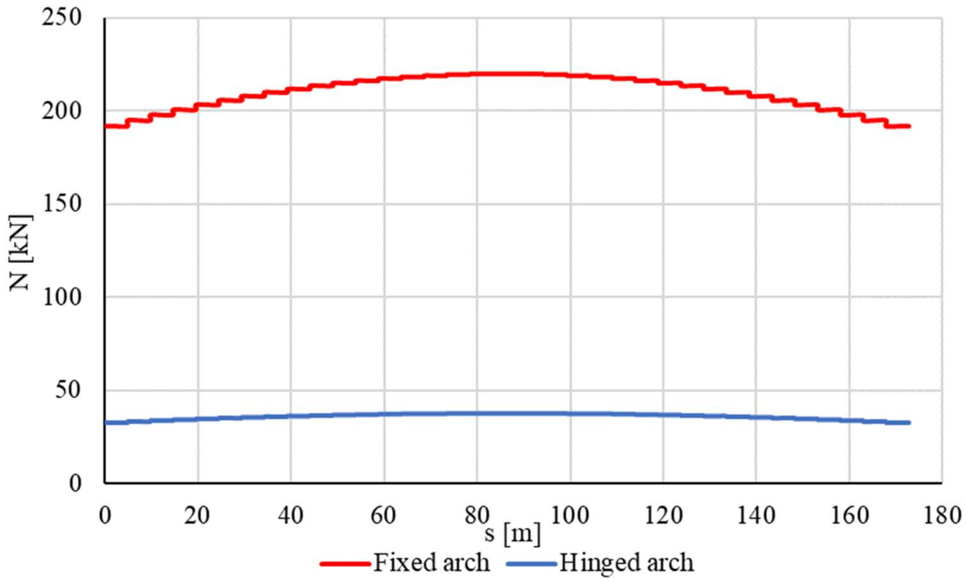

Figure 7.4: Axial force comparison between fixed and hinged arch under imposed deformation of 1cm applied on Tiemblo's arch

As can be seen from Fig. 7.4, the structural response in terms of axial force is completely different among the two configurations of fixed and hinged arch, respectively the first shows greater axial force values rather than the second as well as bending moments. On the contrary, vertical deflections are smaller for fixed arch as the structure is more rigid.

7.1.2 Distributed load

Under distributed vertical load, once again the structural response shows different responses especially for the three-hinged arch.

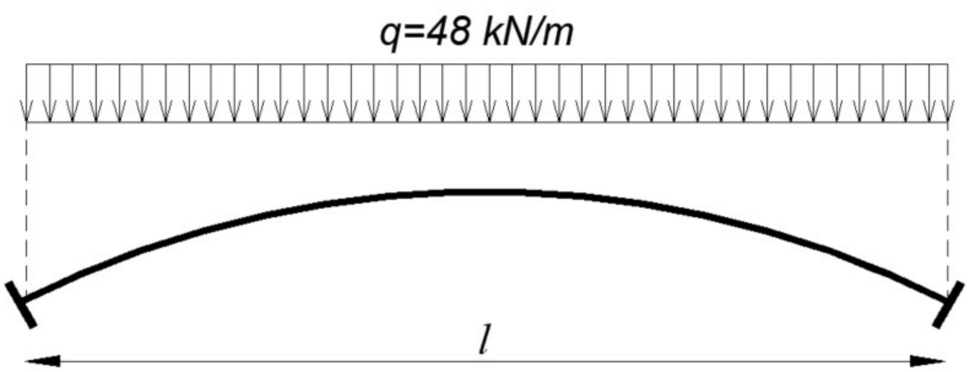

Figure 7.5: Distributed load applied to Tiemblo's arch

Below there are reported the results in terms of vertical deflections, bending moments and axial force. As can be seen from the plots, there are no relevant differences comparing the fixed static scheme with the 2-hinged arch. Significant deflection is observed when looking at the 3-inged arch although the absolute value is about the order of magnitude of $\frac{L}{10000}$ where L is the arch span.

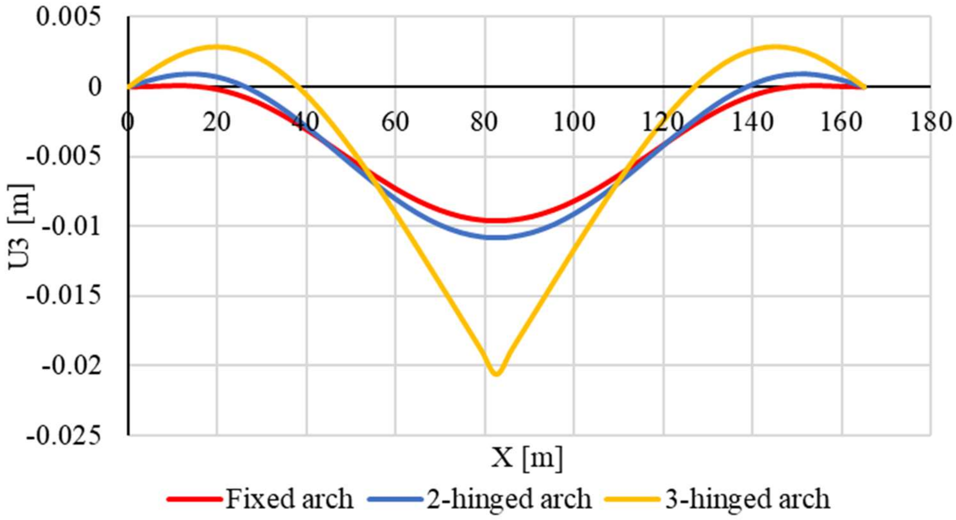

Figure 7.6: Vertical deflections of Tiemblo's arch in three different external vinculation, subjected to distributed uniform load

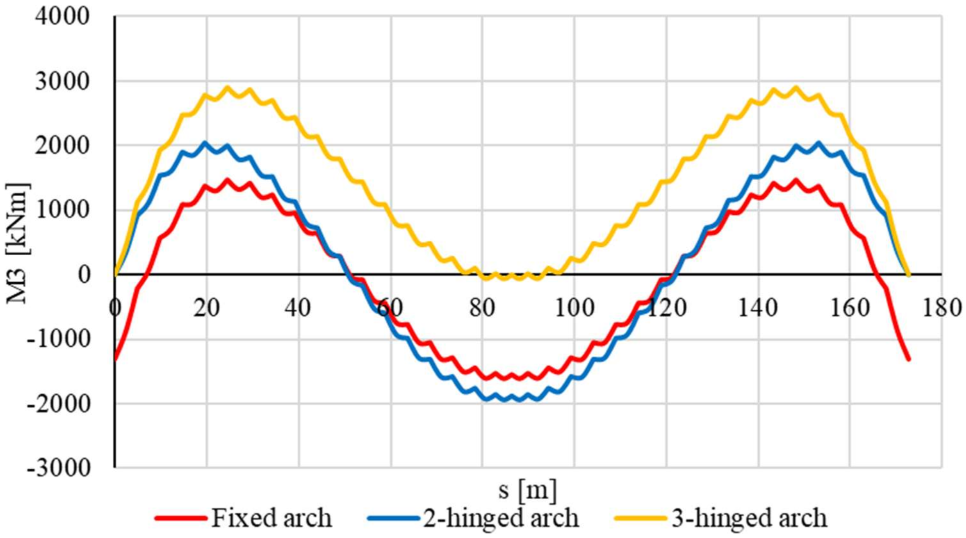

Figure 7.7: Bending moments of Tiemblo's arch in three different external vinculation, subjected to distributed uniform load

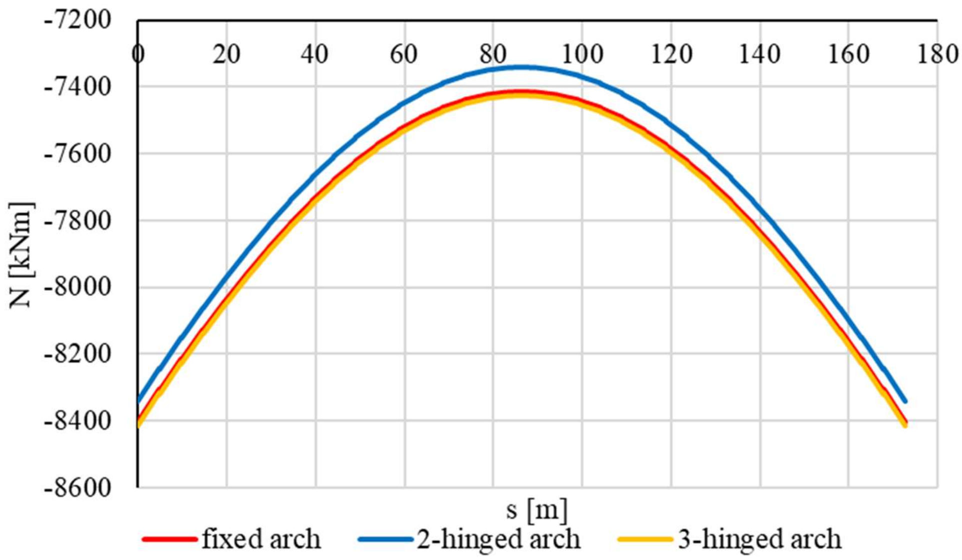

Figure 7.8: Axial force of Tiemblo's arch in three different external vinculation, subjected to distributed uniform load

7.1.3 Concentrated load

Let's now apply a concentrated load as shown in Fig. 7.9. The structural response is now very different among the three types of degree of connection. In the three-hinged arch, the internal actions and the deformations are higher with respect to the fixed and two-hinged arches. The deflection at crown, under a concentrated load applied in midspan, might be 5 or 6 times greater, with the whole arch under negative bending moment, Fig. 7.11.

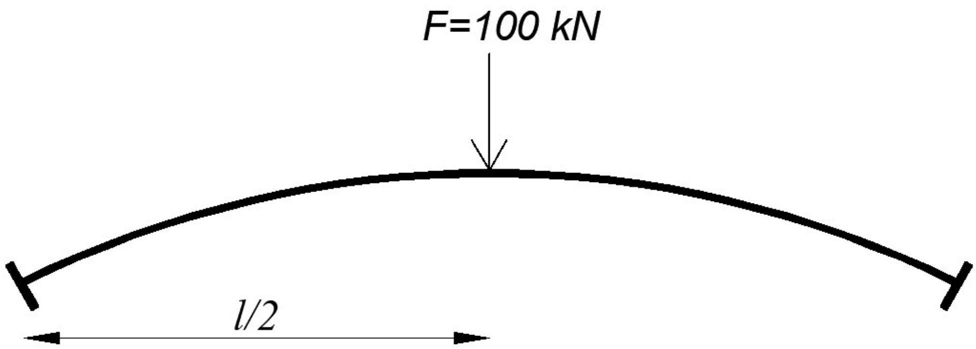

Figure 7.9: Concentrated load applied to Tiemblo's arch

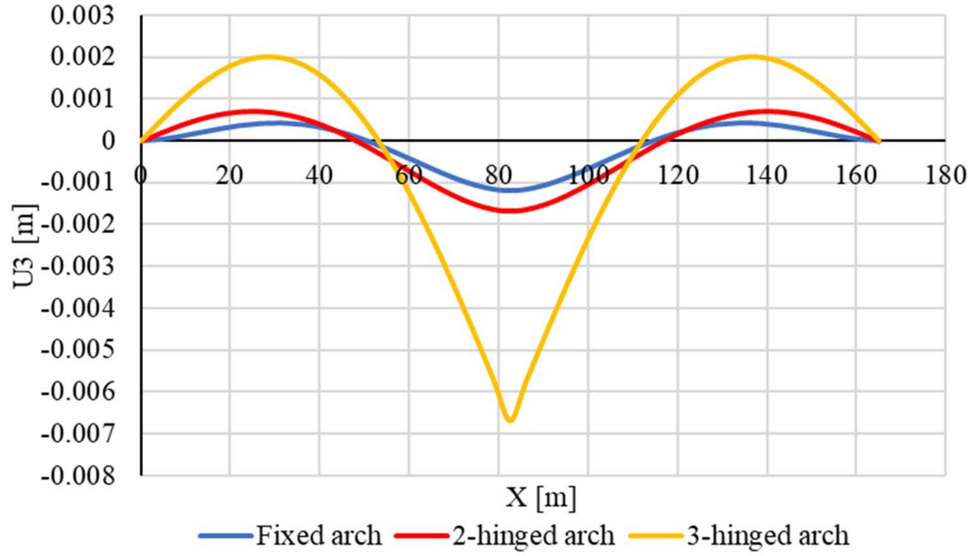

Figure 7.10: Vertical deflections of Tiemblo's arch in three different external vinculation, subjected to midspan concentrated load

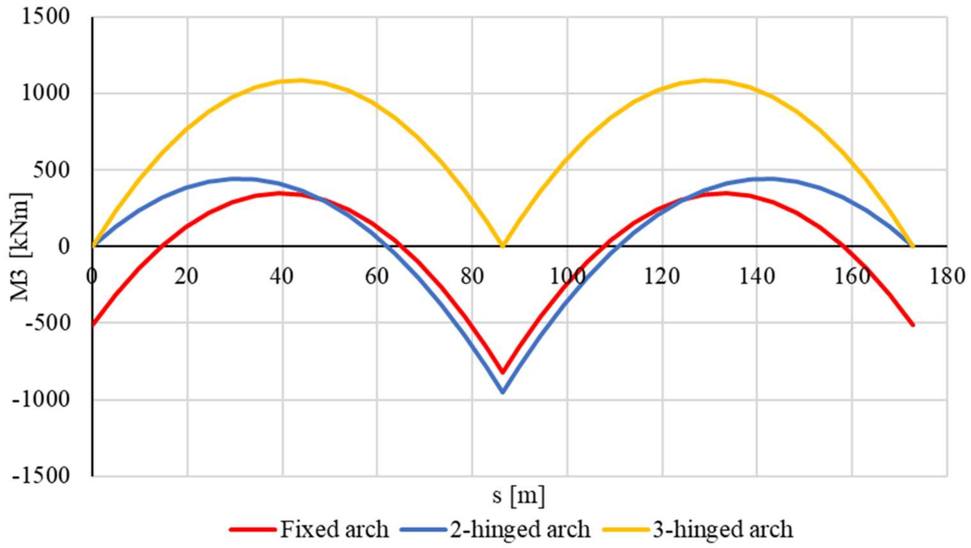

Figure 7.11: Bending moment of Tiemblo's arch in three different external vinculation, subjected to midspan concentrated load

In case of concentrated load applied at quarter-span length, the minimum amount of bending moment is obtained for the fixed arch and vice versa the maximum for the 3-hinged arch. The same occurs for vertical displacements.

Finally, the conclusions are that an arch responds very bad with respect to concentrated loads, as the axis of the arch is far away from the pressure line of such loads, nevertheless, the bending moments are in the order of 4 or 5 times lower than those obtained in a straight beam simply supported over the same span.

7.2 Deck-arch relation under vertical loads

The behavior of the individual arch is not enough to describe a more complex phenomenon as the structural response of an arch bridge. Unless particular cases, the arch is never alone. In its deformation it influences and is influenced by the rigidity of the deck above and by the degree of connection between them. This fact is so fundamental that an arch can be as this as desired, with a very small inertia, since the deck, which must be thick to resist the effect of non-funicolar overloads, stabilizes the arch. Both the problems of instability of the arch in its plane and the effect of non-funicolar overloads hardly affect the stresses in the arch. The inertia of a thin arch bridge is for all these purposes, that of the deck.

In order to validate this statement, it will follow a parametric study in which the inertia of the arch and the deck, and so the relationship between them, are varied.

For the aim, the structural response of Tiemblo bridge will be studied as it comprises a very rigid arch and a thin deck, comparing it with its corresponding opposite Infante bridge designed by Arch. Adao de Fonseca, which is made by a very thin arch and a stiff high deck. In Fig. 7.12 there are reported the typical cross section of the comparative bridges.

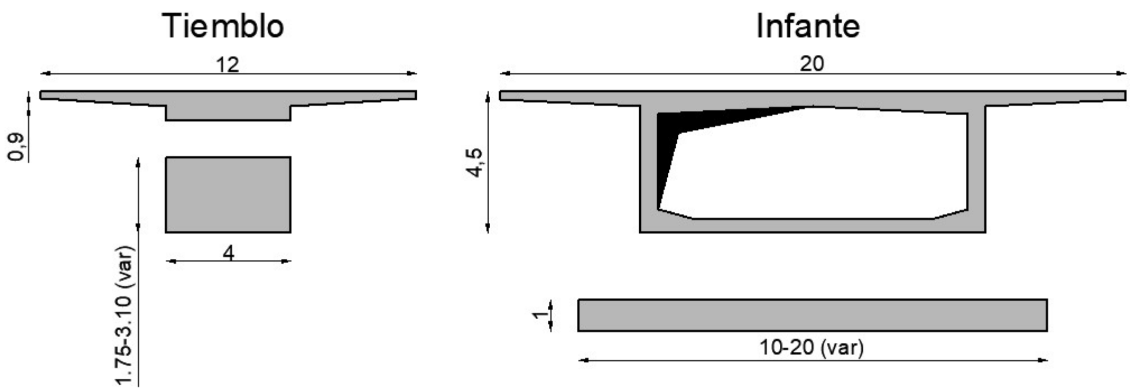

Figure 7.12: Typical cross-section of Infante and Tiemblo bridge, deck above and arch below

The geometrical data as area and inertia of the two sections will be reported in the next paragraph, Tab.7.1.

7.2.1 Influence of the rigidities' relation between arch and deck

Let's now study the structural response in terms of bending moment of the two different arch bridges. Tiemblo is taken as reference bridge and it has been compared with the rigidities of Infante bridge designed by Architect Adao de Fonseca in Oporto. In this way, two limit cases are defined in terms of stiffness distribution among arch and deck. Briefly, the characteristics of the bridges are here resumed:

- Tiemblo: the whole the rigidity is coming from the arch (2.4 x 4 m solid cross-section) with a really slender deck (0.9 m height at centre point);
- Infante: the whole rigidity is hold by the deck which is a box section (4.5 m height) with a really slender arch (1.5 x 10 m solid cross section).

The distribution of the stiffnesses among the two members can be seen in Tab. 7.1. From the ratio I_A/I_D it is clear which member is expected to assume the response to bending of the whole structure.

	A_{Arch} [m^2]	A_{Deck} [m^2]	I_{Arch} [m^4]	I_{Deck} [m^4]	I_A/I_D [-]
Tiemblo	7.00	6.16	4.75	0.39	12.18
Infante	22.50	18.60	4.22	59.70	0.07

Table 7.1: Area and inertia comparison between Tiemblo and Infante bridges.

A FE model has been used as described in section 2.5 where arch, deck and columns are representative of those of Tiemblo. Where the sections varies, as in case of the arch and columns, average values have been adopted, in order to simplify the process.

Then, the section properties have been changed in order to obtain the rigidities of Infante bridge keeping the same span, rise and columns of Tiemblo. The arch is embedded to the foundations resulting in a 3-times hyperstatic scheme and the union between arch and deck is made by columns that are hinged both at the deck and at the arch.

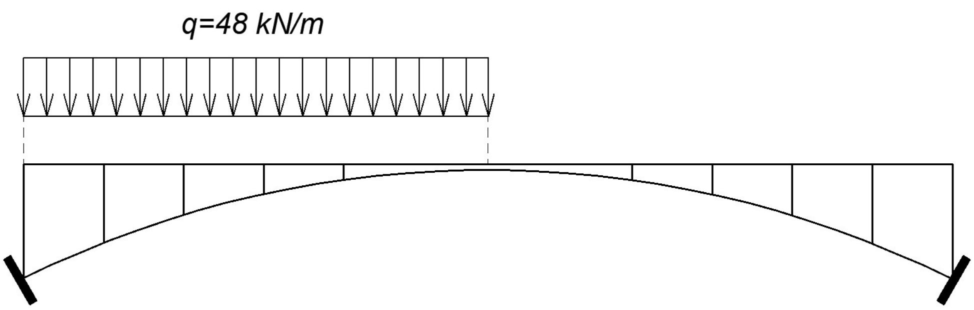

Figure 7.13: Asymmetrical load arrangement on Tiemblo

This load configuration is chosen to shade the bending moments behavior of an arch structure. From Fig. 7.14 and 7.15 is clear that Tiemblo structure shows very high peak moments at foundations despite a lower value at quarter point, moreover, Infante exhibit low moments at foundations despite higher values at quarter point. So that, the soil strength might affect the designer to choose one solution or another. In Fig. 7.10 and 7.11 there are reported the bending moment diagrams first for Tiemblo and then for Infante, under the case of asymmetrical load applied to two identical bridges.

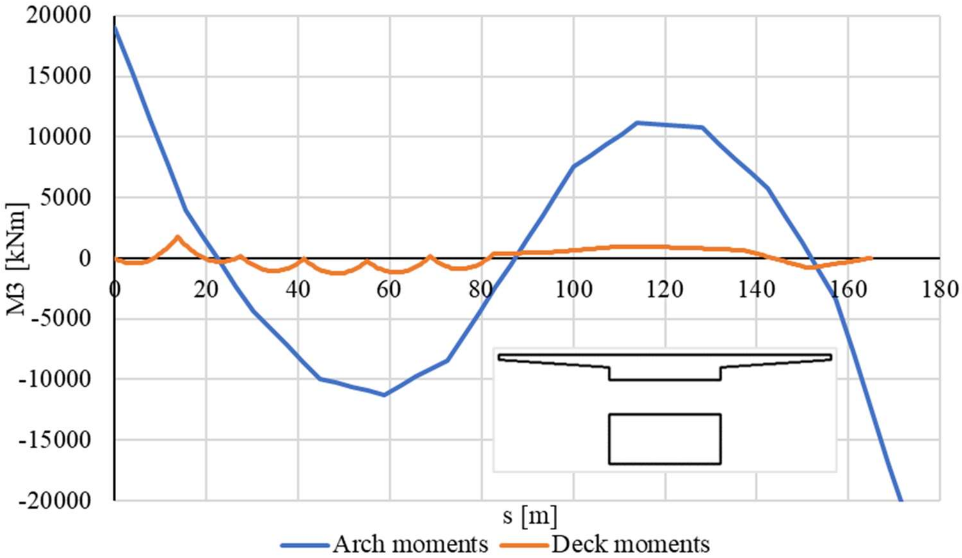

Figure 7.14: Bending moment distribution among arch and girder and typical cross section of the Tiemblo.

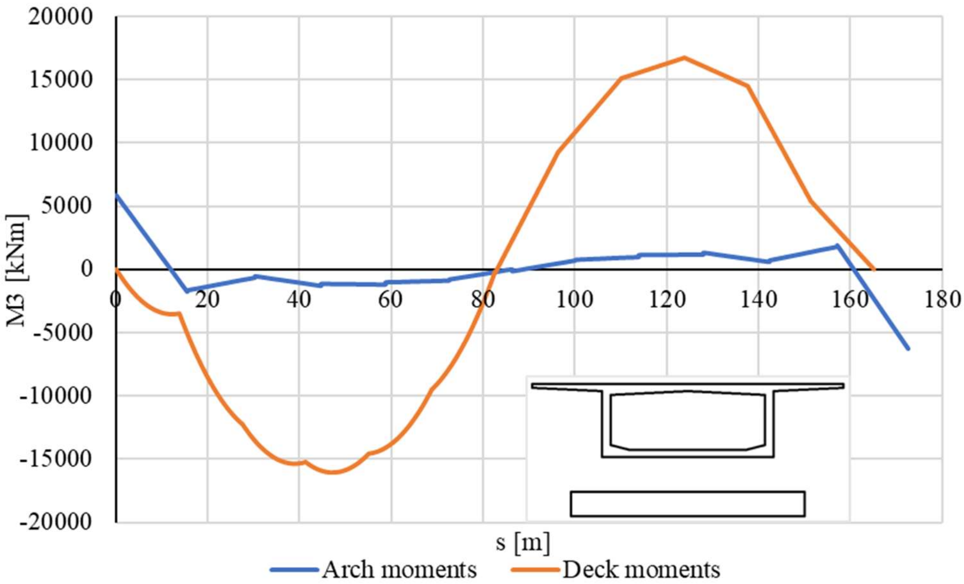

Figure 7.15: Bending moment distribution among arch and girder and typical cross section of the Infante

Results are evident, bending moments coming from non-funicular loads are taken by the element with greater rigidity, the arch or the deck. In the case of Tiemblo, the whole load is taken by the arch meanwhile the deck has the typical bending moment behavior of a continuous beam over simple supports. Morevoer, the opposite happens for Infante bridge, where the deck takes all the bending moment due to its high bending stiffness leaving the arch almost unload. From this consideration, seems more reasonable to choose the first configuration (Tiemblo) more suitable for concrete bridges since the element that carries the compression is the one that must carry the bending.

Moreover, by looking at what happens at the deflections, under the same conditions made above, the exact opposite behavior is noticed, Fig. 7.16. The structure represented by Infante bridge shows a deflection (-0.008 m) that is almost 7 times lower than the one of Tiemblo (-0.058 m). This happens because for Infante bridge, the deck acts like a very rigid beam that spread the load all over the arch. The same cannot happen to the Tiemblo structure which deck transfer the load to the arch as concentrated point loads inducing high moments to the arch as it resists well for antifunicular loads and worst for concentrated loads.

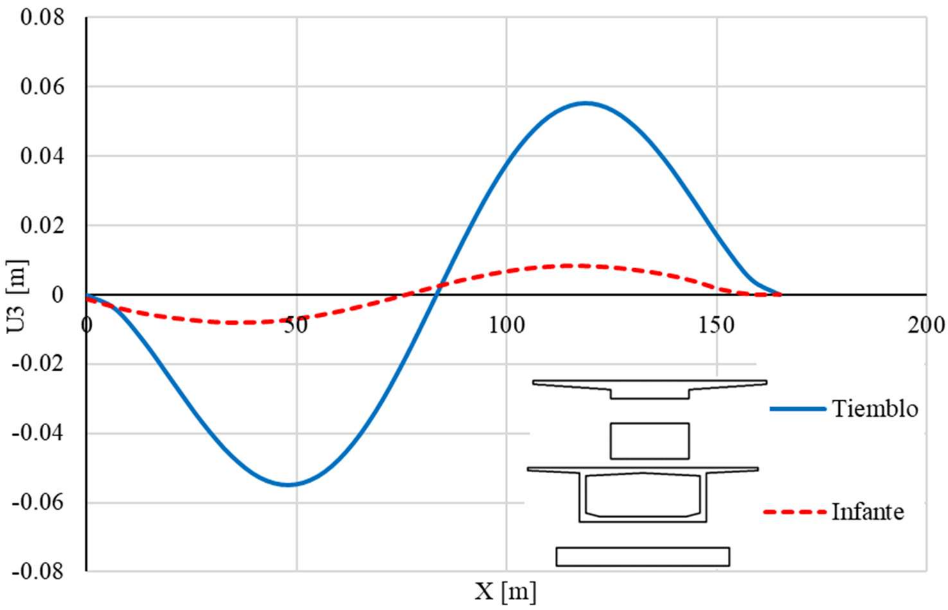

Figure 7.16: Deflection comparison between Tiemblo and Infante structures under asymmetrical load configuration

In the past, in cases of Infante structures, the loads were decomposed in symmetric and asymmetric. The symmetric one was transmitted directly to the arch as funicular load, and the asymmetric stresses only the deck.

Regarding the distribution of the axial force, no difference can be seen between the two different structures, as shown in Fig. 7.17. In particular, all the axial load is taken by the arch as the columns have been considered hinged both at deck and at the arch. Moreover, in the next paragraph, further analysis will be done to the consequences of the degree of connection between arch and deck.

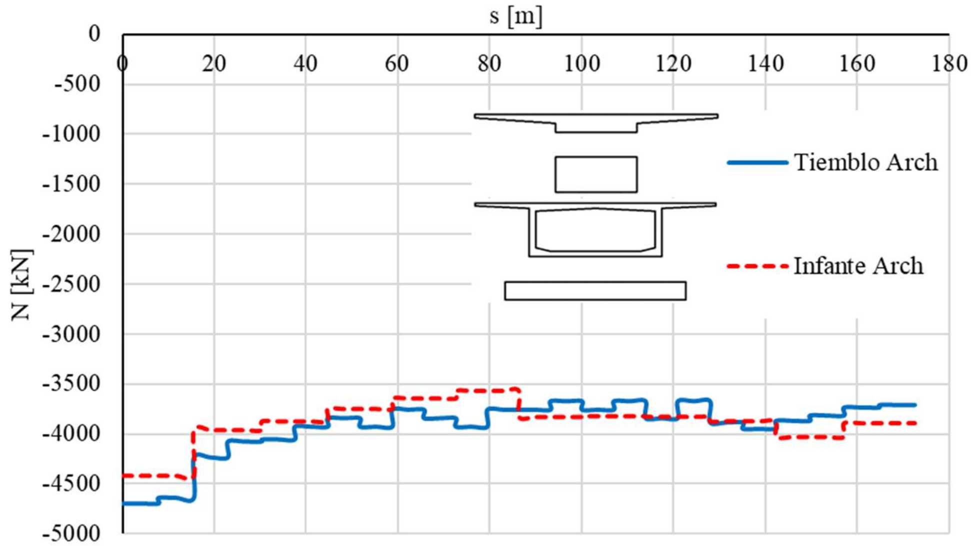

Figure 7.17: Axial load distribution in Tiemblo and Infante arches under asymmetrical load configuration

7.2.2 Embedding of spandrel columns in arch and deck

If, instead of considering the columns hinged, they would be embedded to the arch and to the deck, the structural behavior changes radically. In the first case, their role was to equal the vertical displacement between arch and deck. Now, both elements contribute to the structural response and arch and deck begin to work as a unique element. This behavior can be observed by analyzing the distribution of axial force in the arch and deck. The classic configuration obtained in Fig. 7.17 with hinged columns, becomes the one of Fig. 7.19, under the same load configuration of Fig. 7.13.

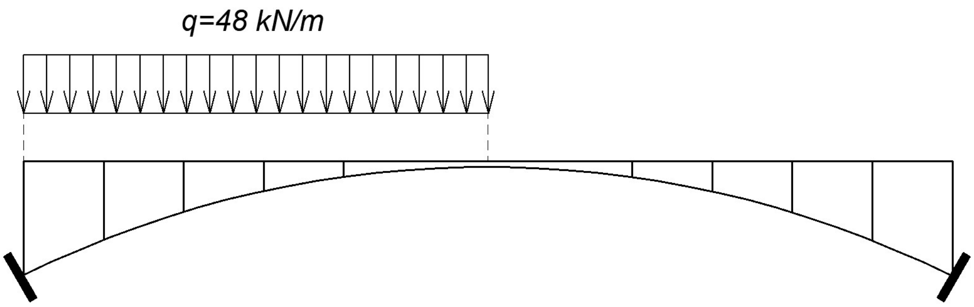

Figure 7.18: Asymmetrical load arrangement on Tiemblo bridge

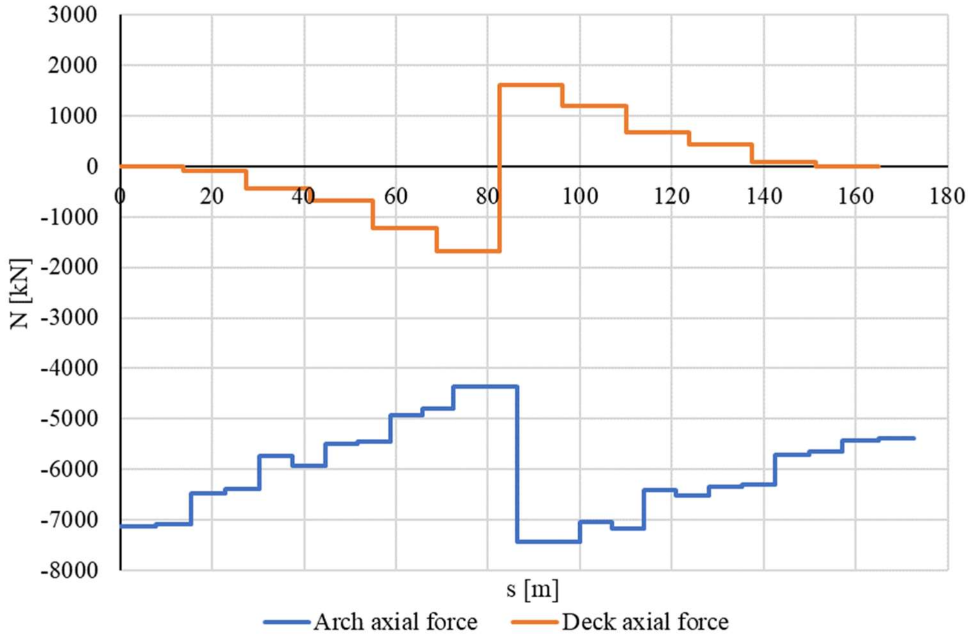

Figure 7.19: Axial load distribution between deck and arch of Tiemblo bridge under asymmetrical load configuration

The resulting plot shows as the high bending stiffness of the shortest pillars in the central area restricts the relative displacement between arch and deck, transferring the horizontal loads on the deck, unloading the arch from it.

The axial load distribution is not only the main consequence of fixing the columns to the arch and deck, interesting results are obtained by looking at bending moments, Fig. 7.20 and at vertical deflections, Fig. 7.21 demonstrating a real joined cooperation between arch and deck. The two main consequences in fixing the columns are:

- there is a clear reduction of bending moment in the arch;
- a significant lower deflection of the structure, quasi the 40% lower.

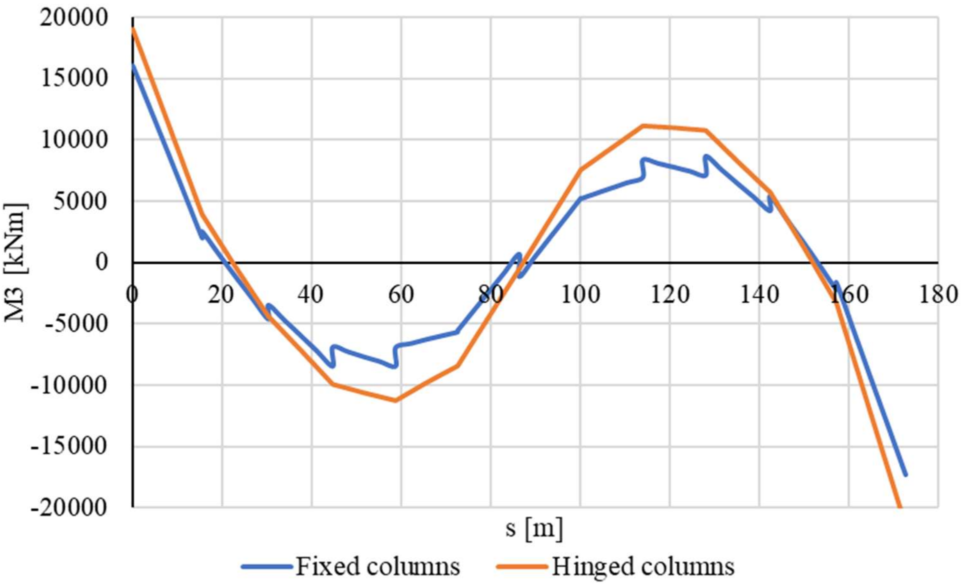

Figure 7.20: Bending moment comparison between the bridge with fixed columns against hinged columns

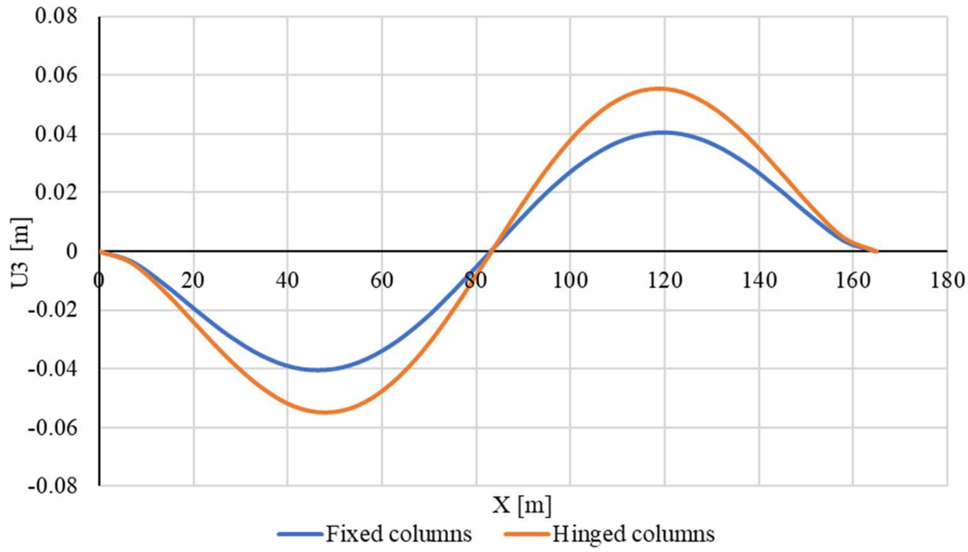

Figure 7.21: Vertical deflection comparison between the bridge with fixed columns against hinged columns

These above described configurations are two limit conditions, in reality, Tiemblo bridge presents a behavior in-between both cases. In fact, the connections of the bridge are made partially by fixed columns and partially by hinged columns, as reported in Fig. 7.22. In particular, the highest columns are embedded between the arch and the deck, meanwhile the last two nearest the crown result hinged to the deck.

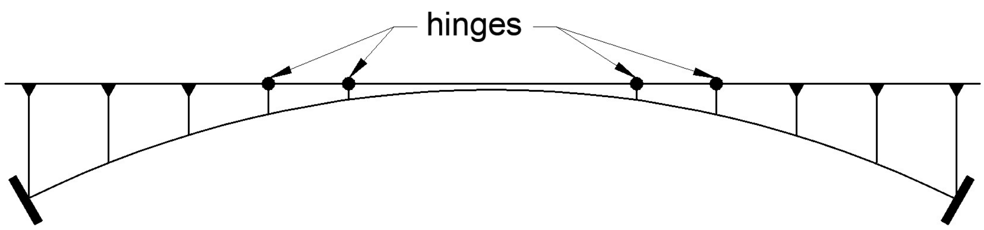

Figure 7.22: Hinge connections of Tiemblo

As expected, the real response of the bridge in terms of vertical deflection, reported in Fig. 7.23, finds out in-between the two limit conditions shown in Fig. 7.21, even though closer to the condition of fully embedded columns.

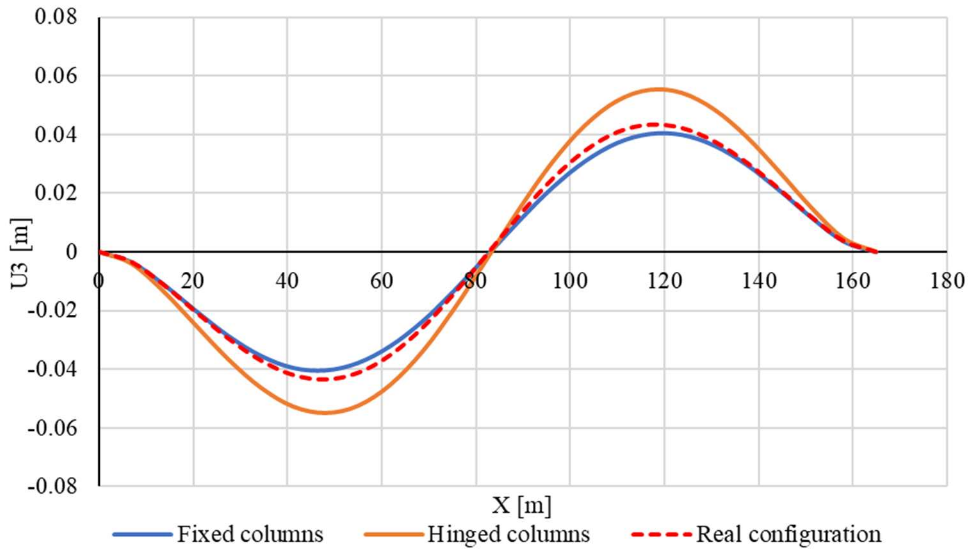

Figure 7.23: Vertical deflection comparison between the bridge with embedded columns, hinged columns and the real configuration of Tiemblo

Let's now analyse what happens to the horizontal longitudinal displacements of the arch and of the deck, for the asymmetric load configuration of Fig. 7.18, both for the case of hinged and fixed columns. The plot is reported in Fig.7.24.

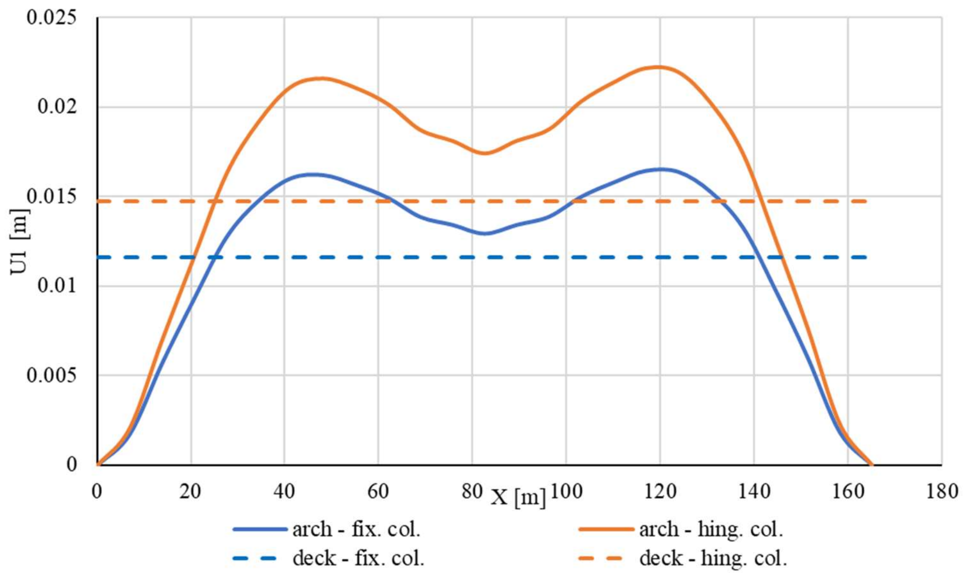

Figure 7.24: Horizontal displacements comparison of deck and arch of Tiemblo bridge with fixed and hinged columns

In both cases, all the points of the deck experiment the same horizontal constant displacement toward right. Both at the beginning as at the end, the horizontal displacements of the arch are much lower than those of the deck, but they it increases as moving toward the central part, clearly overpassing those of the deck.

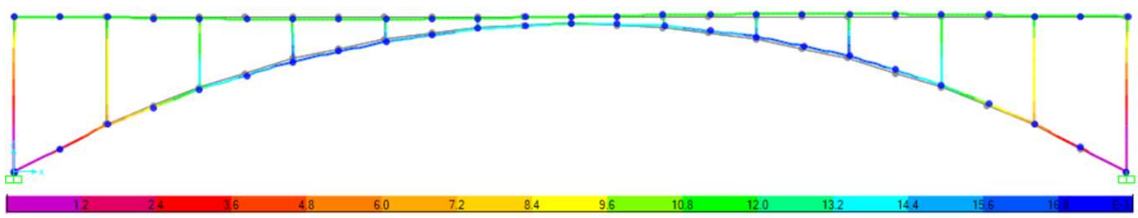

Figure 7.25: Horizontal displacement Ux under asymmetric load

This horizontal movement does not provide any internal actions to the columns when they are hinged. Vice versa, when the columns are fixed, they oppose at this deformation with their rigidity. In this way, the columns are strongly stressed in bending and shear, producing a loss of axial force in the arch and an important value in the deck.

Actually, the real distribution of hinges reported in Fig. 7.22 leads, once again, to a midway behavior as reported in Fig. 7.26, with the real solution revealing closer to the condition of fully embedded columns. The main advantage is clearly a more rigid structure that allows lower displacements.

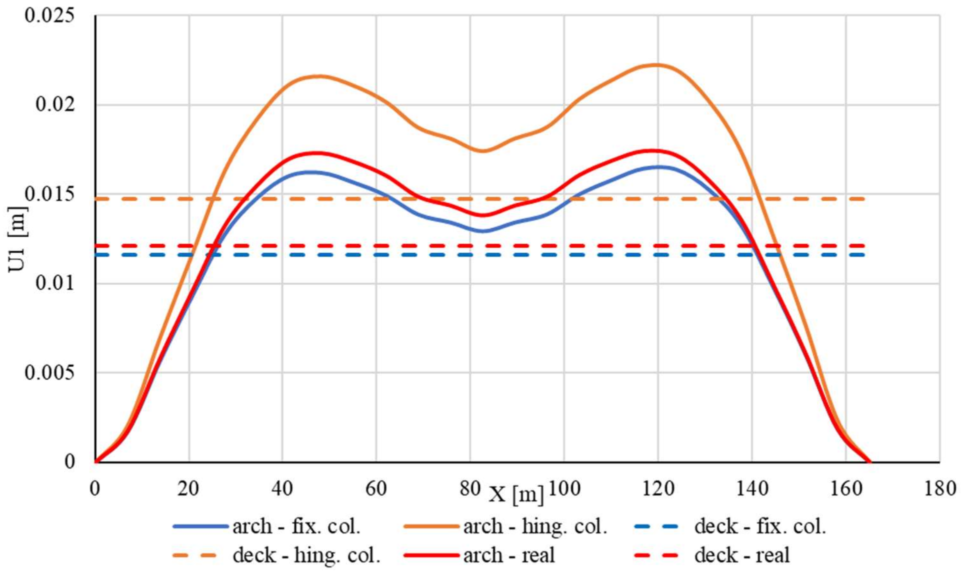

Figure 7.26: Horizontal displacement U1 of Tiemblo bridge under asymmetric load configuration

Thus, the choice of the connection between deck and arch among a fixed solution and a hinged one may lead to many consequences on the horizontal displacements of the bridge. For example, it affects the type of joint required to withstand the displacement or the choice of bearings to adopt

Here below, there is reported the technical drawing of the joint designed for Tiemblo, located at the right end of the bridge. It is possible to see the max allowed value of horizontal displacement equal to 100 mm.

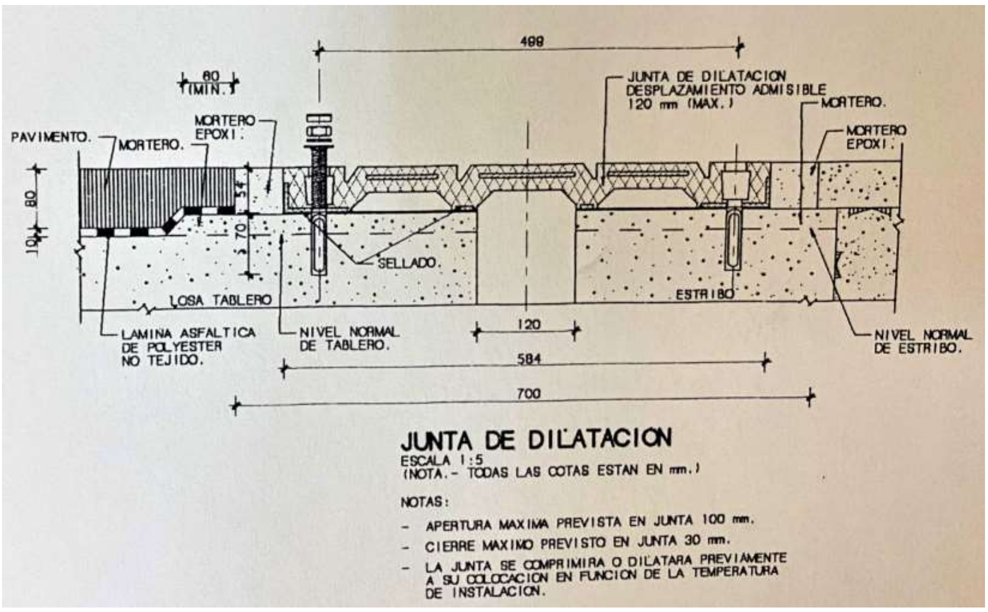

Figure 7.27: Technical drawing of the joint of the Tiemblo bridge situated at right abutment

When the load configuration is symmetrical, Fig. 7.28, this problem does not disappear because even in this case there are horizontal movements in the arch and null in the deck. In the plot there are once again reported the two configurations of connection between deck and arch: through fixed columns and hinged columns. As expected, the structure with fixed column provides slightly lower displacement values as it is more rigid.

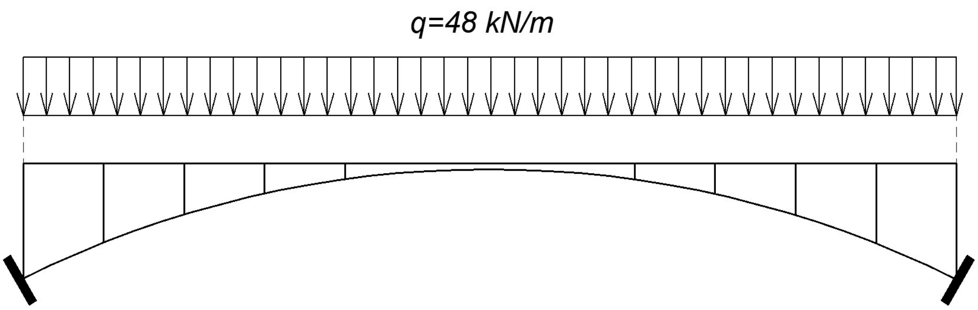

Figure 7.28: Symmetric load configuration

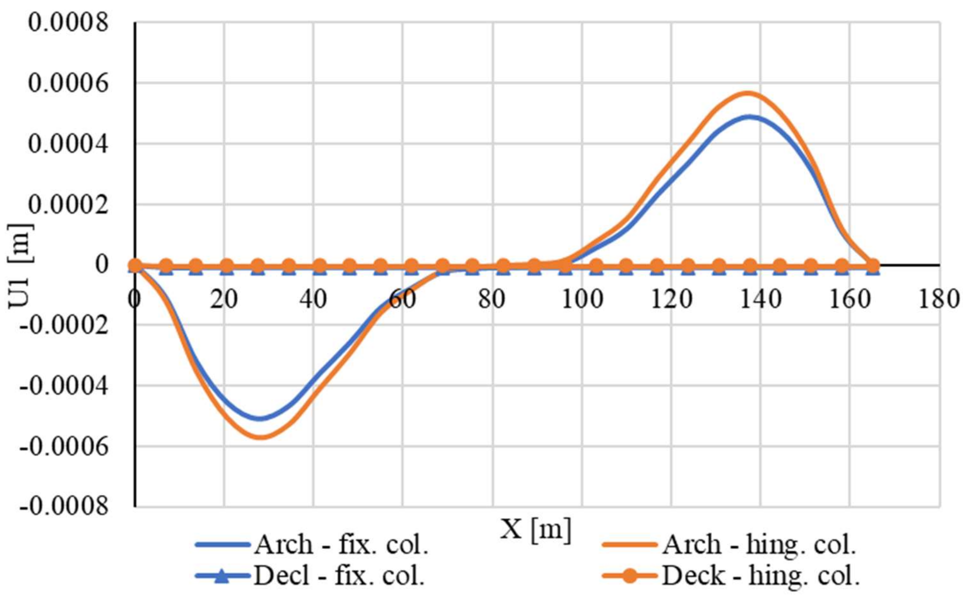

Figure 7.29: Horizontal displacement U1 of Tiemblo bridge under symmetric load configuration

Finally, an interesting behavior occurs by observing the axial load response. The rigid connection between deck and arch through fixed columns allow to have a very high compression force in the central span of the deck, avoiding the need of prestressing cables in that area. In fact, as shown in Fig. 7.30, under permanent loads G1 of arch and deck, there is an axial activation of the deck reaching compression values of 20000 kN.

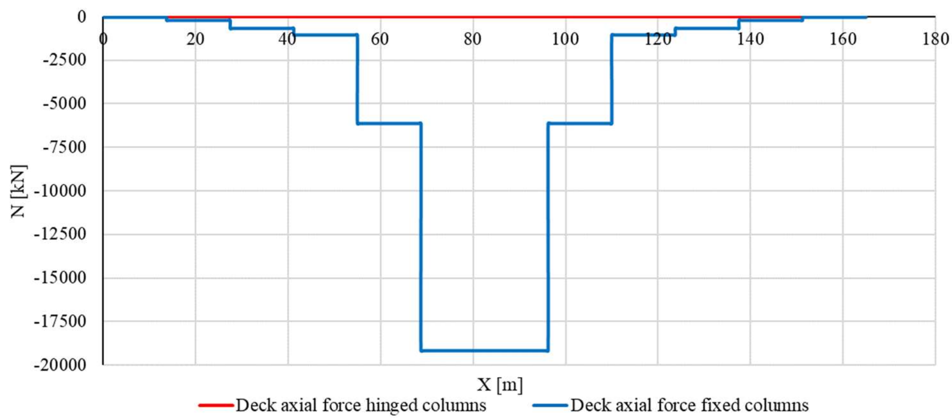

Figure 7.30: Axial load comparison between deck with fixed and hinged columns in the case of Tiemblo

The author of this chapter, wants to remind that the presented results have been obtained by a FE model of the bridge, adopting uniform average dimensions of sections where variable sections were present in order to simplify and highlight each influence of the variables presented. Moreover, further analyses were conducted with the real variable dimensions of the sections, such as the one of the arch and of the columns, and no relevant differences were found in terms of global response in each analyses.

7.3 Freyssinet connections

In the previous paragraphs, many times it has been spoken about the degree of connection between deck and columns making distinction between fixed columns and hinged columns. In this section, the authors want to describe briefly the technology of the hinged connection. Moreover, as shown in Fig. 7.22, Tiemblo bridge present six out of ten Freyssinet connections ahead of the columns near to the crown.

The Freyssinet connection is a joint made in concrete. It has been used first by Freyssinet in 1923 for the bridge of Candelier. It is based on the realization of a deep notch in the concrete that plasticizes the cross section when it is stresses at high compression, which allows it a certain rotation capacity, usually no more than 1%.

This type of joint is very suitable for resisting large loads with no very high turns as occurs in the case of arch bridge. Usually it is not recommended for girder bridges, moreover, it does not require maintenance.

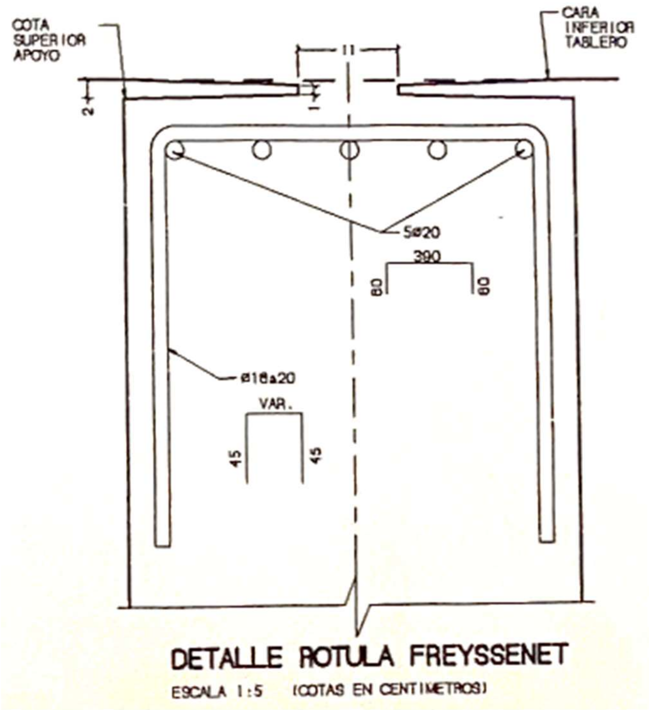

Figure 7.31: Detail of the Freyssinet joint of Tiemblo's columns P6-P7-P8 and P9-P10-P11

The structural response is here briefly analysed:

a. Under axial load with no eccentricity:

The axial load N produces a compression state of stress with a parabolic behavior and maximum values at the edges, $\sigma_{max} = 1.5 \cdot \sigma_m$

In this section, there is a hyper-resistance of the concrete due to the hooped effect provided by the upper and lower part of the concrete which restricts the transversal deformation due to the Poisson effect. This phenomenon has two consequences: i) the height h must be the lowest possible, 1 or 2 cm so that the hoop effect extents to the whole height; ii) h must complain the condition that the maximum rotation of the section will not put in contact the point A and B. In these conditions, the capacity of axial load for the joint is about 5 times the compressive strength of concrete, it means about 150 MPa.

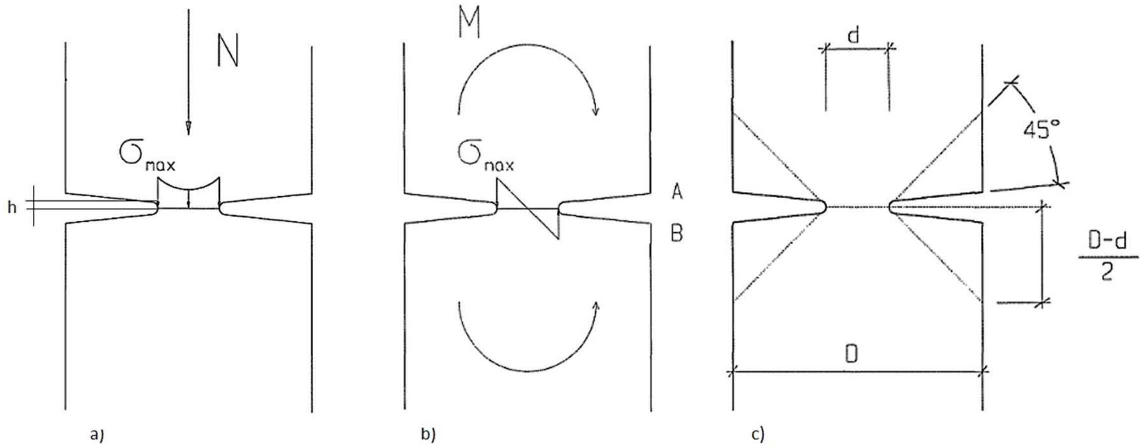

Figure 7.32: Freyssenet connection; a) pure axial load b) eccentric vertical load c) main geometrical characteristics of the connection

b. Under axial load with eccentricity.

In the case of eccentric load, as in Fig. 7.32.b, the joint will undergo a rotation of Θ. The behavior under this load configuration is very controversial, giving rise to both elastic and plastic operating hypotheses. What happens is that the rotation takes place not only in the section height defined by h but also to the nearest upper and lower part of concrete. Therefore, the height h is substitute with a value equal to $h_e = h + k \cdot d$, where k varies according to different authors (Sims and Bridle suggests k=0.5, Leonhardt takes h=d). Therefore, the rotation Θ of the joint provide a maximum tensile stress of $\sigma = \frac{E\Theta d}{2h_e}$, and if it is requested to do not crack, the value of the width d will be:

$$\frac{N}{d} \cdot 1.5 = \frac{E\Theta d}{2h_e} \rightarrow d \leq \sqrt{\frac{3Nh_e}{E\Theta}}$$

Where Θ is the sum of all the rotations due to live loads, permanent loads, temperature, etc. Finally, the moment introduced on the column and deck is $M = \frac{E\Theta d^3}{12\ _e}$.

Moreover, general considerations are:

1. Usually $d \leq 0.3D$ and generally 15 cm
   $h \leq 0.2d$ and lower than 2 cm;
2. The admitted shear of the joint is 1/8 of the axial load;
3. No vertical reinforcement is needed, nor crusade, as it practically will not work;

4. The hinge corners should be rounded as the upper and lower part of the joint, therefore is advisable to adopt the prefabricated assembly.

7.4 Construction process

There are many possibilities to construct an arch bridge, as for example:

- Construction on scaffolding, this procedure is only valid when the site is accessible (Arch over Clariano river in Valencia);
- Construction with self-climbing scaffolding, this procedure it is not competitive nowadays, actually, the lack of alternatives to this method led to the decline of the arches during a good part of the last century;
- Construction of the arch simultaneously to the deck, introducing a provisional diagonal stays and cantilevering. This procedure has drawbacks:
  - The need to anchor the horizontal tensile force to of the upper part of the cantilever that is generates as a consequence of the own weight of the arch and the deck
  - The rigidity of the assembly makes it difficult to introduce adjustments to correct the deviations that occurs in the geometry

  On the contrary, it reveals a good solution for a structure with concrete-steel deck which allows a shorter execution period, moreover, this type of solution does not require auxiliary structures and makes possible the simultaneously execution of both arch and deck;

- Construction of the arch with provisional pylon and provisional stays and execution of the deck subsequently. This method has the drawback that it requires the construction of a provisional pillar which will be demolished later. It also requires completing the execution of the arch before starting to cast the deck. Moreover, this procedure has advantages:
  - It allows to control and adjust the geometry in every moment of the construction process due to the high flexibility of the arch when cantilever;
  - It requires to anchor to the soil only the self-weight of the arch, which can be done with a more vertical component rather than the previous one;

- The provisional bracing allows to put in compression the arch in order to compensate the elastic shortening due to permanent loads, without the need to use hydraulic jaks at crown;

From all the possibilities described above, the one chose was the construction of the arch with a provisional cable stay and subsequent execution of the deck.

In this way, the arch has been built in 17 sections per side, of 4.9 meters of length, by using a travelling formwork and a provisional cable stay. In Fig. 7.33 there is shown the construction of the arch that reaches almost the end with the key-closure.

Figure 7.33: Construction of Tiemblo trough cantilever advancements and provisional cable stay. (Image taken from Hormigon y Acero, n°220)

This bracing allows to ensure the stability of the structure during the construction and to introduce a positive bending moment at the footings of the arch before casting the key-segment compensating, in this way, the shortening effect due to permanent loads (Corres Peiretti et al., 2001). This is a great advantage since it avoids the need to introduce jacks at the crown, whose dismantling carries relevant construction problems. Finally this method permit to avoid auxiliary structures to withstand lateral buckling since the closing of the arch is done with a relatively small axial force, 18000 kN compared to 60000kN of the total permanent load (Corres Peiretti et al., 2001).

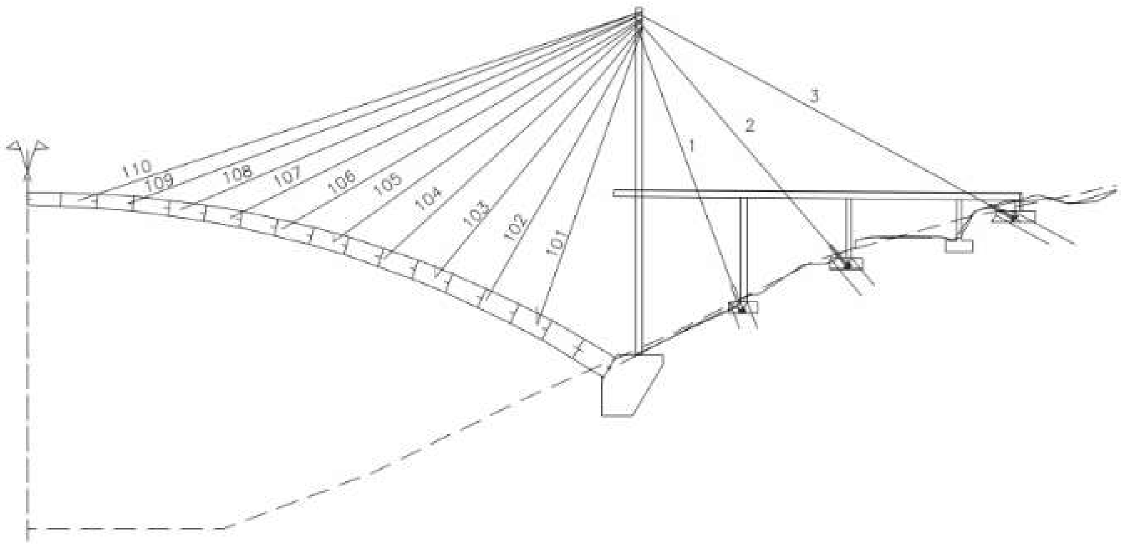

Figure 7.34: Scheme of the construction process and definition of the numbers of provisional cables (image taken from Fhecor)

Finally, the sequence of the construction stages followed to build each of the 17 segments is:

1. Positioning of the travelling formwork relatively to the previous segment;
2. Placing the longitudinal and transversal reinforcement;
3. Correction of the prestressing in cables with the aim to obtain the final geometry which has been disturbed by concreting the segment;
4. Measurement of the arch geometry, cable forces, displacements of the provisional pylon and of the strain gauges placed in specific segments.

The time needed to construct each segment was 1 week.

In order to have the geometry of the arch coinciding with the theoretical one, the cable forces are adjusted after the pouring of each segment. These forces are determined considering an infinite rigid area of the segments allowing to evaluate Fi..Fn to apply to the cables to keep the arch in its theoretical position. In this way, it has been possible to know the lengthening or shortening needed in each cable in order to obtain the theoretical forces Fi..Fn at the end of the process, considering the real stiffness. Adjustments of these forces might be possible when significant deviations in the arch geometry has been measured. Finally, the two sides of the arch have been closed with a 5 cm difference, allowing to achieve a discrepancy lower than L/1000 from the theoretical geometry (Corres Peiretti et al., 2001)

7.5 Conclusions

In conclusion of the chapters 6 and 7, the main achievements are summarized:

- Concrete arches are usually fixed at the springings, and present variable depth rather than uniform.
- Eccentric vertical live load with respect to the center line of the single rib arch applies as torsional moment and vertical loads to the single rib rather than in arches with two ribs where the eccentric load means an increase of vertical load to one rib, in the direction of the eccentricity, and a decrease on the other rib.
- For a fixed concrete arch, the deflection due to live load is quite small, which means that it does not control the design of the arch depth. Buckling in the plane of the arch and moment magnification are the important factors in determining the arch depth. Radius of gyration is a measure of resistance to buckling and moment magnification (Nettleton & Torkelson, 1977).
- The span to rise ratio generally vary over a wide range. Moreover, the rise and the minimum span are controlled by the site conditions, the clearance and the roadway grade. For a bridge crossing a deep valley, either the rise or the span can be increased for economy reason. In order to affect the economy, it's reasonable to reduce the rise and increase the span, like for example, in a single span crossing a canyon, by raising the abutments (Nettleton & Torkelson, 1977).
- The horizontal thrust is reduced for a high-rise arch, for a given span, like also the moments from arch shortening, temperature and shrinkage. On the contrary wind stresses are increased and the resulting added length of the arch provides extra material cost and construction cost (Nettleton & Torkelson, 1977).
- Menn's preliminary design formulation better fit for low arch rise for a given span. Moreover, the number of spandrel columns does not affect significantly the goodness of the suggested bending moments evaluation. Much more important role plays the distribution of stiffness among arch and deck, which shows better results for arch stiffer than the supported deck.
- The effect of the interaction between arch, column and deck against live loads stresses leads to a reduction of bending moment in all the points of the arch. The system in this way would act as a Verendeel truss to resist live moments (Nettleton & Torkelson, 1977).

- Stresses coming from shortening and shrinkage can be opposed by applying jacking forces equal to the crown thrust before the key-closure. The effect of the jacking results in lifting up both side of the halves so that the pouring of the key-section is performed in the opening created by the jacking. When the crown section reaches sufficient strength, the jacking forces are transferred to it. Alternative methods are for example the use of cable forces when constructing the arch by temporary cable-stay as in the case of the construction of Tiemblo, which has the advantage of avoiding the dismantling of the jacks.
- It is common to see very slender arches designed to take only axial load combined with deep decks which will act against bending moment. This structural response is similar to a tied arch in which a slender rib is used with a deep tie that takes the moments.
- Single arch bridges, solid or box sections, are significantly stiffer laterally than vertically so that lateral buckling and lateral moments are of minor consequences. When two or more individual ribs are used, lateral stiffness may play a more important part in the design (Nettleton & Torkelson, 1977).
- If the arch cross-section results understressed there are three main possible ways to reduce the section: reducing the width, the depth or the thicknesses of the members in the case of hollow box sections. Each of these will reduce the moment of inertia, resulting in an increase in live load moment and on the other hand, in a reduction of the dead load thrust. Reducing the depth would significantly affect the moment of inertia but not much the decreasing of dead load. Therefore, the more efficient would be to thin the slabs of the box sections and to reduce the overall width. The thickness of the walls could not be reduced due to difficulties in construction stages.

8 BRIDGE PRELIMINARY DESIGN

In this chapter of the thesis, some simple methods to perform a preliminary design of roadway arch bridges with fixed supports and variable cross-section will be presented, this includes an analysis under permanent and live loads, where no horizontal loads will be considered. The pre-design procedure chosen to be followed is based on the observation of the trends deduced from the empirical parameters plots and discussed in the “Empirical (geometrical and material) trends” chapter. Starting from these values and taking advantage of the empirical relations discussed, the other geometrical parameters have been easily determined, allowing the proposal of a sound procedure for the preliminary design process.

8.1 Description of the methodology

The following data have to be defined to start the process:

- Span length L;
- Rise f;
- Width of the deck B;
- Compressive strength of concrete f_{ck}.

Starting from these values and considering the trends of the empirical relations previously discussed, the other geometrical parameters could be easily determined:

a. Arch cross-section: h_c, h_s, b and type of section

The depths of the arch at crown h_c and springing lines h_s, which are relevant in design process due to their effect on visual qualities and structural response of a given bridge, have been deduced according to the empirical correlations Equation 8.1 and Equation 8.2 defined in Chapter 5. These quantities have been evaluated starting from the plot of the real values collected into the database with respect to the span length L. To reach approximate values as reliable as possible of arch depth both at crown and at springing lines, a wider dataset has been considered, taking into account the roadway bridges collected for the present research, the ones considered into Salonga and Gauvreau work and the ones analyzed by Manterola (Salonga & Gauvreau, 2014)(Manterola, 2006). By looking at the slope of the linear regression (Fig.8.1 and Fig.8.2), h_c and h_s could be evaluated from the interpolation as in the following two equations:

$$h_c = 0.015L = L/67 \tag{8.1}$$

$$h_s = 0.019L \approx L/50 \tag{8.2}$$

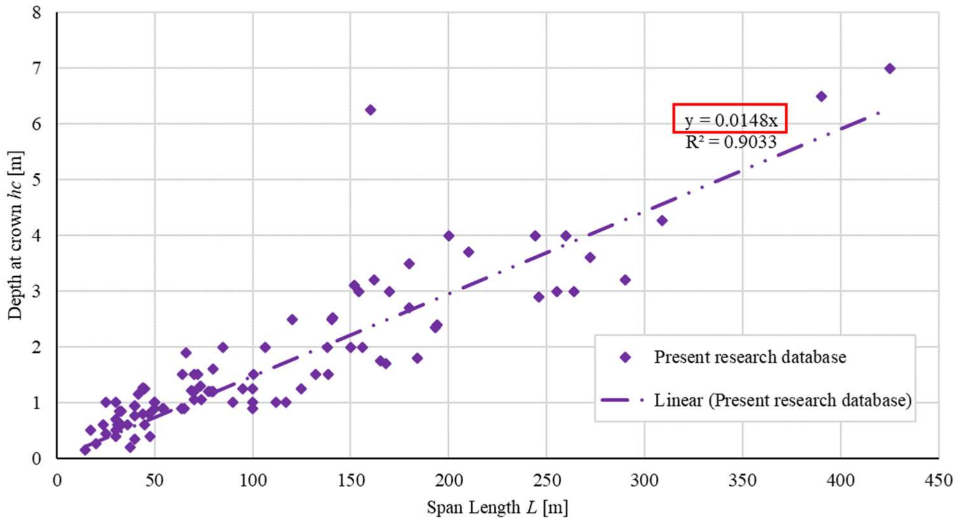

Figure 8.1: Arch depth at crown h_c versus span length L of roadway bridges of the entire database (present research, Salonga and Gauvreau (Salonga & Gauvreau, 2014) *and Manterola* (Manterola, 2006)*)*

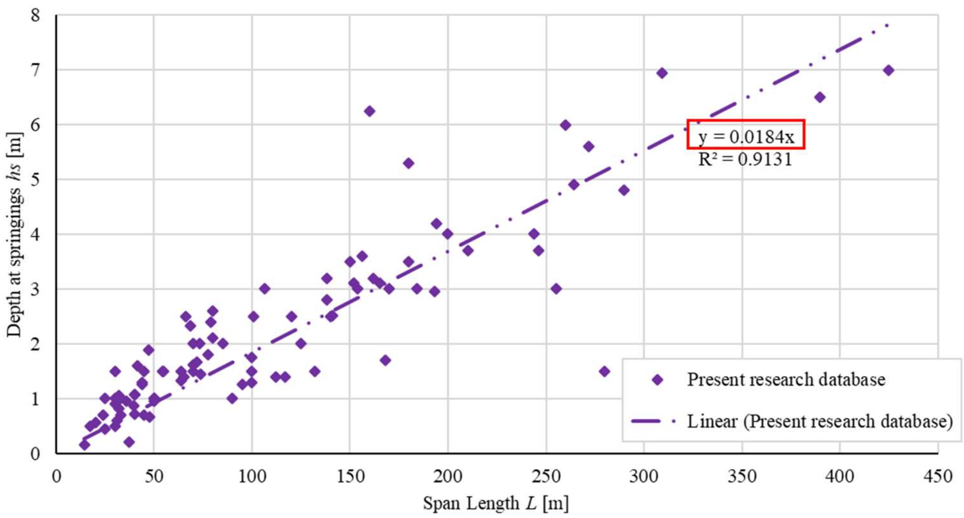

Figure 8.2: Arch depth at springing lines h_s versus span length L of roadway bridges of the entire database (Present Research, Salonga and Gauvreau (Salonga & Gauvreau, 2014) *and Manterola* (Manterola, 2006)*)*

From both the upper graphs it can be also noticed that the coefficient of linear regression R^2 is high (around 90%). This value measures the proportion of variation of the dependent variable that is explained by the regression line. It represents the coefficient of determination which is used as an indicator of the goodness of fit, it shows how many points fall on the regression line and must be a value between zero and one, often expressed as a percentage. Usually, an R^2 value of more or less 90% is considered a good fit.

Once the arch depth has been found by linear interpolation, the arch width b can be derived by plotting the roadway data collected in the present work with respect to the span length L (Fig.8.3) deriving the following Equation 8.3:

$$\bar{b} = 0.042L = L/24 \tag{8.3}$$

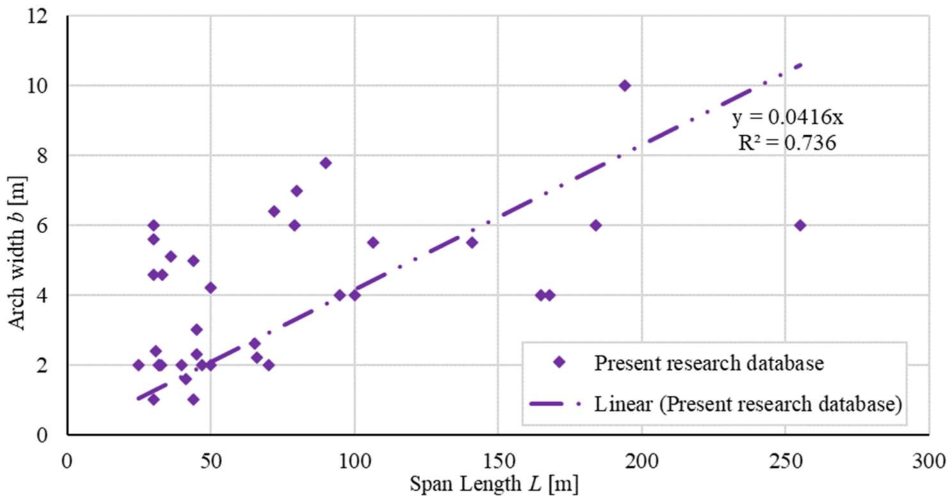

Figure 8.3: Arch width b with respect to the span length L of roadway bridges of the present research database

The entire roadway database (present research, Salonga and Gauvreau (Salonga & Gauvreau, 2014) and Manterola (Manterola, 2006)) has not been used to find a recommended arch width value, because a clear and exhaustive trend were not identified due to the assumption of an average arch width value in the case of Salonga and Gauvreau dataset and for the lack of information in Manterola one.

For the cross-section type of the arch, the threshold suggested by Menn at L=100m has been assumed for distinguish between solid and box sections (Fig.8.4): *"The cross section of the arch is primarily a function of the arch* ***span length*** *and the* ***ratio of arch stiffness to girder stiffness*** *[…] For L>100m solid arches are* ***relative expensive****. Ratio of flexural resistance to material cost is small […]. High stresses for falseworks […]"*(Menn, 1990).

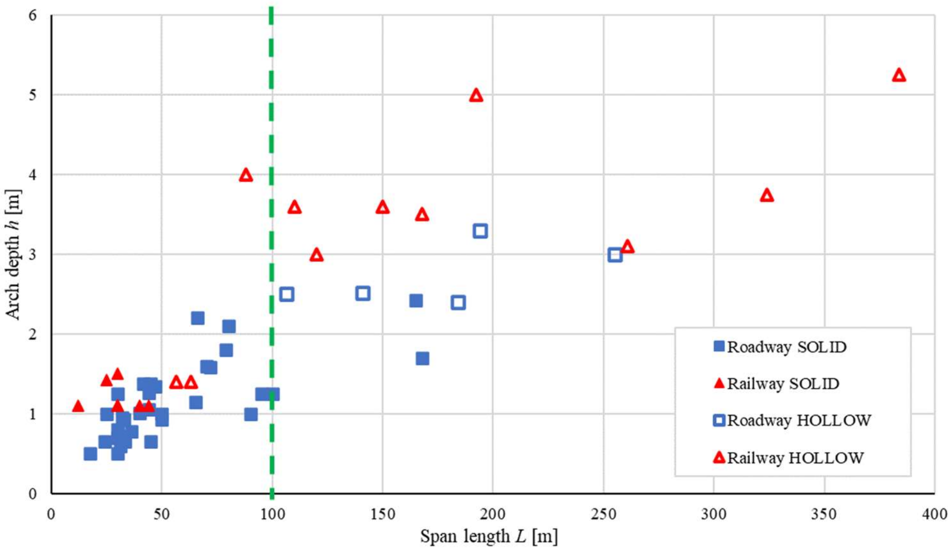

Figure 8.4: Arch section type h (Solid or Hollow) according to the span length L (L>100m or L<100m) of the present research database

From the graph above can be easily noticed that the simplified approximation for the arch cross-section proposed by Menn (L>100m or L<100m) fits well with the real data collected for the present research and so, for that reason, can be used during the pre-design process (Menn, 1990).

b. Column number

Regarding the number of columns, a fix value of 10 has been selected. This choice is based on the data collected in both the databases (present research and Salonga and Gauvreau (Salonga & Gauvreau, 2014)), and on the values recommended by Manterola: *"Relationship between the arch and the deck occurs by means of vertical pillars. Its separation is, at least, the division of the arch into* ***8 equal parts****, being* ***more frequent, 10 or 12 parts****, or the odd ones in between, when a pillar is not arranged in the key […]"* (Manterola, 2006) (Fig.8.5).

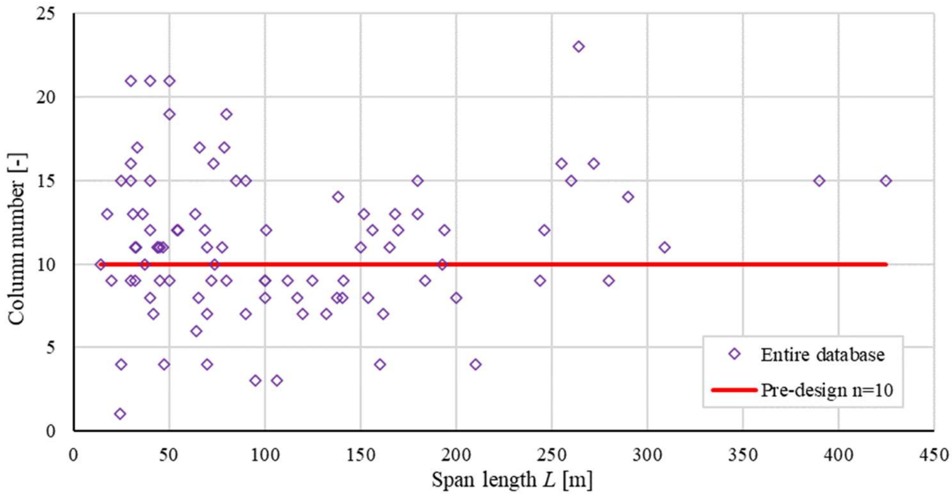

Figure 8.4: Column number check on the entire roadway bridges database (present research and Salonga and Gauvreau (Salonga & Gauvreau, 2014)*) with respect to the span length L*

c. Depth of the deck h and type of section

For the girder depth h evaluation, the relationship proposed by Menn between column span length l and h has been assumed (Menn, 1990):

$$\frac{l}{h} \cong \frac{12}{1} \quad \text{over the arch} \tag{8.4}$$

Comparing this relation with the trend of values obtained from the entire database (present research and Salonga and Gauvreau (Salonga & Gauvreau, 2014)) *(*Fig.8.7*)*, it emerges that the Menn proposal and the slope of the linear regression line are quite similar, confirming the reliability of this approach for the preliminary design process (Menn, 1990).

The analysis of the data collected in both databases (present research and Salonga and Gauvreau (Salonga & Gauvreau, 2014)) reveals that almost all the girders with a column span length l higher than 12m have a prestressed box section. This last consideration is shown in Fig.8.8, where the girder depth h is plotted versus the column span length l gathering the bridges in prestressed and not prestressed cross sections.

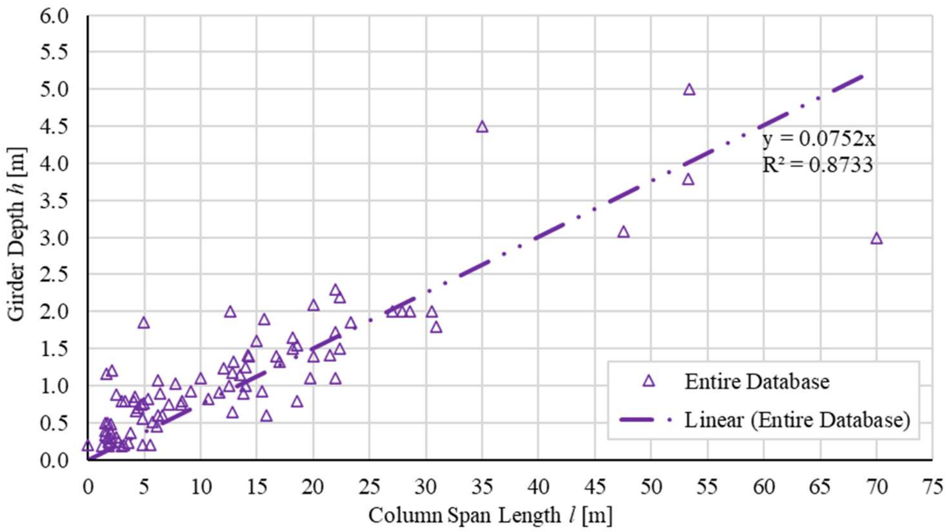

Figure 8.5: Girder depth h with respect to the column span length l of roadway bridges of the entire database (present research and Salonga and Gauvreau (Salonga & Gauvreau, 2014)*)*

An additional consideration can be done by looking at the prestress. An empirical graphical distinction, by looking simply at the graph Fig.8.8, between the prestressed (l>12m) and not prestressed (l<12m) case could be done by comparing the girder depth *h* and the column span length *l* coming from the present research database.

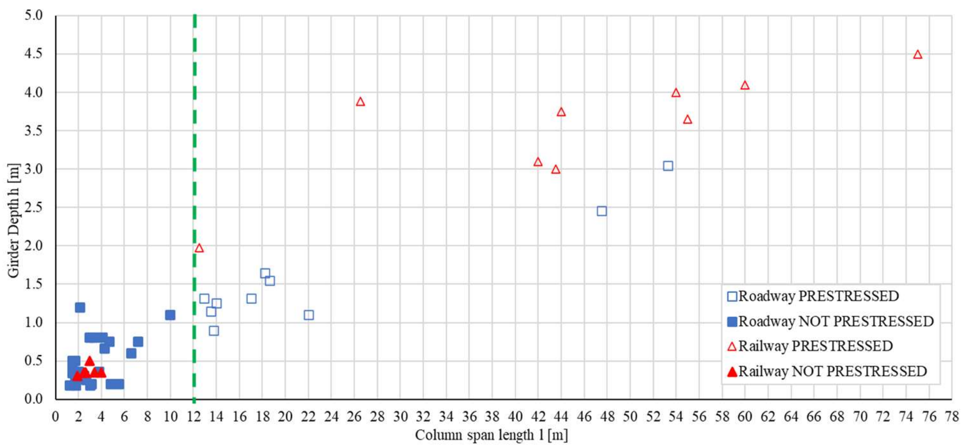

Figure 8.8: Girder section type h (Prestressed or Not) according to the column span length l (l>12m or l<12m) of the present research database

Another observation can be done by comparing the estimation formula of the effective slab thickness t_{eff} proposed by Menn Equation 8.5 for posttensioned concrete girder bridges with the linear regression line obtained plotting the t_{eff} value of present research roadway bridges with respect to their span length L (Menn, 1990). As can be observed in Fig.8.9, the two equations are very similar, underlining a clear correlation between the Menn's formula and the interpolation line of the real data, confirming what Menn proposed about the consumption of concrete in the superstructure. Although most of the arch points stay above the continuous line, it is possible to design concrete arch bridges consuming less concrete than girder bridges as discussed in the "Empirical (geometrical and material) trends" chapter (Menn, 1990).

$$t_{eff} = 0.35 + 0.0045L \tag{8.5}$$

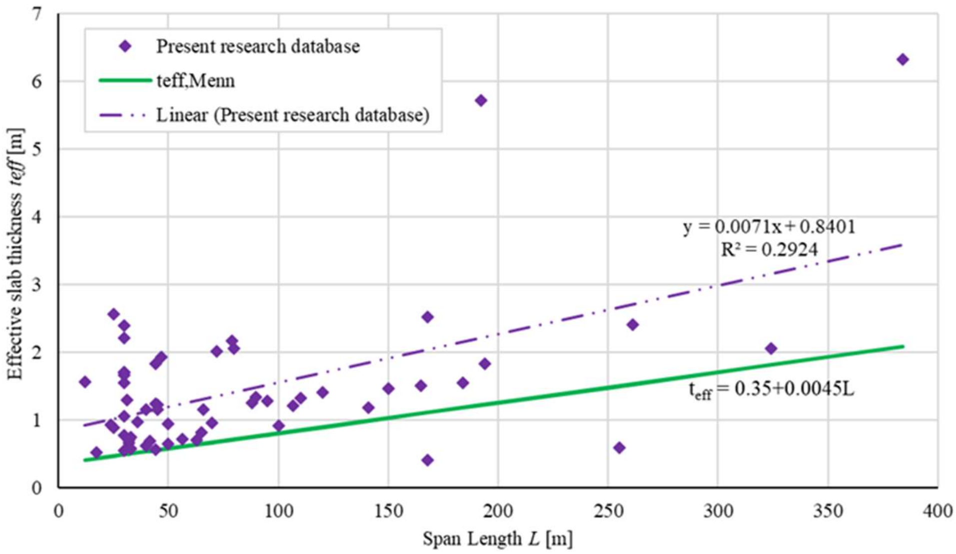

Figure 8.9: Effective slab thickness t_{eff} comparison between the present research roadway bridges and the empirical Menn's formula (Menn, 1990)

Moreover, it can be observed by looking at the relation between the time *t* and the column span to girder depth ratio *l/h* which can affect the type and the usage of concrete during the years. In the following graph (Fig.8.10), the complete database (present research and Salonga and Gauvreau (Salonga & Gauvreau, 2014)) has been used to collect the information, but it seems that there is not a clear trend and correlation between the time and *l/h* as can be seen also from the low values of the linear regression coefficients R^2.

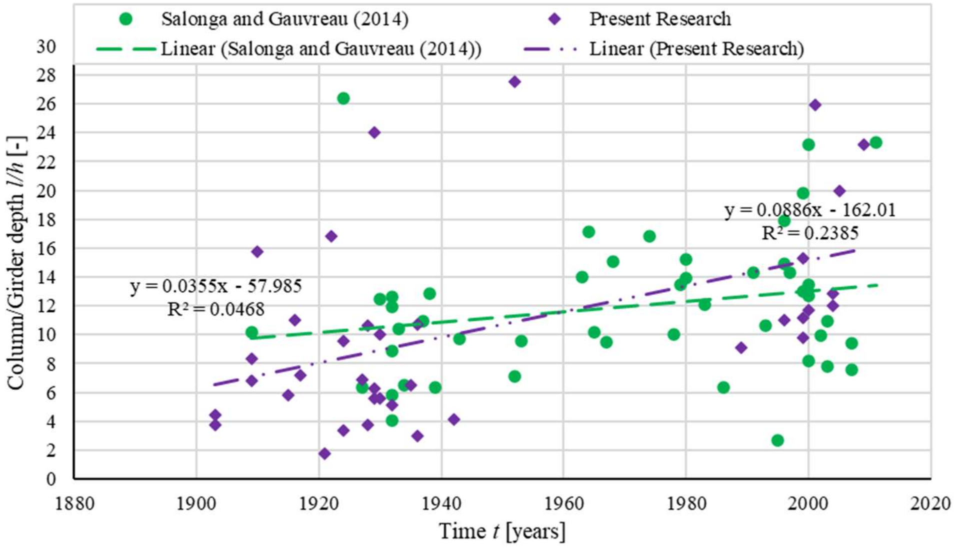

Figure 8.10: Column/Girder depth l/h with respect to time t of the entire database (present research and Salonga and Gauvreau (Salonga & Gauvreau, 2014)*)*

8.2 Application of the methodology

Once all the needed geometrical parameters are defined, the preliminary load analysis could be performed including an analysis under permanent and live loads, where no horizontal loads are considered by defining:

a. self-weight of the girder $G_{1,girder}$:

$$G_{1,girder} = h_{girder} \cdot B \cdot \gamma_{cls}\ [kN/m] \text{where } \gamma_{cls} = 25\ [kN/m^3] \tag{8.6}$$

$$h_{girder} = l/12\ [m]\ \textit{(Menn, 1990)} \tag{8.7}$$

b. non-structural permanent load of the pavement G_2:

$$G_2 = B \cdot h_{pav} \cdot \gamma_{cls}\ [kN/m] \quad h_{pav} = 0.1\ [m] \tag{8.8}$$

c. self-weight of the arch $G_{1,arch}$:

$$G_{1,arch} = b \cdot \bar{h} \cdot \gamma_{cls}\ [kN/m] \tag{8.9}$$

$$\bar{h} = \left(\frac{h_c + h_s}{2}\right)\ [m] \tag{8.10}$$

d. permanent load of the girder Q:

$$Q = B \cdot 4 \; [kN/m] \tag{8.11}$$

The reason of choosing a simplified value of live load Q equal to 4 [kN/m] equally distributed comes from previous Spanish specifications;

e. load combination q (ULS) and load arrangement (uniformly distributed):

$$q_{ULS} = 1.35 \cdot \Sigma G_1 + 1.35 \cdot G_2 + 1.5 \cdot Q \; [kN/m] \tag{8.12}$$

f. axial forces at springing lines $N_{Ed,springs}$ (ULS), being the most critical section for the axial load:

$$N_{Ed,springs} = \sqrt{\left(\frac{ql^2}{8f}\right)^2 + \left(\frac{ql}{2}\right)^2} \tag{8.13}$$

g. check using the recommended reduced axial force value:

$$v = \frac{N_{Ed,springs}}{A_{springs} \cdot f_{cd}} = 0.3 \div 0.4 \tag{8.14}$$

The parameter used for assessing the pre-design is the reduced axial force v. This parameter could be used to perform the check at the Ultimate Limit State (ULS) on the data collected into the database, ensuring if, during the preliminary design process, the guessing geometrical and structural quantities can be reliable or not. This value also guarantees an efficient instrument to assess the reliability of the empirical formulas and relations suggested to be followed in the pre-design procedure. From the plot of v (ULS) at springing lines with respect to the bridge ID (Fig.8.11), it cannot be distinguished a clear trend helping to suggest a limit value of reduced axial force to perform the checks.

On the other hand, if the arch has a continuous perimetral reinforcement, the bending moments will be high ensuring a v value closed to 0.4 from the interaction domain, validating the chosen methodology. In most of the cases (24 over 33 total roadway bridges), the reduced axial force respects this threshold.

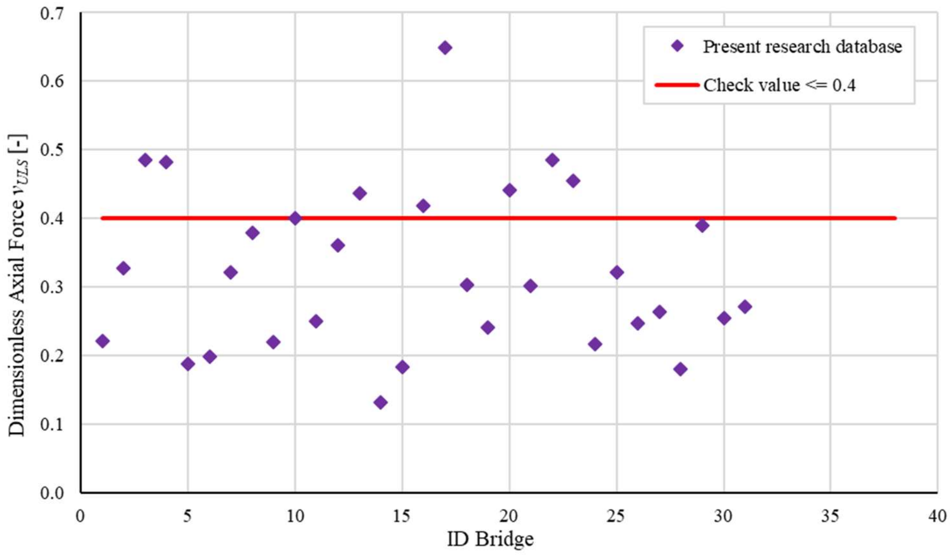

Figure 8.11- Reduced axial force at ULS v_{ULS} trend with respect to the bridge ID for the roadway bridges obtained from the preliminary design process

The preliminary design process discussed in this chapter has been calibrated on the collected roadway bridges data only, without considering the railway ones to validate the proposed empirical formulations and trends. That is because of the lack of information about railways from both the Salonga and Gauvreau and Manterola study cases (Salonga & Gauvreau, 2014) (Manterola, 2006). Despite that, a dataset of around 130 roadway bridges has been employed to perform this analysis, ensuring to get reliable results. Only for the discretization of the section type for girder and arch and the analysis about the prestressing of the section itself, the entire database, roadways and railways collected in the present research, has been used.

In the next chapter will be performed a comparison between firstly, the real and the preliminary design values of the geometrical parameters discussed in this section and secondly, the real and the pre-design values of dimensionless axial force, computed on the dataset of the present research, using the ULS combination to check if the geometric parameters chosen to pre-dimensioning a bridge are reliable or not.

9 COMPARISON WITH DATABASE TRENDS

This section of the thesis presents a comparison between the real values collected and the preliminary design results of the geometrical parameters discussed in the "Bridge preliminary design" chapter. The following procedure highlights that there is a good agreement, especially for the arch h_c, h_s and girder h depths, between the actual values of roadway bridges collected into the entire database (present research and Salonga and Gauvreau (Salonga & Gauvreau, 2014)) and the ones computed following the empirical relations proposed in "Empirical (geometrical and material) trends chapter.

a. Arch depth at crown h_c and at springing lines h_s

From the results comparison (Fig.9.1 and Fig.9.2), between the real geometrical values computed for the entire deck arch bridges database (present research and Salonga and Gauvreau (Salonga & Gauvreau, 2014)) and the ones obtained using the empirical formulas, arises a good fit in the results. For both the arch depth at crown and at springing lines, the preliminary design values obtained by using simplified formulations fit well the real data collected. So, it can be said that the simplified procedure chosen to follow in this work reports reliable results, ensuring a dependable tool for a preliminary assessment of a certain design concept as a guide for the designers.

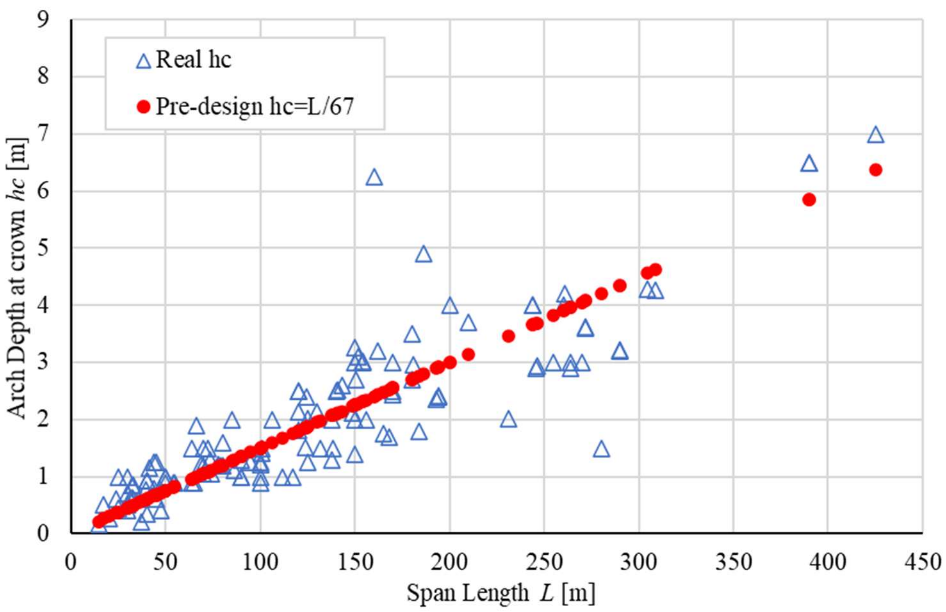

Figure 9.1: Arch depth at crown h_c comparison between the real values from the entire database (present research and Salonga and Gauvreau (Salonga & Gauvreau, 2014)*) and the ones obtained using the empirical formula*

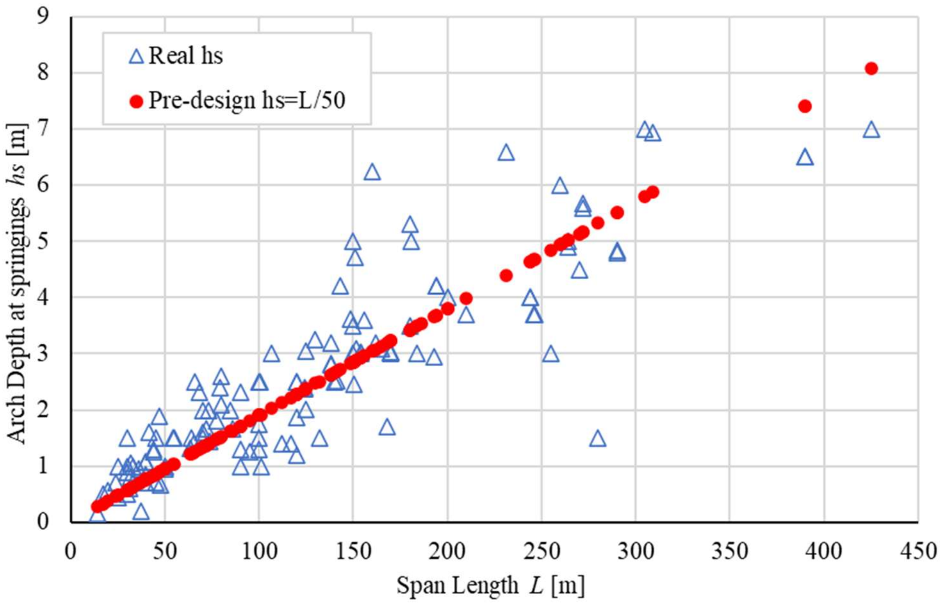

Figure 9.2: Arch depth at springing lines h_s comparison between the real values from the entire database (present research and Salonga and Gauvreau (Salonga & Gauvreau, 2014)*) and the ones obtained using the empirical formula*

From the collected results, in 57 cases over 130 total concrete arch bridges the arch depth at crown results to have a higher value in pre-design rather than in reality. For the arch depth at springing lines, instead, in 50 over 130 cases the pre-design results are higher that the real ones.

b. Arch width *b*

From the data comparison (Fig.9.3) between the real geometrical values computed for the entire deck arch bridges database (present research and Salonga and Gauvreau (Salonga & Gauvreau, 2014)) and the ones obtained using the empirical formulas, the results seem to move a bit away from the pre-design trend. That can be since for the data collected by Salonga and Gauvreu an average value of arch width has been assumed due to the lack of more detailed information. Instead, in the case of the present research, the data present into the dataset is exact (Salonga & Gauvreau, 2014).

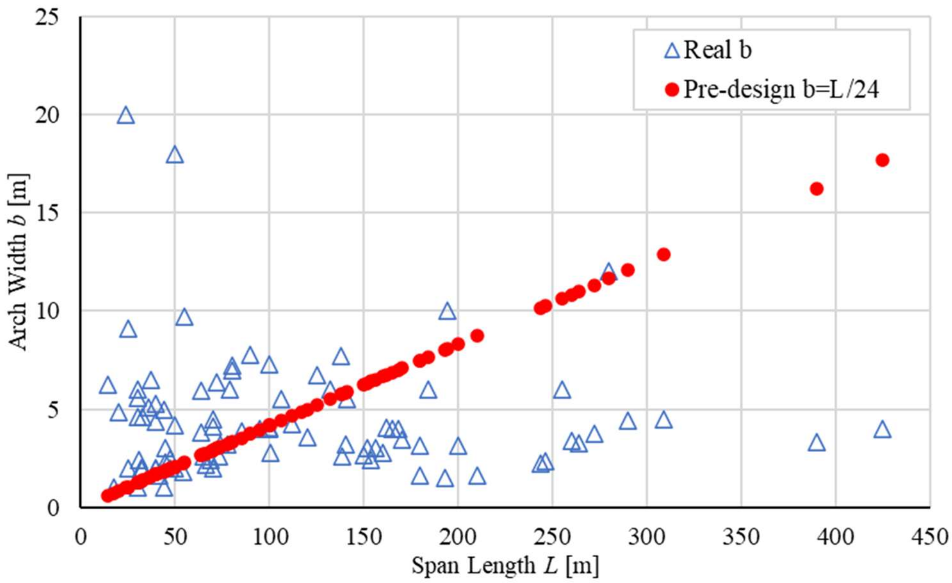

Figure 9.3: Arch width b comparison between the real values from the entire database (present research and Salonga and Gauvreau (Salonga & Gauvreau, 2014)*) and the ones obtained using the empirical formula*

From the collected results, in 46 cases over 93 concrete arch bridges the arch width results to have a higher value in pre-design rather than in reality.

c. Girder depth *h*

From the results comparison (Fig.9.4), between the real geometrical values computed for the entire deck arch bridges database (present research and Salonga and Gauvreau (Salonga & Gauvreau, 2014)) and the ones obtained using the empirical formulas, arises a good fit of the results. For the girder depth, the pre-design values obtained by using simplified formulations fit well the real data collected once again.

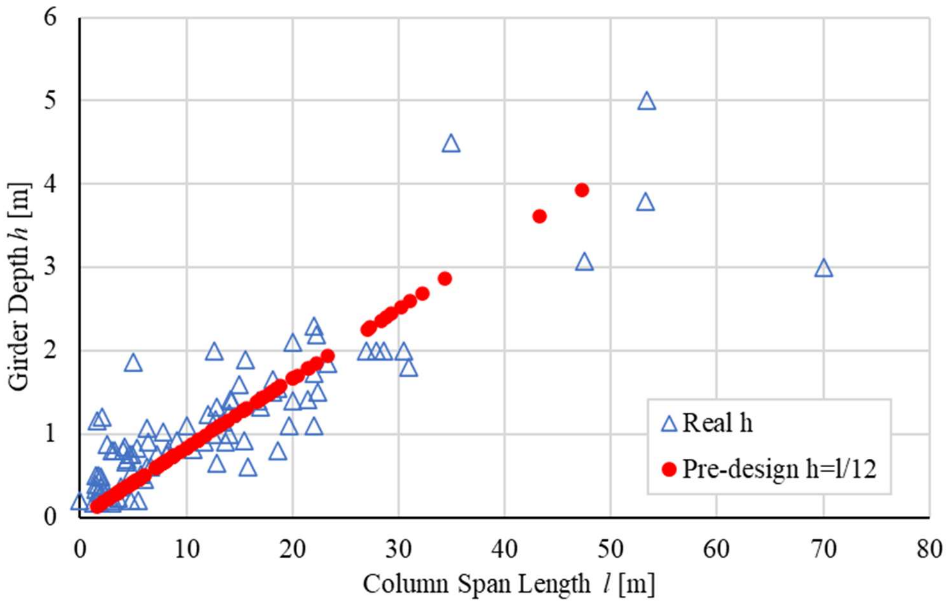

Figure 9.4: Girder depth h comparison between the real values from the entire database (present research and Salonga and Gauvreau (Salonga & Gauvreau, 2014)*) and the ones obtained using the empirical formula*

From the collected results, in 37 cases over 93 concrete arch bridges the girder depth results to have a higher value in pre-design rather than in reality.

d. Reduced axial force *v*

Specifically, the preliminary design assessment is performed in terms of dimensionless axial force v. This parameter could be used to perform the check at the Ultimate Limit State (ULS) on the data collected into the database, ensuring if, during the preliminary design process, the guessing geometrical and structural quantities can be reliable or not. Fig.8.5 illustrates the dimensionless axial force *v* versus the span length *L* at ULS. The results show that the mean value of *v* according to the preliminary design procedure is 0.32. This value is similar to the optimal *v* for achieving the highest flexural strength of the cross section. Therefore, such procedure would enable the designer to define material-efficient cross sections. On the other hand, in most of cases (63%) the dimensionless axial force is lower than 0.4. Therefore, the methodology, although its simplicity, represents a conservative procedure for the preliminary design of arch bridges. The authors are aware that the methodology does not include a complete analysis of the bridges, but the procedure proposed may represent a first approach to the design of such bridges.

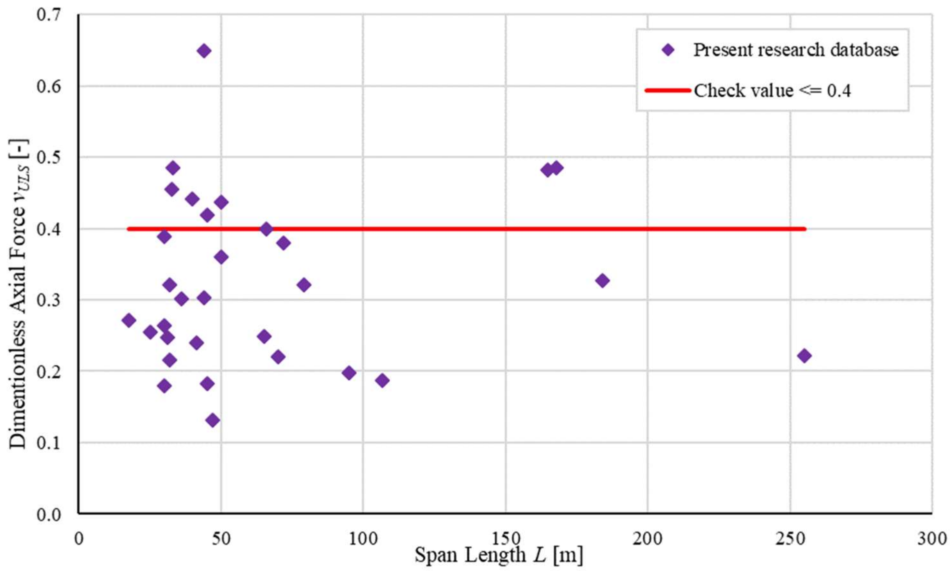

Figure 9.5: Reduced axial force v_{ULS} at ULS with respect to the span length L of the results of the present research database obtained from the preliminary design check

10 CONCLUSIONS

In the present research, a pre-design method for concrete arch bridges has been presented. It was obtained basing the research only on concrete deck arch bridges, both roadway and railways typologies, built in Spain. Anyway, the simplified predesign method found and suggested in this work can be applied also to other concrete deck arch bridges, beyond Spain. Moreover, it can be applied to all kinds of sections for both arch and girder just changing some geometrical properties establishing an out-and-out law for different kind of arch structures. In the proposed design process, as objective information, the database and the historical analysis have been used. Then, together with the geometrical and mechanical proportions, the methodology to trace an exhaustive pre-design method has been identified.

Some sensitivity analyses were carried out to obtain the optimal solutions studying the structural behavior of these kind of bridges basically by analyzing the most relevant books on the topics including determinate and indeterminate systems and relations as the relevance of the bending stiffness between arch and deck on the structural behavior. The idea was to study and better understand the main structural behavior in terms of resisting response of arch bridges by looking at real structures as the Tiemblo bridge in Spain designed by Fhecor in 1999.

Then some checks have been performed to verify if the common preliminary design rules applied on arch bridges belong to the response behavior of the Tiemblo bridge. In particular, a back analysis of the simple rules suggested by Menn is performed to understand and validate those rules exploiting their limits of applicability by varying some parameters of the model.

Fixing the geometrical and mechanical parameters validated by the empirical trends proposed by Salonga and Gauvreau's work and design proposals suggested by Menn, it can be said that the simplified procedure chosen to follow in this work shows reliable results, ensuring a dependable tool for a preliminary assessment of a certain design concept as a guide for the designers.

10.1 Future works

Future works can be performed in terms of maintenance interventions of the bridges during their service life or in terms of construction processes influence on the bridges' life. Inadequate attention to durability issues sometimes in combination with very aggressive maritime environment has led to expensive and technically demanding repair works on older arch bridges. The design of more recent constructed bridges considered the experience from the in-service performance of older arch bridges. Moreover, structural health monitoring systems could be a solution for those bridges, a numerical model, which can realistically simulate effects of reinforcement corrosion in concrete to predict service life of new or already damaged structure. These aspects can be evaluated and exploited by looking at the type and usage of concrete during the years, perspective that was not examined in this work.

Every resistant structure has a shape, but when considering the arch, it can be said that the structure is a shape in itself. Hence the arch continues to resist due to its shape, which is also its greatest advantage and its biggest inconvenience: because to be able to work as an arch, it needs to be complete. Therefore, all partial structures that may arise during the construction of the arch have little to do with final structure: in fact, the construction of arches stem from this difficulty. Throughout history, different uses of construction methods, created through the different uses of materials and with the evolution of the technologies applied on the work site can be identified. The construction methods could be subdivided mainly into two fields: the first collects the use of auxiliary structures that support the arch until it is completed; the second represents the building of the arch by means of partial structures, using different resistant structures, until closing it at the keystone, which is when the arch begins to work. These are just some preliminary considerations regarding the construction processes, each situation and case has its own influence on the bridge life, another aspect that has not been treated in the present research.

These issues are additional and different aspects that could be treated and further analyzed in order to enlarge the concrete arch bridges research topic.

Bibliography

Austin. (1971). In-plane bending and buckling of arches. *J.Struct.Div.*, *97(5)*, 1575–1592.

Bastos. (2002). El congreso de ache puentes y estructuras edificación Realizaciones Puentes.

Bruun. (2014). *Robert Maillart: the evolution of reinforced concrete bridge forms*. In *9th International Conference on Short and Medium Span Bridges*.

Chen, Su, Lin, Chen, Zhuang, & Tabatabai. (2017). Development and application of concrete arch bridges in China. *Journal of Asian Concrete Federation*, *3*(2), 12–19. doi:10.18702/acf.2017.06.3.1.12

Delgado, Peiretti, Caldentey, Martín, & Herranz. (2001). Puente arco sobre el embalse de El Burguillo (Ávila): diseño y control de la ejecución. *Hormigon y Acero*, (220), 3–17.

Eurocode 0 - Basis of structural design. (1990).

Fhecor. Bridge over " El Burguillo " reservoir (1999).

Fonseca, & Bastos. (1972). The Infante Dom Henrique bridge over the river Douro: construction method, monitoring equipment and structural control, *32*(7), 587–594.

Fonseca, & Mato. (2005). Infant henrique bridge over the River Douro, Porto. *Structural Engineering International: Journal of the International Association for Bridge and Structural Engineering (IABSE)*, *15*(2), 85–87. doi:10.2749/101686605777963251

Fox. (2000). Arch bridges. In *Bridge Engineering Handbook*.

Galambos. (1998). *Guide to stability design criteria for metal structures*.

Johnson, Klein, & Lawler. (2019). Extending the Life of Historic Concrete Arch Bridges: State of the Art. *Structural Engineering International*, *29*(1), 60–73. doi:10.1080/10168664.2018.1513778

Kindij. (2008). History of Concrete Application in Development of Concrete and Hybriad Arch Bridges. *Chinese-Croatian Joint Colloquium on LONG ARCH BRIDGES*, *LONG ARCH*, 20.

Leonhardt. (1979). *I ponti dimensionamento - tipologia costruzione*. (Edizioni tecniche, Ed.).

Manterola. (2006). *Puentes, Tomo VI*. In C. y P. E.T.S. Ingenieros de Caminos (Ed.), *Puentes* (pp. 2–14).

Martínez. (2005). *Arches: evolution and future trends.*

Menn. (1990). *Prestressed Concrete Bridges*.

Mermigas, & Wang. (2020). Comparative Study of the Proportions and Efficiency of Steel Arch Bridges. *Structural Integrity*, *11*, 280–288. doi:10.1007/978-3-030-29227-0_28

Nettleton, & Torkelson. (1977). Arch Bridges. *Department of Transportation*, (Federal Highway Administration), 124.

Palaoro. (2011). *Arch bridges. Design - Construction - Perception*. *University of Trento*.

Peiretti, Martin, Caldentey, & Herranz. (2001). Puente arco sobre el embalse de El Berguillo (Avila). Diseno y control de la ejecucion. *Hormigon y Acero*, *200*, 3–17.

Radic, Kuster, & Bleiziffer. (2013). Sustainable Large Arch Bridge Maintenance through Inspections, Assessments, Monitoring, Repairs and Service Life Modelling. *IABSE Congress Report*, *18*(23), 619–626. doi:10.2749/222137912805110943

Ribera. (1930). *Puentes de fabrica y hormigon armado - Tomo III* (Vol. 3).

Ridruejo. (2018). Ribera. Retrieved from dbe.rah.es/biografias/21336/jose-eugenio-ribera-dutaste

Salonga, & Gauvreau. (2014). Comparative Study of the Proportions, Form, and Efficiency of Concrete Arch Bridges. *Journal of Bridge Engineering*, *19*(3), 04013010. doi:10.1061/(asce)be.1943-5592.0000537

Schanack. (2016). Arch Bridges. In *Innovative Bridge Design Handbook*.

Suarez. (2020). *Optimization of shape and arch cross-section for arch bridges*. Politecnico di Torino.

Teknoring. (n.d.). Arco (costruzioni). Retrieved from https://www.teknoring.com/wikitecnica/costruzioni/arco-costruzioni/

Treccani. (2021). “Treccani. L’enciclopedia italiana.” www.treccani.it